siam

12th Annual Meeting of the Bulgarian Section of SIAM
December 20-22, 2017
Sofia

BGSIAM'17

EXTENDED ABSTRACTS

HOSTED BY THE INSTITUTE OF MECHANICS
BULGARIAN ACADEMY OF SCIENCES

siam

12th Annual Meeting of the Bulgarian Section of SIAM
December 20-22, 2017
Sofia

BGSIAM'17

EXTENDED ABSTRACTS

PREFACE

The Bulgarian Section of SIAM (BGSIAM) was formed in 2007 with the purpose to promote and support the application of mathematics to science, engineering and technology in Republic of Bulgaria. The goals of BGSIAM follow the general goals of SIAM:

- To advance the application of mathematics and computational science to engineering, industry, science, and society;

- To promote research that will lead to effective new mathematical and computational methods and techniques for science, engineering, industry, and society;

- To provide media for the exchange of information and ideas among mathematicians, engineers, and scientists.

During BGSIAM'17 conference a wide range of problems concerning recent achievements in the field of industrial and applied mathematics will be presented and discussed. The meeting provided a forum for exchange of ideas between scientists, who develop and study mathematical methods and algorithms, and researchers, who apply them for solving real life problems. The conference support provided by the SIAM is highly appreciated.

List of the Invited Speakers include:

- Krassimir Atanassov (Bulgarian Academy of Sciences) "Generalized Nets - Theory and Applications"

- Peter Minev (University of Alberta, Canada) "High-order Artificial Compressibility for the Navier-Stokes Equations"

- Maya Neytcheva (Uppsala University, Sweden) "Enhanced degree of parallelism when solving optimal control problems constrained by evolution equations"

- Zahari Zlatev (Aarhus University, Denmark) "Application of repeated Richardson Extrapolation in the treatment of some chemical modules of environmental pollution models"

The present volume contains extended abstracts of the presentations (Part A) and list of participants (Part B).

Krassimir Georgiev
Chair of BGSIAM Section

Michail Todorov
Vice-Chair of BGSIAM Section

Ivan Georgiev
Secretary of BGSIAM Section

Sofia, December 2017

.

Table of Contents

Part A

Extended abstracts[1]

Method for indoor localization optimization of AoA based mobile devices

Alexander Alexandrov, Vladimir Monov

The paper presents a method for improving the accuracy of indoor positioning approach for commercial mobile devices based on the existing Angle of Arrival (AoA) technology. We propose an optimization method for indoor positioning released by two-stage data fusion process using Extended Kalman filter approach for the first stage and Central Limit Theorem/Fraser-Potter equation techniques for the second stage. Test results show that the proposed method can achieve 10-15% better accuracy in a real-world environment compared to existing AoA methods and techniques.

In our study, the locator with integrated data fusion algorithm realizes a number of consistent measurements with 100ms period. It fuses the results, using Kalman filtering method and sends the fused data of the localization measurements to the control center (Fig. 1).
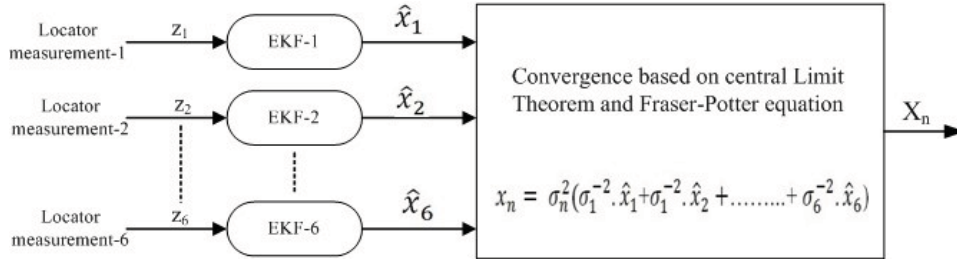
Figure 1

The control center optimizes a criterion based on the Central Limit Theorem and the Fraser-Potter fixed interval smoother in the form $x_n = \sigma_n^2(\sigma_1^{-2}.\hat{x}_1 + \sigma_1^{-2}.\hat{x}_2 + ... + \sigma_6^{-2}.\hat{x}_6)$, where $\sigma_n^2 = (\sigma_1^{-2} + \sigma_1^{-2} + ... + \sigma_6^{-2})$ is the variance of the combined estimate.

The data fusion method presented in the paper allows the information from consistent number of measurements realized by AoA locators to be combined and integrated in real time. Extended Kalman filters (EKF) work as data fusion devices on the locator base station and in the second stage data fusion is realized at the server side.

As a whole, the paper presents a novel indoor positioning system using three efficient mechanisms: signal strength filter, user location filter and path tracking assistance to improve the positioning accuracy of the system. The comprehensive performance of the proposed system was analyzed in detail and compared with a radar system.

Cross-validated sequentially constructed multiple regression

Slav Angelov, Eugenia Stoimenova

Let observe the multiple regression as a tool for prediction. A well known fact is that under the Gaus-Markov conditions the least squares estimator is the best linear unbiased estimator for multiple regression. Let assume that the G-M conditions hold, the input data are suitable for linear model and that the coefficients are estimated by the least squares estimator. Another important thing is that we are assuming that we have independent model variables. But usually in practice we have correlations between the variables and as a result the model has multicollinearity problem. Multicollinearity causes some of the coefficients in the model to be estimated with high variance or even to be biased because of the presence of suboptimal solutions. This is leading to unstable model and the final result is poor predictions. Moreover, if there is presence of multicollinearity and the model is recalculate by a data set with outliers than the negative effects will be increased. If we examine the outliers as a separate problem we should say that they can be influential to the model or not. Usually even if they are not too influential they have higher variance than the other observation and their individual or group effect causes the model to be biased which again may lead to poor prediction results for observations out of the learning set. Additionally, poor prediction results may be caused by overfitting the model - there is a small number of observations per model variable and as a results the estimated model is misleading. Under our initial assumptions we can summarize that in order to obtain a linear model with better prediction performance than a multiple regression we need to take into consideration all of the mentioned factors.

In this paper will be proposed a technique that transforms some of the model variables into components reducing in that manner the total number of variables. The components are forged in a procedure where the most poorly estimated model variable (based on the t value) is combined in a linear relation with another model variable(or component) which is the most highly correlated with it. This linear relationship is estimated iteratively where the values for the coefficients for this component are chosen while minimizing the *Root mean squared error after cross-validation* for the multiple regression with all other model variables (except the mentioned two) and the new component. The procedure that forms the components stops when a chosen minimum of variables is reached or/and when all the model variables and components in the model are well estimated (a chosen threshold for the t values). Because of the way in which the components are constructed the newly obtained set of variables is with lower correlations between each other than the initial set and are more robust to influence while adding more observations to recalculate the model. The final results are less multicollinearity, smaller number of coefficients to be estimated and bigger robustness. This means more consistent model estimation that leads to more reliable prediction results.

The proposed step by step procedure for obtaining components is tested on a real example concerning accounting and macroeconomic information from the firms in the bulgarian gas distribution sector in the period 2007-14. The goal is to predict the *Return on assets* financial ratio for the next observed period based on accounting information from that period. The components are obtained from the data in the period 2007-10, than the model is recalculated with the data in period 2007-11 and tested for the data in period 2012-14. The result shows

enhanced model stability and better prediction results than the multiple regression. Based on the same derived components a second test is performed. The model is recalculated for years 2007-12 with added and without three outliers (not strongly influential but outliers). Than the both models are tested for the data in the period 2013-14. For the model with the added outliers the components again have better prediction results.

How to Assess Multi-population Genetic Algorithms Performance Using Intuitionistic Fuzzy Logic

Maria Angelova, Tania Pencheva

Aim: In this investigation the quality of multi-population genetic algorithms performance is going to be assessed applying a step-wise "cross-evaluation" procedure based on the intuitionistic fuzzy logic. When search for an optimal solution, three multi-population genetic algorithms, applying main genetic operators selection, crossover and mutation in different implementation order, have been here applied in such a challenging object as parameter identification of a fermentation process model.

Methods: The objective function value and the algorithm convergence time are the most representative criteria that might be used to assess the quality of algorithms performance. Although, from a biotechnological point of view those criteria are not quite informative. As an alternative of conventional criteria, intuitionistic fuzzy logic (IFL) is going to be implemented in order to assess the algorithms performance considering the values of the model parameter evaluations as well. A step-wise "cross-evaluation" procedure, developed in [1], is going to be applied aiming to assess performances of three multi-population genetic algorithms (MpGA) modifications using intuitionistic fuzzy logic (IFL). Up to now the procedure has been successfully applied to assess the performance of different modifications of standard simple genetic algorithms (SGA), different modifications of MpGA, standard SGA towards standard MpGA, as well as to assess the performance of SGA and MpGA at different values of the generation gap (GGAP), proven as the most sensitive genetic algorithm parameter.

Object: Here for the first time two modifications of standard MpGA, here denoted as MpGA_SCM (coming from selection, crossover, mutation), in which the selection operator is performed as the last one (after crossover and mutation) are going to be evaluated, implementing the "cross-evaluation" procedure. As such, the algorithms performance of standard MpGA_SCM and two modifications, respectively denoted as MpGS_MCS (mutation, crossover, selection) and MpGA_CMS (crossover, mutation, selection) have been here investigated for the purposes of parameter identification of *S. cerevisiae* fed-batch cultivation.

Results and discussion: As a result, MpGA_SCM has been approved as a leader between three considered here MpGA modifications. The leadership between MpGA_CMS and MpGA_MCS depends on the researcher choice between a bit slower, but more highly evaluated MpGA_CMS towards faster one, but a bit less highly evaluated MpGA_MCS.

Keywords: Modelling; Yeast; Genetic Algorithms; Quality Assessment; Intuitionistic Fuzzy Logic.

References

[1] Pencheva T., M. Angelova, K. Atanassov. Chapter 11. Genetic Algorithms Quality Assessment Implementing Intuitionistic Fuzzy Logic. In: Vasant P. (Ed.), Handbook of Research on Novel Soft Computing Intelligent Algorithms: Theory and Practical Applications, IGI Global, Hershey, Pennsylvania (USA), 2013, 327-354.

6

Perturbation analysis for a nonlinear matrix equation arising in Tree-Like stochastic processes

Vera Angelova

In this contribution the nonlinear matrix equation

$$X \; = \; \Phi(S); \quad \Phi(S) = C - \sum_{i=1}^{m} A_i X^{-1} D_i,$$

with $S = (A_1, A_2, \ldots, A_m, D_1, D_2, \ldots, D_m, C) \in \Psi = \underbrace{\mathbb{R}^{n \times n} \times \mathbb{R}^{n \times n} \times \dot\times \mathbb{R}^{n \times n}}_{2m+1}$ - the collection of matrix coefficients A_i, D_i, $C \in \mathbb{R}^{n \times n}$ for $i = 1, \ldots, m$ and a non-singular solution $X \in \mathbb{R}^{n \times n}$ is considered. This equation is encountered in the analysis of certain discrete-time bivariate Markov processes called Tree-Like stochastic processes [3] and is introduced by Bini et al. in [1] under the assumptions: $C = B - I$ is the transition matrix within a node, with B - sub-stochastic real $n \times n$ matrix; the transition matrices A_i (from a node to its left child) and D_i (from the left child to its parent) have non-negative entries; the matrices $I + C + D_i + \sum_{j=1}^{m} A_j$ for $i = 1, \ldots, m$ are stochastic. Recall that a matrix $P = \{p_{ij}\} \in \mathbb{R}^{n \times n}$ with non-negatives elements p_{ij} is stochastic if $\sum_{j=1}^{n} p_{ij} = 1$.

The perturbation analysis of equation (1) is presented. Based on the Fréchet derivatives, Lyapunov majorants and fixed-point principles, norm-wise, mixes and component-wise condition numbers are formulated and linear perturbation bounds are derived. The condition numbers are formulated according to the definitions given in [2]:

The absolute norm-wise condition number for the problem $X = \Phi(S)$ is the finite quantity

$$K(S) := \lim_{\varepsilon \to 0} \sup \left\{ \frac{\|\Phi(S + \delta S) - \Phi(S)\|}{\|\delta S\|} : \delta S \neq 0, \|\delta S\| \leq \varepsilon \right\}$$

and the corresponding relative condition numbers are $k(S) := K(S) \frac{\|S\|}{\|X\|} = K(S) \frac{\|S\|}{\|\Phi(S)\|}$.

For the vector representation $x = \varphi(s)$ of the problem $X = \Phi(S)$, with $x := \mathrm{vec}(X) = [x_j] \in \mathbb{R}^{n^2}$, $s = \left[\mathrm{vec}(A_1)^\top, \mathrm{vec}(A_2)^\top, \ldots, \mathrm{vec}(A_m)^\top, \mathrm{vec}c(D_1)^\top, \ldots, \mathrm{vec}(D_m)^\top, \mathrm{vec}(C)^\top \right]^\top = [s_j]$, $j = 1, 2, \ldots, (2m+1)n^2$, $\varphi := (\mathrm{vec} \circ \Phi)$. The mixed relative condition number is the quantity

$$
\begin{aligned}
m_\infty(\varphi, s) \quad &:= \quad \frac{\|\varphi'(s) \mathrm{diag}(s_1, s_2, \ldots, s_{(2m+1)n^2})\|_\infty}{\|x\|_\infty} = \frac{\||\varphi'(s)||s|\|_\infty}{\|x\|_\infty} \\
&\leq \quad k_\infty(s) := \frac{\|\varphi'(s)\|_\infty \|s\|_\infty}{\|x\|_\infty}
\end{aligned}
$$

and he relative component-wise condition number, defined for the case when all elements x_k of x are non-zero is

$$
\begin{aligned}
c(\varphi, s) \quad &:= \quad \|\mathrm{diag}(1/x_1, 1/x_2 \ldots, 1/x_v) \varphi'(s) \mathrm{diag}(s_1, s_2, \ldots, s_{2v})\|_\infty \\
&= \quad \|(|\varphi'(s)||s|)./|x|\|_\infty.
\end{aligned}
$$

7

Here $k_\infty(s)$ is the standard relative condition number with respect to the infinity norm $\|\cdot\|_\infty$. For the nonlinear matrix equation (1) norm-wise non-local residual bounds in terms of the computed approximate solution $\hat{X} = X + \delta X$ are obtained as well. These bounds are appropriate for a stop criteria of the iterations, when using a numerically stable iterative algorithm: Denote $r := \|R(\hat{X})\|_{\mathrm{F}} = \|\hat{X} + \sum_{i=1}^{m} A_i \hat{X}^{-1} D_i - C\|_{\mathrm{F}}$, $\zeta_i := \|D_i^\top \hat{X}^{-1} \otimes A_i\|_2 \|\hat{X}^{-1}\|_2$ and $\chi := \|\hat{X}^{-1}\|_2$. For $r \in \Omega = \left\{ 0; \sum_{i=1}^{m} \zeta_i - r\chi + 2\sqrt{r\chi} \le 1 \right\}$, the following bounds for the error δX in the approximate solution $\hat{X}$ are valid:

- non-local absolute residual bound

$$\|\delta X\|_{\mathrm{F}} \le \phi(r),$$

$$\phi(r) := \frac{2r}{1 - \sum_{i=1}^{m} \zeta_i + r\chi + \sqrt{(1 - \sum_{i=1}^{m} \zeta_i + r\chi)^2 - 4r\chi}}$$

- non-local relative residual bound in terms of the right solution X

$$\frac{\|\delta X\|_{\mathrm{F}}}{\|X\|_2} \le \frac{\phi(r)}{\|X\|_2}$$

- non-local relative residual bound in terms of the computed approximate solution $\hat{X}$

$$\frac{\|\delta X\|_{\mathrm{F}}}{\|X\|_2} \le \mathrm{est}; \quad \mathrm{est} := \frac{\phi(r)/\|\hat{X}\|_2}{1 - \phi(r)/\|\hat{X}\|_2}.$$

The effectiveness of the bounds proposed is demonstrated by numerical examples.

References

[1] D. A. Bini, G. Latouche, and B. Meini. Solving nonlinear matrix equations arising in Tree-Like stochastic processes. *Linear Algebra Appl.*, 366:39–64, 2003.

[2] M.M. Konstantinov, D.W. Gu, V. Mehrmann, and P.H. Petkov. *Perturbation Theory for Matrix Equations*. North-Holland, Amsterdam, 2003. [ISBN 0-444-51315-9].

[3] G. Latouche and V. Ramaswami. *Introduction to Matrix Analytic Methods in Stochastic Modeling*. ASA-SIAM Series on Statistics and Applied Probability 5. SIAM, Philadelphia, 1999.

Decision Support System in cases of wildland fires

Atanas Angov, Stefan Stefanov, Nina Dobrinkova

Wildland fire is part of the natural life cycle of the forest. It plays a key role in shaping ecosystems by serving as an agent of renewal and change. However fires have negative side too, which comes up to air pollution, harmful emissions, infrastructural destruction, flora and fauna disappearance. Wildland fires release carbon dioxide, a key greenhouse gas, into the atmosphere which in some areas is a factor for this phenomenon. The Joint Research Centers of European Union (JRC) have annual forest fires report that confirms a trend towards longer and more intense fire seasons all over Europe including northern areas like Norway, Finland and Scotland. The report coincides with an international study which finds that global wildfire trends could have significant health implications due to rising harmful emissions. Despite authorities' efforts, the current statistics shows that the fire seasons are longer and with peaks of fire intensity that can cause catastrophic fires like the ones that had happened in Portugal in 2016 and 2017. The National Oceanic and Atmospheric Administration (NOAA) had funded a study about the climate warming effects that considers the increasing greenhouse gases emissions will rise up the risk of very large, damaging wildfires over the next several decades. Given the increase of wildfires' number and size in the period 2008 - 2017 the firefighter and volunteer groups will be with crucial role in the years to come. However the reality nowadays when it comes to volunteer groups in Bulgaria is that they have significant lack of basic trainings, knowledge and tools to help them battle better with the nature on the field. Points of Interest (POIs) which this people need to know like logistic centers for water supplies and firefighting tools are usually well done instructions on a paper documents. There are no Information and Communication Technologies (ICT) that can ease their orientation or provide them with information what type of equipment is placed in the near by locations. Thus in our article we will present an idea for a system that can be used on the field and in operational rooms by firefighting and volunteer groups acting in cases of wildland fires. For our application we will use different open source software solutions as Geoserver, Qgis, pgAdmin and PostgreSQL:

• The Geoserver allows the user to display spatial information to the world. Implementing the Web Map Service (WMS) standard, Geoserver can create maps in a variety of output formats. OpenLayers, is a free mapping library, that is integrated into Geoserver, making map generation quick and easy. Geoserver also conforms to the Web Feature Service (WFS) standard, which permits the actual sharing and editing of the data that is used to generate the maps. Others can incorporate the collected data into their websites and applications, freeing the data and permitting greater transparency. Geoserver is free software. This significantly lowers the financial barrier to entry when compared to traditional GIS products. In addition, it is also open source and easy to distribute. GeoServer can display data on any of the popular mapping applications such as Google Maps, Google Earth, Yahoo Maps, and Microsoft Virtual Earth. GeoServer can connect with traditional GIS architectures such as ESRI ArcGIS;

• QGIS is a professional GIS (Geographic Information System) cross-platform application that is Free and Open Source Software (FOSS). GIS Applications are normally programs with a graphical user interface (GUI). QGIS is application that supports viewing, editing, and

analysis of geospatial data. QGIS can create, edit, visualize, analyze and publish geospatial information. QGIS supports both raster and vector layers. Vector data is stored as either point, line, or polygon features. Multiple formats of raster images are supported, and the software can georeference images. QGIS supports shapefiles, coverages, personal geodatabases, dxf, MapInfo, PostGIS, and other formats. Web services, including Web Map Service and Web Feature Service, are also supported to allow use of data from external sources.

● pgAdmin is a free multiplatform management tool for PostgreSQL and derivative relational databases such as EnterpriseDB's EDB Advanced Server. It may be run either as a web or desktop application;

● PostgreSQL is a powerful, open source object-relational database system. It runs on all major operating systems, including Linux, UNIX (AIX, BSD, HP-UX, SGI IRIX, macOS, Solaris, Tru64), and Windows. It also supports storage of binary large objects, including pictures, sounds, or video. It has native programming interfaces for C/C++, Java, .Net, Perl, Python, Ruby, Tcl, ODBC and others. An enterprise class database, PostgreSQL boasts sophisticated features such as Multi-Version Concurrency Control (MVCC), point in time recovery, tablespaces, asynchronous replication, nested transactions (savepoints), online/hot backups, a sophisticated query planner/optimizer, and write ahead logging for fault tolerance. It supports international character sets, multibyte character encodings, Unicode, and it is locale-aware for sorting, case-sensitivity, and formatting. It is highly scalable both in the sheer quantity of data it can manage and in the number of concurrent users it can accommodate. There are active PostgreSQL systems in production environments that manage in excess of 4 terabytes of data.

In our article we will describe two PhD studies in their initial stage that will implement the presented open source tools into one system having desktop application for operational room decision support and second mobile option of the system where field data collection and response is in place.

Generalized Nets: Theory and Applications

Krassimir Atanassov

The Generalized Nets (GNs, [1-5]) are defined as extensions of the ordinary Petri Nets (PNs) and their modifications, but in a way that is in principle different from the ways of defining the other types of PNs. The additional components in the GN-definition give more and better modelling capabilities and determine the place of GNs among the separate types of PNs, similar to the place of the Turing machine among the finite automata.

By analogy with the PNs, GNs contain places, transitions and tokens, but their transitions have essentially more complex structure. Besides the input and output places, the GN-transitions contain moment of activation, by analogy with Time PNs; duration of the active state, by analogy with e-nets; index matrix with predicates that determine whether a token from i-th input place can go to the j-th output place; index matrix with natural numbers that determine the capacities of the arc between i-th input and j-th output place; and a special condition, by analogy with the PRO-nets, that determine whether the transition can be activated. GN-tokens enter the net with initial characteristics, that include as a very partial case the idea for colours with which the tokens of the Coloured PNs are coloured and for the symbols, with which the tokens of the Predicate-Transition Nets are marked. Entering a new place, the GN-tokens obtain new characteristics. In contrast to the Coloured PNs and the Predicate-Transition Nets, GN-tokens can keep all their characteristics and they can be used for evaluation of the truth-values of the transition condition predicates. Also in contrast to the remaining types of PNs, the GNs contain global temporal scale.

The GNs have more than 20 conservative extensions (i.e., extensions for which their functioning and the results of their work can be represented by an ordinary GN). The most important of them are:

• four types of intuitionistic fuzzy GNs
• Colour GNs
• GNs with global memory
• GNs with optimization components
• GNs with additional clocks
• GNs with stop-conditions
• GNs with volumetric tokens
• GNs with complex transition type
• GNs with characteristic functions of the places and arcs
• GNs with 3-dimensional structure.

Some of these GN- extensions have many real-world applications. For example, the intuitionistic fuzzy GNs of different types are used for models in chemical and, specifically, in petrochemical industry. Some of these models contain additional clock and/or stop-conditions. They are suitable, e.g., for the models of rectification columns in a petrochemical refinery. The GNs with optimization components can be used for describing of decision making and control processes, and for some more theoretical GN-models, e.g., for ant-colony optimization and genetic algorithms. The GNs with volumetric tokens are used for models of Internet processes, while GNs with place characteristics – in some medical and ecological models.

11

The GNs with 3-dimensional structure, the colour GNs and the GNs with complex transition type provide better visualization of the modeled processes.

The GNs theory contains some aspects:

• algebraic aspect: different operations and relations are defined both over the transitions, and over GNs in general. The operations, defined over GNs –"union", "intersection", "composition" and "iteration" do not exist anywhere else in the PN theory. They can be transferred to virtually all other types of PNs (obviously with some modifications.

• topological aspect: to each GN a graph is juxtaposed and its properties can be used for searching the GN-properties.

• logical aspect: the logical conditions for reachability of the output places from the input places are studied.

• operator aspect: six types of operators are defined in its framework. Every operator assigns to a given GN a new GN with some desired properties. The comprised groups of operators are from global, local, hierarchical, reducing, extending and dynamic types.

During the last 30 years, the GNs have found applications in the areas of Artificial Intelligence (AI) and Data Mining (DM), medicine, biology and ecology, chemistry and economics, university administration processes and many others.

The GNs are object of intensive research and applications in different countries in the world: Australia, Bulgaria, Poland, Portugal, South Korea, Spain, UK, USA and others.

References

[1] Alexieva, J., E. Choy, E. Koycheva. Review and bibloigraphy on generalized nets theory and applications. In:– A Survey of Generalized Nets (E. Choy, M. Krawczak, A. Shannon and E. Szmidt, Eds.), Raffles KvB Monograph No. 10, 2007, 207–301.

[2] Atanassov, K. Generalized Nets, Singapore, New Jersey, London, World Scientific, 1991.

[3] Atanassov, K. On Generalized Nets Theory, "Prof. M. Drinov" Academic Publishing House, Sofia, 2007.

[4] Atanassov, K., S. Sotirova. Generalized Nets. Prof. M. Drinov Academic Publishing House, Sofia, 2017 (in Bulgarian).

[5] Radeva, V., M. Krawczak, E. Choy. Review and bibliography on generalized nets theory and applications. Advanced Studies in Contemporary Mathematics, Vol. 4, 2002, No. 2, 173–199.

Parametric study of a classifying rotor

**Ana Avdzhieva, Stefka Dimova, Sylvi-Maria Gurova, Tihomir Ivanov,
Galina Lyutskanova-Zhekova, Spasimir Nonev, Slavcho Slavchev,
Vladimira Souvandjieva**

In the present work, we consider a classifying rotor, used in air classifiers. The latter are industrial machines that separate materials by a combination of size, shape, and density. Air classifiers are commonly employed in industrial processes where a large volume of mixed materials with differing physical characteristics need to be separated quickly and efficiently [1].

The principle of the rotor's work is as follows. After entering the machine, the air flows through the classifying rotor in centripetal direction. In the process, the classifying rotor extracts the fines from the feed material. The coarse material is rejected by the classifying rotor. Product fineness is controlled by adjustment of the classifier rotor speed and airflow.

One problem in this process is the fact that near the bottom of the rotor, in the center, there exists a region of low velocity, which leads to poor productivity of the classification process. A possible solution, which we investigate, is to modify the shape of the bottom in a way that such a region exists no more.

In the present work, we study the geometry of the rotor in air classifiers, in order to improve their effectiveness. Using computational fluid dynamics simulations for an idealized geometry, we identify the area, where the profile of the air flow leads to worse performance and propose different modifications of the geometry, in order to improve it. Then, we derive a semi-empirical 2D model that helps refine the parameters, once a shape is chosen.

References

[1] Wikipedia, Air classifier, up-to-date on October 10, 2017, `https://en.wikipedia.org/wiki/Air_classifier`.

Enhanced degree of parallelism when solving optimal control problems constrained by evolution equations

Owe Axelsson, Maya Neytcheva, Zhao-Zheng Liang

The recent development of the high performance computer platforms shows a clear trend towards heterogeneity and hierarchy. In order to utilize the computational power, particular attention must be paid to finding new algorithms or adjust existing ones so that they better match the computer architecture of the nowadays available high performance computer platforms.

In this work we consider an alternative to classical time-stepping methods based on use of time-harmonic properties and discuss solution approaches that allow efficient utilization of modern HPC resources.

The idea is as follows. Assume that we deal with a problem with a solution that is periodic. To be specific, let the solution function be time-dependent and periodic in time. Then the problem becomes time-harmonic and the solution can be expressed in terms of a Fourier series. The Fourier expansion offers the possibility to construct an approximation of the solution by truncating the infinite series appropriately.

Further, due to the orthogonality of the trigonometric functions in the expansion, for linear problems the computation of the Fourier coefficients separate and one can compute the solution for each period (frequency) separately, fully in parallel. Hence, the solution process is perfectly parallelizable across the different frequencies.

To overcome the restriction on the solution to be periodic, we show an approach to first symmetrically extend a non-periodic to a periodic function and then use the truncated Fourier expansion.

This approach is used to solve optimal control problems, constrained by a (non-periodic) evolutionary equation. We define the algebraic systems. resulting from a suitable discretization and describe the solution method. Due to the large size of the discretized systems one must use preconditioned iterative solution methods. We show some efficient preconditioning techniques, expected also to be well parallelizable, and illustrate the overall performance with some (so far serial) numerical tests. The structure of the proposed preconditioning technique The detailed description is to be found in [1], containing also various relevant publications, in perticular, [2].

References

[1] O. Axelsson, M. Neytcheva, Z.-Z. Liang, Parallel solution methods and preconditioners for evolution equations. Department of Information Technology, Uppsala University, TR 2017-017 August 2017, http://www.it.uu.se/research/publications/reports/2017-017/

[2] U. Langer. M. Wolfmayr, Multiharmonic finite element analysis of a time-periodic parabolic optimal control problem, *J. Numer. Math.*, 21 (2013), 265–300.

Geometric Visualization of a Polygon Area Partitioning

Todor Balabanov, Stanislav Darachev, Ivan Jordanov, Aleksandar Karakushev, Nikolai Kitanov, Alexander Manov, Georgi Nikolov, Spasimir Nonev, Zdravka Nedyalkova, Emiliyan Rogachev, Natasha Stojkovikj, Petar Tomov, Iliyan Zankinski

In the process of modeling sewerage networks, the main component is the drained area (catchment) from which water is collected to each conduit (pipe). If the area for a single sub-catchment is derived from a mathematical model, we have to create the geometry of that territory, Exactly, in this paper, we want to make geometric visualization for partitioning of a given living area, with respect to the known water debit, relative to each pipe. If each pipe is represent as edges and these edges formed polygon then our main goal is to make geometric visualization of a polygon area partitioning.

Proposed Solutions

1. Monte Carlo Flooding - With this algorithm the polygon will be divided in irregular shapes. The final result of the algorithm is similar to liquid foolding from different sides.

(a) Test case 1.   (b) Test case 2.

Figure 1: Monte Carlo Flooding algorithm results.

2. Percent Distributed Clustering - The given area is divided into a fine grid of pixels. The sides of the polygon are also divided into sixty line segments each. For each pixel of the area the algorithm finds the line segment that gives the lowest value for the distance between the pixel and the line segment multiplied by 100 minus the required percentage of the area: distance * (100 - f(x)). The side that the line segment belongs to is the side that the area taken by the pixel will drain into.
3. Offsetting Polygon - The main idea of the offsetting polygon approach is to fill the initial polygon with smaller ones of which each side is parallel to the corresponding one of the initial polygon.

(a) Test case 1.

(b) Test case 2.

Figure 2: Percent Distributed Clustering algorithm results.

(a) Initial step.

(b) Final result.

Figure 3: Offsetting Polygon algorithm results.

Conclusions

Experimental results show that usage of Percent Distributed Clustering and Offsetting Polygon can produce much better accepted results than Monte Carlo Flooding.

Variational methods for stable time discretization of linear differential equations

Simon Becher, Gunar Matthies, Dennis Wenzel

We have derived a new class of discretization methods for systems of ordinary differential equations. These problems can arise in various fields of application, e.g. after the semi-discretization in space of parabolic problems. Important features for numerical time discretization schemes include order of convergence and stability. Especially the latter one is of significant relevance when considering semi-discretized partial differential equations as the systems tend to become more and more stiff for high resolution in space. We thus aim to construct methods providing *A*- or even *L-stability*. In addition, assuming sufficient regularity of the data, the need for higher regularity of the numerical solutions can arise. The constructed class of methods has the three key features *stability*, *high order of convergence* and *high regularity* under reasonable assumptions on the problem.

Starting from the well-known *discontinuos Galerkin (dG)* and *continuos Galerkin-Petrov (cGP)* methods we use a specific class of interpolatory quadrature formulas to construct variational time discretization methods of higher regularity. Instead of choosing all quadrature points as roots of specific Jacobi polynomials (*Gauss* quadrature) we additionally use function values and derivatives at the beginning and end point of the interval. This can be seen as a generalization of the *Gauss-Radau* and *Gauss-Lobatto* formulas.

If we now consider some division of the time interval, the underlying interpolation operator of any one of the constructed quadrature rules can be defined for every subinterval by an affine transformation. Transferring concepts known from *Finite Element* discretization we combine the local interpolation operators with certain global conformity conditions describing the relation of adjacent subintervals to form a global space of ansatz functions. In each subinterval those functions are polynomials of a degree determined by the underlying interpolation operator while the conformity conditions influence the global regularity.

In order to compute the polynomial coefficients locally we use a combination of different sources of information. Firstly we demand our numerical solution to fulfill the differential equation or one of its derivatives at the beginning and end point of every subinterval, the so-called *collocation equations*. Additionally we need a certain number of *variational equations* in each step to assemble a linear system for the coefficients. Thus we choose a space of test functions of appropriate order with some basis, multiply the problem with those basis polynomials and integrate the resulting equation over the subinterval.

It could be shown that each of the constructed methods inherits the stability properties of either the *dG* method, which is *L-stable*, or the *cGP* method, which is *A-stable*. According to this observation we use the notation *dG-Cs* and *cGP-Cs* for the unique method giving *s* times continuosly differentiable solutions while inheriting the stability properties of *dG* and *cGP* respectively.
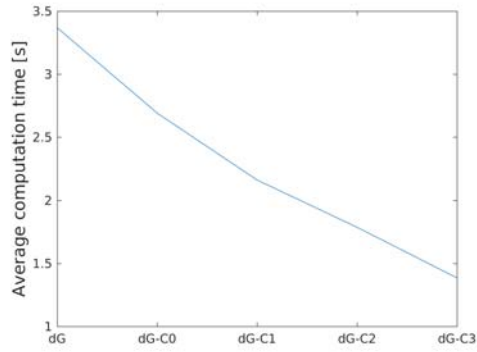
Figure 1: Computation times for a parabolic test problem showing significant performance increase for methods of higher regularity.

The methods were tested on different examples indicating promising results in terms of both convergence order and efficiency. In fact we could observe the convergence rates for different error types depending on both polynomial degree and regularity of the method. To establish the higher regularity of the numerical solution we used *collocation equations* at the beginning and end point of the subintervals. In one case this means an information transfer between the intervals reducing the number of free coefficients. In the other case the assembly costs are cheaper than for *variational equations* leading to a significantly improved performance compared to methods of lower regularity, e.g. the *discontinuos Galerkin method*.

Statistical characteristics of a flow of substance in a network channel containing two arms

Roumen Borisov, Kaloyan N. Vitanov, Nikolay K. Vitanov

Statistical modeling is widely used for understanding processes and characteristics of of complex systems [1, 2]. Often the studied complex systems have a network structure. Because of this the research on network properties is much performed nowadays. In this presentation we shall continue our research based on models for flow of substance in channels of networks [3, 4]. The models in [3, 4] have been used for description of charateristics of human migration through simple channels, i.e. in channels that do not have arms. We extend these models in the presentation. In more detail we discuss the stationary regime of a kind of flow of substance in a channel of network. The new point is that the channel consists of a main channel and two arms. We study the distribution of the substance in the nodes of the channel and the influence of the changes in the flows in the arms of the channel on the distribution of the substance in the main part of the channel. The distributions of the substance in the nodes of the main part of the channel as well as in the two arms are of the kind of the long tail distributions that generalize the famous distributions of Waring, Yule-Simon and Zipf. The results of the study are also discussed from the point of view of flows in channels of technological and other systems.

References

[1] Nikolay K. Vitanov. Science dynamics and research production. Indica- tors, indexes, statistical laws and mathematical models. Springer, Cham, (2016)

[2] Nikolay K. Vitanov, Marcel Ausloos. Test of two hypotheses explaining the size of populations in a system of cities. *Journal of Applied Statistics* **42**, 2686 - 2693 (2015).

[3] Nikolay K. Vitanov, Kaloyan N. Vitanov. Box model of migration chan- nels. *Mathematical Social Sciences* **80**, 108 - 114 (2016).

[4] Nikolay K. Vitanov, Kaloyan N. Vitanov. On the motion of substance in a channel of network and human migration. *Physica A* **490**, 1277 - 1294 (2018).

Material science theory in Industry 4.0 for phase transition technologies

Stefan Bushev

The Fourth Industrial Revolution (Industry 4.0) emerges and opens its way alone, unlike all previous industrial revolutions [1]. Industry 4.0 has: 1. non-linear (exponential) rate of development; 2. scale of impact: 2.1 new technologies merge the physical, digital and biological world with a global influence on the global economy, politics, society and the individual. Dozens of professions and millions of jobs are closed down; 2.2 danger: the new economy based on Industry 4.0 to make smart machines and artificial intelligence follow man rather than them [1]; 3. The challenge for governments is generally: the creation of conditions for a policy of "a comfortable adaptation" of society and the individual with the rapid changes. We think this is possible through knowledge, but it is developing very intensively, and this is an essential reason for lifelong learning.

Material Science [2] is an interdisciplinary science exploring the relationship between the structure of materials (atomic level) and their properties with their applications in scientific and engineering fields. Some studied properties are: electronic, thermal, chemical, magnetic, optical, semiconductor, mechanical. With the development of nanotechnology, material science has become an important university discipline. Some research areas are nanotechnology, crystallography, ceramics, metal science, metallurgy, biomaterials, metal physics [2]. Some used scientific areas are solid state physics, solid state chemistry, liquid crystals, physics chemistry.

It is known that an area of knowledge becomes a science after using mathematics in it. In [3] the definition of mathematics is: Mathematics contains mathematical knowledge, the foundation of mathematics, the methodology of mathematics and philosophy of mathematics in a complex interconnectivity and continuous development. The definition represents the very complex development of mathematical knowledge. The huge advantage of mathematics is that it develops itself. For example, an unresolved pure mathematical problem is canceled and remembered even for centuries until a corresponding solution is found which is involved in mathematical knowledge. Mathematical knowledge is differentiated in particular areas - mathematical disciplines (sciences), but Gödel's theories prove that there is no complete theory.

Let us assume from a methodological point of view that the pure application of mathematics is mathematical physics i.e. an approximate equation between mathematics and physics induced by the results of fundamental experiments. The main difference between mathematics and mathematical physics is the (internal) heavy, unresolved problems of pure mathematics. The full range of knowledge about material science is mathematics and mathematical physics. According to the principles of material science [2] and mathematical modeling [4, 6, 7], a methodology for Basic Knowledge is proposed:

1. general evaluation of the structure (on the meso level) and the properties of the material;

2. select a section of mathematics and mathematical physics for multi-scale description;

3. a specific mathematical model of the structure, with the working properties, the technological process, the work and the life of the material.

A very important point is the use of this methodological framework for the additive capabilities of the 3D printer technology i.e. 3D printer interaction with die casting and heat treatment. 3D printer + die casting + heat treatment are an essential task of Industry 4.0. Mathematical modeling in Industry 4.0, in our view, is close to pure mathematics [3]. Such an assumption can also be accepted on the basis of works [4, 6, 7]. The 3D printer technology has a great application (from food, medicine and weapons) and is an incentive for its mathematical modeling [5].

References

[1] K. Schwab, The fourth industrial revolution, Hermes, Plovdiv, 2016.

[2] W. D. Callister, Jr., Fundamentals of Materials Science and Engineering, 2001, John Wiley and Sons, Inc., Fifth Edition, CD-ROM.

[3] S. Bushev, Industrial mathematics - phase transitions, scattering, structures, Innovations, year V, ISSUE 2/2017, Sofia, 57-63.

[4] Mathematical Modeling Handbook II: The Assessments, The Consortium for Mathematics and Its Applications Bedford, 2013, USA.

[5] I. Akinola, Modelling the Stereo-lithography Process, Electrical Engineering, Stanford University

[6] S. Heinz, Mathematical modeling, Springer-Verlag Berlin Heidelberg, 2011.

[7] K. Velten, Mathematical Modeling and Simulation: Introduction for Scientists and Engineers, WILEY-VCH Verlag GmbH and Co. KGaA, Weinheim, 2009.

Mechanical characterization of multilayer thin film system via nanoindentation and numerical simulations

M. Datcheva, S. Cherneva, D. Iankov , V. Kyrychok, D. Stoychev

Multilayer systems made up of thin films are widely used in electronics. Very often this is a technology for making sensors and functional coatings with various industrial applications. In such constructions, it is important to know the mechanical characteristics of the structures as a whole as well as those of the thin coating layers. The determination of the mechanical characteristics is challenginge due to the fact that the separation of a layer and its characterization with classical experimental techniques is practically impossible or presumes destruction of the sample.

The instrumented indentation (IIT), also known as nanoindentation is a relatively new and promising technique used for characterization of materials in a local point[1,2]. Moreover, nanoindentation has become a commonly approved tool for the measurement of mechanical properties at small scales, but may have even greater importance as a technique for experimental studies of fundamental materials physics.

In the present work a strategy is presented for using IIT data to investigate the mechanical properties of multi-layer systems[3]. For this purpose the nanoindentation deformation process was numerically simulated employing appropriate and adequate finite element models. The adequate numerical simulation of the nanoindentation process allows for performing a back analysis for identification of the constitutive parameters in the mathematical model describing the material behavior[4,5,6]. The results of numerical simulations for a system with four layers are presented and discussed in details.

References

[1] Oliver, Warren Carl, and George Mathews Pharr. "An improved technique for determining hardness and elastic modulus using load and displacement sensing indentation experiments." Journal of materials research 7, no. 6 (1992): 1564-1583.

[2] Iankov, R., S. Cherneva, and D. Stoychev. "Investigation of material properties of thin copper films through finite element modelling of microindentation test." Applied Surface Science254, no. 17 (2008): 5460-5469.

[3] Datcheva, Maria, Sabina Cherneva, Maria Stoycheva, Roumen Iankov, and Dimitar Stoychev. "Determination of anodized aluminum material characteristics by means of nano-indentation measurements." Materials Sciences and Applications 2, no. 10 (2011): 1452.

[4] Cherneva, Sabina, Roumen Iankov, Nenad Radic, Bosko Grbic, and Dimitar Stoychev. "Nanoindentation investigation of mechanical properties of ZrO 2, ZrO 2-Y 2 O 3, Al 2 O 3 and TiO 2 thin films deposited on stainless steel OC 404 substrate by spray pyrolysis." Materials Science and Engineering: B 183 (2014): 12-16.

[5] Bolzon, Gabriella, Giulio Maier, and Michele Panico. "Material model calibration by indentation, imprint mapping and inverse analysis." International Journal of Solids and Structures 41, no. 11 (2004): 2957-2975.

[6] Bocciarelli, M., and G. Bolzon. "Indentation and imprint mapping for the identification of constitutive parameters of thin layers on substrate: perfectly bonded interfaces." Materials Science and Engineering: A 448, no. 1 (2007): 303-314.

A novel method for improving the numerical solutions of fractional differential equations

Yuri Dimitrov, Ivan Dimov, Venelin Todorov

The fractional differential equations (FDEs) have a natural singularity at the initial point of fractional differentiation. The Caputo derivative of order α, where $0 < \alpha < 1$ is defined as:

$$y^{(\alpha)}(x) = D^\alpha y(x) = \frac{1}{\Gamma(1-\alpha)} \int_0^x \frac{y'(\xi)}{(x-\xi)^\alpha} d\xi. \tag{1}$$

The Miller-Ross sequential derivative and the fractional Taylor polynomials of the function y are defined as:

$$y^{[n\alpha]}(x) = D^{n\alpha}y(x) = D^{\alpha+\alpha+\cdots+\alpha}y(x) = D^\alpha D^\alpha \cdots D^\alpha y(x),$$

$$T_m^{(\alpha)}(x) = \sum_{n=0}^m \frac{y^{[n\alpha]}(0)x^{\alpha n}}{\Gamma(\alpha n + 1)}.$$

In this paper we consider the following ordinary and partial FDEs

$$y^{(\alpha)}(x) + by(x) = 0, \quad y(0) = 1, \tag{2}$$

$$y^{[2\alpha]}(x) + by^{(\alpha)}(x) + cy(x) = 0, \quad y(0) = 1, y^{(\alpha)}(0) = 1, \tag{3}$$

$$\begin{cases} \dfrac{\partial^\alpha y(x,t)}{\partial t^\alpha} = \dfrac{\partial^2 u(x,t)}{\partial x^2}, \\ u(x,0) = \sin x, \; u(0,t) = u(\pi,t) = 0. \end{cases} \tag{4}$$

Equation (1) has the solution $y(x) = E_\alpha(-Bx^\alpha)$. The Miller-Ross derivatives of the solution satisfy $y^{[n\alpha]}(0) = (-b)^n$. The solutions of equations (1), (2) and (3) have a singularity at the initial point of fractional differentiation. The accuracy of the numerical solutions of equations (1) and (2) which use the L1 approximation of the Caputo derivative is $O(h^\alpha)$ and the numerical solution of equation (3) has an accuracy $O(\tau + h^2)$. We use the fractional Taylor polynomials of the solutions of equations (1), (2) and (3) for transforming the equations to FDEs whose solutions have higher-order continuous derivatives. Substitute

$$z(x) = y(x) - T_m^{(\alpha)}(x) = y(x) - \sum_{n=0}^m \frac{y^{[n\alpha]}(0)x^{\alpha n}}{\Gamma(\alpha n + 1)}.$$

Equations (1) and (2) are transformed as:

$$z^{(\alpha)}(x) + bz(x) = -\frac{by^{[\alpha m]}(0)x^{\alpha m}}{\Gamma(\alpha m + 1)}, \quad z(0) = 0. \tag{5}$$

$$z^{(2\alpha)}(x) + bz^{(\alpha)}(x) + cz(x) = -\frac{cy^{[\alpha m]}(0)x^{\alpha m}}{\Gamma(\alpha m + 1)} - \tag{6}$$
$$\frac{x^{\alpha(m-1)}}{\Gamma(\alpha m + 1 - \alpha)}\left(by^{[\alpha(m-1)]}(0) + cy^{[\alpha m]}(0)\right).$$

Substitute

$$z(x,t) = y(x,t) - \sin x \sum_{n=0}^{m}(-1)^n \frac{t^{n\alpha}}{\Gamma(n\alpha + 1)}.$$

Equation (3) is transformed as

$$\begin{cases} \dfrac{\partial^\alpha z(x,t)}{\partial t^\alpha} = \dfrac{\partial^2 z(x,t)}{\partial x^2} + (-1)^{m+1}\sin x \dfrac{t^{m\alpha}}{\Gamma(m\alpha + 1)}, \\ z(x,0) = z(0,t) = z(\pi,t) = 0. \end{cases} \tag{7}$$

When m is a positive integer and $m\alpha \geq 2$, the solutions of equations (4), (5) and (6) have continuous second derivatives in the direction of fractional differentiation. The accuracy of the numerical solutions of equations (4), (5) and (6) which use the L1 approximation of the Caputo derivative is $O\left(h^{2-\alpha}\right)$ and $O\left(\tau^{2-\alpha} + h^2\right)$.

References

[1] W. Deng, C. Li, Numerical Schemes for Fractional Ordinary Differential Equations, In Numerical Modeling, Peep Miidla (editor). InTech; 2012.

[2] Y. Dimitrov, Second-order approximation for the Caputo derivative, Journal of Fractional Calculus and Applications 7(2), (2016), 175–195.

[3] F. Zeng, Z. Zhang, G.E. Karniadakis, Second-order numerical methods for multi-term fractional differential equations: Smooth and non-smooth solutions, Computer Methods in Applied Mechanics and Engineering (2017)

Modelling for Price Accuracy in the Airline Tickets Domain

Peter Dojnow

The discrepancy and volatility of the advertised and the selling prices on the Internet markets (online purchase) is a growing problem and is a broad field for investigation [1, 2, 3] and its managing [4]. This is due to elaborate data transaction organisation of information systems and long chain from air carriers, (re)seller agents to travel search sites such as Skyscanner company. More than 3.5 billion people fly every year; thousands of seats are sold every minute. Many transactions are accomplished which cost time and inevitable delays thereby leads to discrepancies of prices from travel search sites and actual selling costs. The problem concerns all these people. The aim is the discrepancies to be diminished to an acceptable limit. Skyscanner company sets the 4 USD limit loss to passengers. The length (size) of data set supplied by Skyscanner company is 766300 records. The inaccurate price denoted here as $Error\_USD$ is every difference of $Partner\_Price - Skyscanner\_Price > 4$ USD. All differences out of the (4,104) range are discarded so 61329 records are left and are used for this study. The prices are tested with two-sample Kolmogorov-Smirnov test [5] to compare the distributions of the $Partner\_Price$ and $Skyscanner\_Price$. The null hypothesis was rejected so the alternative hypothesis is approved that they are from different statistical distributions. The histogram of the inaccurate prices represents empirical distribution of the $Error\_USD$. There are univariate point outliers (anomalies) in 3 price error ranges: $11,5 \pm 0.5, 17.5 \pm 0.5, 23.5 \pm 0.5$ USD are single data points that lay far from the rest of the distribution. There is no appointed mathematical definition of what is an outlier (anomaly); determining whether or not an observation is an outlier or is ultimately a subjective exercise [6, 7, 8] and the different methods which were used gave different result thus the obvious ones are indicated. Detecting outliers (anomalies) and understanding the reason of their existence is very important in data mining as they can skew the results and can reveal intrinsic defects of the processes generating the data. There are different causes of outliers but in this case the observed data set is not from experiment measurement errors but rather a data processing error in the chain of the information retrieval and the delivery from the company partners. The coefficients of some models of statistical distributions [9, 10] with outliers and without outliers are evaluated. The exponential distribution occur in many different connections such as the radioactive or particle decays or the time between events in a Poisson process [9]. The power-law probability distributions occur in trading volumes on the stock market. The most important special case where $b < 0$ is the Pareto distribution, which has a power-law tail. It is originally explored as a model of business failure [10]. The composite additive distributions *Exponential2* and *Power2* are better fitted to the empirical one and they represent the diverse distributions of prices as the goodness of fit indicators *SSE*, the sum of squares due to error and *RMSE*, the root mean squared error with and without outliers are evaluated and the values are closer to 0 which indicates that these fits are more useful for prediction [11].

The problem is submitted at the 132 European Study Group with Industry, September 18-22, 2017, Sofia, Bulgaria.

References

[1] Eric K. Clemons, Il-Horn Hann, and Lorin M. Hitt. Price dispersion and differentiation in online travel: An empirical investigation. *Management Science*, 48(4):534–549, 2002.

[2] Rob Law and Rita Leung. A study of airlines' online reservation services on the internet. *Journal of Travel Research*, 39(2):202–211, 2000.

[3] Peng-Sheng You. Dynamic pricing in airline seat management for flights with multiple flight legs. *Transportation Science*, 33(2):192–206, 1999.

[4] J.S. Walker, T.S. Case, J.A. Jorasch, and T.M. Sparico. Method, apparatus, and program for pricing, selling, and exercising options to purchase airline tickets, August 18 1998. US Patent 5,797,127.

[5] Taylor B. Arnold and John W. Emerson. Nonparametric Goodness-of-Fit Tests for Discrete Null Distributions. *The R Journal*, 3(2):34–39, 2011.

[6] D.M. Hawkins. *Identification of Outliers*. Monographs on applied probability and statistics. Chapman and Hall, 1980.

[7] Varun Chandola, Arindam Banerjee, and Vipin Kumar. Anomaly detection: A survey. *ACM Comput. Surv.*, 41(3):15:1–15:58, July 2009.

[8] Charu C. Aggarwal. *Outlier Analysis*. Springer, 2013 edition, 2013.

[9] Christian Walck. *Hand-book on STATISTICAL DISTRIBUTIONS for experimentalists*. Particle Physics Group Fysikum University of Stockholm, 2007.

[10] Gavin E. Crooks. *Field Guide to Continuous Probability Distributions*, v 0.11 beta edition, 2017.

[11] MathWorks. *Evaluating Goodness of Fit*, 2017 edition, 2017.

Preliminary analysis of the dynamics of multifractal parameters of the Dow Jones Industrial Average

Peter Dojnow

The Dow Jones Industrial Average (DJIA) is an index for key industrial enterprises [1]. It represents large and well-known U.S. companies and covers almost all industries [2]. It is presented on May 26, 1896 [3]. The DJIA is an indicator for the state of the U.S. economy [4], which as a complex nonlinear system can be studied with a various statistical mathematical analytical methods [5] that can give different, seemingly noncomparable estimates. The DJIA, like other time series originating from the self-organizied large systems containing many interacting agents is non-stationary, noisy-like with power law spectrum density, with positive trend, with multitude fluctuations which conditions a multifractal characteristic.

The following methods are used: Multifractal Detrended Fluctuation Analysis (MDFA) [6], Wavelet Transform Modulus Maxima Method (WTMM) [7]. The MDFA in the developed MFA toolbox is a modified version of the original one with double sliding windows for smoothing of the fluctuation function and extracting the dynamics of the (multi)fractal parameters in the course of time in the case of nonstationarity. The evaluated parameters are generalised Höledr (Hurst) correlation exponent $h(q)$, scaling exponent $\tau(q)$, multifractal spectrum $f(\alpha)$ and the multifractality - the multifractal spectrum with Mf [6, 7]. From the initial series labelled as Index after random shuffling by the surrogate time series method [8] the Index_{rp} values are obtained. The amplitude (Am) and the phase (Ph) are derived from analytical signal [9] with the Hilbert transform from the initial series and thence the Amplitude_{rp} and the Phase_{rp} components.

The obtained values of the correlation exponent $h_2 \sim 1.5 \pm 0.2$ are of the Brownian motion process, which in this case is related to the economy [10]. The random permutation of the series leads to destruction of the correlations and the strong diminution of the multifractality which means it is of the second type. The index and its phase have similar trends but the phase sharpens the variations which coincide with great historical events in economy: The Great Depression 1929-1941 [11]; the 1980s oil glut and the price of oil, which had peaked in the 1980 and the Reaganomics of the 1980s; the Black Monday (1987) [12]; the Dot com bubble aftermath in 2000. A sharp break-down of the multifractality is manifested in the period 1929-1941. An example for a sharp leap of the multifractality is in the Reaganomics of the 1980s. The Dot com bubble aftermath crisis in 2000 reflected in a decreased multifractality of the index and its phase. The amplitude of the correlation $h_2(t)$ and the multifractality $Mf(t)$ differs - qualitatively and quantitatively from the other two components so the extraction and investigation of the separated components of the index - the amplitude and the phase make sense and can extract additional information. The investigation of the influence of the time-window length - $w_t' = 2048$ and $w_t'' = 4096$ revealed that the length doesn't change qualitatively the course of the correlation and the multifractality. The main peaks and the transitions in both curves are the same but the estimated multifractality at w_t'' is a lesser than the other one with w_t'. The longer length smooths the variations in the curves but worsens the time-resolution of the variations.

References

[1] S&P Dow Jones Indices LLC. Dow jones industrial average fact sheet. *S&P Dow Jones Indices LLC*.

[2] P. Kahn. *A Reference Manual on the Dow Jones Industrial Average*. Gann Research Institute, 1982.

[3] P.M. Parker. *Dow Jones Industrial Average: Webster's Timeline History, 1896-2007*. Webster's online dictionary. ICON Group International, 2009.

[4] R.J. Stillman. *Dow Jones industrial average: history and role in an investment strategy*. Dow Jones-Irwin, 1986.

[5] Garnett P. Williams. *Chaos Theory Tamed*. National Academy Press, 1997.

[6] Jan W. Kantelhardt, Stephan A. Zschiegner, Eva Koscielny-Bunde, Shlomo Havlin, Armin Bunde, and H. Eugene Stanley. Multifractal detrended fluctuation analysis of nonstationary time series. *Physica A: Statistical Mechanics and its Applications*, 316(1-4):87–114, December 2002.

[7] J.F. Muzy, E. Bacry, and A. Arneodo. Multifractal formalism revisited with wavelets. *International Journal of Bifurcation and Chaos in Applied Sciences and Engineering*, 04, April 1994.

[8] T. Schreiber and A. Schmitz. Surrogate time series. *Physica D*, 142(3-4):346–382, 2000.

[9] D. Gabor. Theory of communication. Part 1: The analysis of information. *Electrical Engineers - Part III: Radio and Communication Engineering, Journal of the Institution of*, 93(26):429–441, November 1946.

[10] Roumen Tsekov. Brownian markets. *Chinese Physics Letters*, 30(8):088901, 2013.

[11] R.S. McElvaine. *The Great Depression: America, 1929-1941*. Three Rivers Press, 1993.

[12] Wikipedia. Black monday (1987). *en.wikipedia.org*.

A single server retrial queue with finite population and two types of customers

Velika Dragieva

We consider in this article a queueing model with one server (an operator, or a company) that serves N customers of two types - regular customers, and subscribed customers. The numbers of both types customers are fixed - K regular and $(N-K)$ subscribers, $K < N$. Each of these customers produces a Poisson flow of demands with intensity λ_R and λ_S, respectively. We assume that the subscribed customers more often use the services of the company so that $\lambda_S > \lambda_R$.

If the server is idle at the time moment of a regular customer arrival, the customer starts to be served. Otherwise it enters a vertual waiting room, called orbit and after an exponentially distributed interval repeats its attempt for service. These attempts are repeated until the customer finds the server idle. Thus, each regular customer in the orbit produces a Poisson flow of demands with intensity μ. The customers in the orbit are called secondary or repeated customers, while those that are outside it - primary regular customers or regular customers in free state. The service duration of primary and secondary regular customers follows the same arbitrary law with common probability distribution function $B_1(x)$. After the service is over the regular customers of both types (primary or secondary) move to a free state, i.e. can produce a Poisson flow of demands with intensity λ_R.

Similarly, if the server is idle at the time moment of a subscribed customer arrival, the customer starts to be served. Otherwise the system state does not change. The service duration of subscribers follows an arbitrary law with common probability distribution function $B_2(x)$. After the service any subscribed customer is free to produce his/her usual demands that form a Poisson flow with intensity λ_S.

Thus, after each service the next customer to be served is determined by a competition between three Poisson flows of demands - demands of the primary regular customers, of the secondary regular customers (the customers in the orbit) and of the subscribed customers.

Introducing a suplementary variable $z(t)$, equal to the elapsed service time, the state of the system at time t can be described by the Markov process

$$X(t) = \{C(t), N_O(t), z(t)\}$$

where $C(t)$ denotes the server state at time t (0, 1 or 2, according to the server is idle, busy with a regular customer or busy with a subscribed customer, respectively) and $N_O(t)$ is the number of repeated regular customers at time t, i.e. the orbit size. Because of the finite state space of this Markov process the stationary regime exists and we can define the limiting probabilities (densities):

$$p_{ij}(x)dx = \lim_{t\to\infty} P\{C(t) = i, N_O(t) = j, x \le z(t) < x + dx\}, i = 1, 2,$$

$$p_{ij} = \lim_{t\to\infty} P\{C(t) = i, N_O(t) = j\}, \ i = 0, 1, 2, \ \ j = 0, 1, \dots, K.$$

In a general way we obtain the equations of statistical equilibrium and applying the discrete transformation method (see for example [1]) derive formulas for the stationary probabilities

p_{ij}. These formulas allow to obtain expressions for the main macro characteristics of the system performance: distribution of the server state, mean number of the customers in orbit and mean waiting time, spent by a customer in the orbit.

The main purpose of this work is to evaluate the influence of the subscribed customers on the system performance characteristics. To this end we compare our results with the results for the corresponding model without subscribers, obtained in [2] and [1]. A cost function and values of the system input parameters that minimize this function are also considered. It should be noted that a similar model but with infinite population and general retrial times is extensively studied in [3].

References

[1] V. Dragieva, A finite source retrial queue: number of retrials, Communications in Statistics - Theory and Methods, 42: 5, (2013), 812 – 829.

[2] G. Falin, J. Artalejo, A finite source retrial queue, Eur. J. Oper. Res., 108, (1998), 409-424.

[3] P. Moreno, An M/G/1 retrial queue with recurrent customers and general retrial times, Appl. Math. Comput. , 159, (2004), 651-656.

Analyses and boolean operation for 2D Cutting Stock Problem

Georgi Evtimov, Stefka Fidanova

The 2D cutting stock problem (CSP) arises in many industries as paper industry, glass industry, biding construction and so on. In paper and glass industries the cutting shapes are rectangles. In building constructions industry the cutting shapes are postilions, which ca have irregular form and can be convex and concave. This increases the difficulty of the problem. In our work we concentrated on 2D cutting stock problem, coming from building industry. Many manufactures companies which build steel structures have to cut plates and profiles. The CSP is well known like NP-hard combinatorial optimization problem. The plates are represented like 2D polygons in any CAD environment. The aim of this issue is to apply some mathematical algorithms on each polygon and to prepare them for subsequent processing for solving the main problem. This task is first basic step (preprocessor) for solving a 2D CSP - arrange all given plates from the project in minimum area. Our preprocessing includes following main steps: Is polygon clock wise; Remove Wasted Points; Find Intersections Points; Create Boolean tables for the polygons.

Ant Colony Optimization Algorithm for Workforce Planning, Influence of the Algorithm Parameters

Stefka Fidanova, Olimpia Roeva

The workforce planning is a difficult optimization problem. It is important real life problem which helps organizations to determine workforce which they need. A workforce planning problem is very complex and needs special algorithms to be solved using reasonable computational resources. The problem consists to select set of employers from a set of available workers and to assign this staff to the tasks to be performed. The objective is to minimize the costs associated to the human resources needed to fulfill the work requirements. A good workforce planing is important for an organization to accomplish its objectives. The mathematical description of the problem is as follows:

A set of jobs $J = \{1, \ldots, m\}$ must be completed during the next planning period. Each job j requires d_j hours during the planing period. There is a set $I = \{1, \ldots, n\}$ of available workers. The availability of the worker i is s_i hours. For reasons of efficiency a worker must perform a minimum number of hours (h_{min}) of any job to which he is assigned and no worker capable assigned to more than j_{max} jobs. A_i is the set of jobs that worker i is qualified to perform. No more than t workers can be assigned during the planed period and the set of selected workers can be capable to complete all the jobs. The goal is to find a feasible solution which minimizes the assignment cost.

The complexity of this problem does not allow the utilization of exact methods for instances of realistic size. Therefore we will apply Ant Colony Optimization (ACO) method which is a stochastic method for solving combinatorial optimization problems. The ACO algorithm was inspired by real ants behavior. ACO algorithm is population based approach, which has been successfully applied to solve hard combinatorial optimization problems. One of its main ideas is the indirect communication among the individuals of a colony of agents with distributed numerical information called pheromone. The problem is represented by graph and the ants walk on the graph to construct solutions. The solutions are represented by paths in the graph. On this work we investigate on influence of ACO parameters on algorithm performance.

Convergence of homotopy perturbation method for solving of two-dimensional fuzzy Volterra functional integral equations

Atanaska Georgieva, Artan Alidema

The study of fuzzy Volterra integral equations begins in Kaleva [7], Seikkala [11] and Mordeson and Newman [8], such integral equations being applied in control mathematical models. Homotopy perturbetion method has been recently intensively studied by scientists and engineers and used for solving nonlinear problems. This method [5], [6] was proposed first by He which is, in fact, a coupling of the traditional perturbation method and homotopy in topology. Homotopy perturbetion method yields a very rapid convergence of the solution series in most cases, usually only few iterations leading to very accurate solution. This method has been applied to many problems [3], [4], [9].

The homotopy perturbation method proposed by He for solving linear and nonlinear integral equations, has been subject of extensive numerical and analytical studies. Allahviranloo and Hashemzehi [1], proposed homotopy perturbetion method to solve fuzzy Fredholm integral equations, respectively Allahviranloo, M.Khezerloo, Ghanbari, S.Khezerloo [2], proposed method to solve fuzzy Volterra integral equations. Also, Rivaz, Yusefi [10] proposed mofidied homotopy perturbetion method for solving two-dimensional fuzzy Fredholm integral equations.

The subject of this paper is to apply the homotopy perturbation method for solving fuzzy Volterra functional integral equation in two variables

$$u(s,t) = g(s,t) + f(s,t,u(s,t)) + \int_c^t \int_a^s H(s,t,x,y,u(x,y))dxdy, \tag{1}$$

where $H : [a,b] \times [c,d] \times [a,b] \times [c,d] \times E^1 \to E^1$, $f : [a,b] \times [c,d] \times E^1 \to E^1$ are a continuous functions on E^1 and g, $u : [a,b] \times [c,d] \to E^1$ are continuous fuzzy-number valued functions.

We use the parametric form of this equation with respect to the definition and find its approximate solution. By Banach's fixed point theorem we prove in details the existence and uniqueness of the solution and the convergence of the proposed method. Also, we give the error estimation between the exact and the approximate solution. Finally, we present some numerical examples to demonstrate the accuracy of the method. From the computational view point, the homotopy perturbation method is more efficient and easy to use.

References

[1] Allahviranloo T., Hashemzehi S.: The homotopy perturbation method for fuzzy Fredholm integral equations.: Journal of Applied Mathematics. **5** 1–12 (2008)

[2] Allahviranloo T., Khezerloo M., Ghanbari M. and Khezerloo S.: The homotopy perturbation method for fuzzy Volterra integral equations. International Journal of computional cognition. **12** 31–37 (2010)

[3] Chun C.: Integration using He's homotopy perturbation method. Chaos, Solitons and Fractals **34** 1130-–1134 (2007)

[4] Cveticanin L.: Homotopy perturbation method for pure nonlinear differential equation. Chaos, Solitons and Fractals **30** 1221-–1230 (2006)

[5] He J. H.: A coupling method of homotopy technique and perturbation technique for nonlinear problems. International Journal Non-Linear Mechanics **35** 37-–43 (2000)

[6] He J. H.: Homotopy perturbation technique. Computer Methods Applied Mechanics Engineering **178** 257-–262 (1999)

[7] Kaleva O.: Fuzzy differential equations. Fuzzy Sets and Systems **24**, 301–317 (1987)

[8] Mordeson J., Newman W.: Fuzzy integral equations. Information Sciences **87** 215-–229 (1995)

[9] Ozis T. and Yildirim A.: A note on He's homotopy perturbation method for van der pol oscillator with very strong nonlinearity. Chaos, Solitons and Fractals **34** 989-–991 (2007)

[10] Rivaz A., Yusefi F.: Modified homotopy perturbation method for solving two-dimensional fuzzy Fredholm integral equations. Journal of Applied Mathematics **25** 591–602 (2012)

[11] Seikkala S.: On the fuzzy initial value problem. Fuzzy Sets Systems **24** 319—330 (1987)

Iterative method for numerical solution of two-dimensional nonlinear Urysohn fuzzy integral equations

Atanaska Georgieva, Albena Pavlova, Svetoslav Enkov

The concept of fuzzy integrals was initiated by Dubois and Prade [1] and then investigated by Kaleva [4], Goetschel and Voxman [3], Nanda [5] and others. Since many real-valued problems in engineering and mechanics can be expressed in the form of two-dimensional fuzzy integral equations, it is important to develop quadrature rules and numerical methods for solving such integral equations.

In this paper, we investigate the following two-dimensional nonlinear Urysohn fuzzy integral equation (2DNUFIE)

$$F(s,t) = g(s,t) \oplus FR \int_c^d (FR) \int_a^b H(s,t,x,y,F(x,y)) \, dx \, dy, \qquad (1)$$

where $H : [a,b] \times [c,d] \times [a,b] \times [c,d] \times \mathbf{R}_{\mathscr{F}} \to \mathbf{R}_{\mathscr{F}}$ is a continuous functions on $\mathbf{R}_{\mathscr{F}}$ and $g, F : [a,b] \times [c,d] \to \mathbf{R}_{\mathscr{F}}$ are continuous fuzzy-number valued functions.

By Banach's fixed point theorem, we give sufficient conditions for existence of unique bounded solutions for 2DNFFIE. We construct an efficient iterative numerical method for equation (1) based on the Picard's technique of successive approximations and on a recent Simpson type fuzzy cubature rule applied at each iterative step. We establish the uniform boundedness of the sequence of successive approximations, and present the steps of the iterative algorithm. The error estimation of the proposed method is obtained in terms of uniform and partial modulus of continuity by using the error estimate for the Simpson fuzzy cubature rule in [2]. We prove the convergence and numerical stability with respect to the choice of the first iteration of the proposed method. We present some test numerical examples, and confirm the obtained theoretical results concerning the convergence and numerical stability with respect to the choice of the first iteration of the method.We also illustrate the accuracy of these results.

References

[1] Dubois D., Prade H.: Towards fuzzy differential calculus. Fuzzy Sets and Systems **8**, 1-7, 105-116, 225-233 (1982)

[2] Enkov S., Georgieva A. and Pavlova A.: Quadrature rules and iterative numerical method for two-dimensional nonlinear Fredholm fuzzy integral equations. Communications in Applied Analysis **21**, 479-498, (2017)

[3] Goetschel R., Voxman W.: Elementary fuzzy calculus. Fuzzy Sets Systems **18**, 31-43 (1986)

[4] Kaleva O.: Fuzzy differential equations. Fuzzy Sets and Systems **24**, 301-317 (1987)

[5] Nanda S.: On integration of fuzzy mappings. Fuzzy Sets and Systems **32**, 95-101 (1989)

Greedy Low-Rank Approximation in Tucker Tensor Format

Irina Georgieva, Clemens Hofreither

For low-rank approximation of tensors with order d higher than two, several different formats have been described in the literature. The most straightforward approach is the approximation by sums of outer products of d vectors, often referred to as the canonical or CP (CANDECOMP/PARAFAC) format. Unfortunately, there are certain difficulties associated with low-rank approximation in this format for orders $d > 2$ stemming from the fact that the set of tensors with a given maximum rank R is not closed if $d > 2$, a crucial difference from the matrix case.

For this reason, alternative formats have been devised. One of these is the so-called Tucker format or tensor subspace format. Here, instead of storing a full tensor, say $A \in \mathbb{R}^{N_1 \times \dots \times N_d}$, one stores d factor matrices $U_j \in \mathbb{R}^{N_j \times r_j}$, $j = 1, \dots, d$, along with a smaller core or coefficient tensor $X \in \mathbb{R}^{r_1 \times \dots \times r_d}$. The assumption is that the ranks are significantly smaller than the size of the original tensor, $r_j \ll N_j$. The entries of the Tucker tensor $T \in \mathbb{R}^{N_1 \times \dots \times N_d}$ described by $\{U_j\}$ and X are then given by

$$T_{i_1,\dots,i_d} = \sum_{\alpha_1=1}^{r_1} \dots \sum_{\alpha_d=1}^{r_d} [U_1]_{i_1,\alpha_1} \cdots [U_d]_{i_d,\alpha_d} X_{\alpha_1,\dots,\alpha_d}.$$

An interpretation of this format is that the columns of U_j form a basis for a r_j-dimensional subspace of $\mathbb{R}^{N_j}$. A tensor product basis for a subspace of the space of d-dimensional tensors in which A lies is obtained by constructing a tensor product basis from these univariate bases. The core tensor X gives the coefficients for the approximation within this subspace.

We propose a novel algorithm for approximation of tensors in the Tucker format. It is an iterative method that, in each iteration, computes an optimal rank one approximation $x_1 \otimes \dots \otimes x_d$ to the residual by means of an Alternating Least Squares (ALS) method. Each of the univariate bases U_j is then enriched by the corresponding vector x_j, leading to an increase in dimension by one. The univariate bases are kept orthonormal throughout, which permits a fast computation of the updated coefficient tensor X. After k iterations, we obtain an approximation with Tucker ranks $r_1 = \dots = r_d = k$.

A crucial advantage of this method is that it applies not only to approximation of given tensors, but can be straightforwardly extended to approximation of tensors which are given implicitly as the solution of linear equations with a low-rank linear operator. Such equations arise naturally in tensor product discretizations of partial differential equations and, more recently, in Isogeometric Analysis.

We give several examples which demonstrate the convergence of the method. It generally converges much faster than a corresponding Greedy Rank-One Update (GROU) scheme. Furthermore, the obtained approximations are in many cases reasonably close to the best Tucker approximation, which is much more costly to compute.

Riemann-Hilbert problems, reduction groups, and spectral properties of Lax operators

Vladimir Gerdjikov

The classical approach to the analysis of integrable nonlinesr evolution equations (NLEE) is to start from its Lax representation. Given the Lax pair, e.g.

$$L_0\psi \equiv i\partial_x\psi + U_0(x,t,\lambda)\psi(x,t,\lambda) = 0, \qquad U_0 = [J,Q_0(x,t)] - \lambda J$$
$$M_0\psi \equiv i\partial_t + V_0(x,t,\lambda)\psi(x,t,\lambda) = 0, \qquad V_0 = [K,Q_0(x,t)] - \lambda K \tag{1}$$

related to the simple Lie algebra $\mathfrak{g}$. In this example J, K belong to the Cartan subalgebra $\mathfrak{h} \subset \mathfrak{g}$. The compatibility condition $[L_0, M_0] = 0$ leads to the N-wave equations [1]. Next one solves the inverse scattering problem for (1) usually reducing it to a Riemann-Hiblert problem (RHP). This allows one to i) use Zakharov-Shabat dressing method for calculating the soliton solutions; ii) apply Mikhailov reduction group to derive new NLEE; iii) use Wronskian relations and prove that the inverse scattering method can be understood as generalized Fourier transform, see e.g. [2, 3].
Let us apply the above scheme, say to Lax pairs which are polynomial in λ, e.g.

$$L\psi \equiv i\partial_x\psi + U(x,t,\lambda)\psi(x,t,\lambda) = 0, \quad M\psi \equiv i\partial_t\psi + V(x,t,\lambda)\psi(x,t,\lambda) = 0,$$
$$U(x,t,\lambda) = \sum_{s=0}^{k-1} U_{k-s}(x,t)\lambda^s - \lambda^k J, \quad V(x,t,\lambda) = \sum_{s=0}^{k-1} V_{k-s}(x,t)\lambda^s - \lambda^k K, \tag{2}$$

where $k \geq 2$, one meets substantial difficulties already on the first step, trying to parametrize adequately $U(x,t,\lambda)$ and $V(x,t,\lambda)$.
Our aim here is to propose a more adequate approach which could allow us to tackle polynomial bundles (2) for any $k \geq 2$.
To this end we start with the RHP, see [4]. Generic RHP is defined by introducing the contour Γ which splits the complex λ-plane into h domains Ω_s, $s = 0, \ldots, h-1$. The solution of the RHP consists of h functions $\xi_s(x,t,\lambda)$ analytic for $\lambda \in \Omega_s$ which are related by:

$$\xi_s(x,t,\lambda) = \xi_p(x,t,\lambda)G_{sp}(x,t,\lambda), \quad \lambda \in \Omega_s \cap \Omega_p, \tag{3}$$

and satisfying $i\partial_x G_{sp} = \lambda^k[J, G_{sp}]$ and $i\partial_t G_{sp} = \lambda^k[K, G_{sp}]$. The canonical normalization of the RHP (say of $\xi_p(x,t,\lambda)$ for $\lambda \to \infty$) allows us to parametrize it by:

$$\xi_p(x,t,\lambda) = \exp(\mathscr{Q}(x,t,\lambda)), \qquad \mathscr{Q}(x,t,\lambda) = \sum_{s=1}^{\infty} Q_s\lambda^{-s}. \tag{4}$$

Then $U(x,t,\lambda)$ and $V(x,t,\lambda)$ can be naturally parametrized by the first few coefficients $Q_a(x,t)$, $a = 1,\ldots,k$. To this end we can use the fact that [5]:

$$U(x,t,\lambda) = -(\lambda^k\xi_p J\xi_p^{-1}(x,t,\lambda))_+, \quad V(x,t,\lambda) = -(\lambda^k\xi_p K\xi_p^{-1}(x,t,\lambda))_+, \tag{5}$$

where the subscript $+$ means the polynomial part of the corresponding expression.

The next steps are as follows.

First, apply Mikhailov reduction group G_R [6] on the solution $\xi_p(x,t,\lambda)$ of the RHP and on $\mathscr{Q}(x,t,\lambda)$. In order that the RHP be compatible with G_R we request, that the contour Γ is invariant with respect to G_R. The same should hold true also for the x and t-dependencies of the sewing functions $G_{sp}(x,t,\lambda)$. We will also search for additional reductions on $\mathscr{Q}(x,t,\lambda)$.

Second, the solution of the RHP is directly related to the fundamental analytic solution $\chi_p(x,t,\lambda) = \xi_p(x,t,\lambda)e^{-\lambda^k(Jx+Kt)}$ of L and M. In terms of $\chi_p(x,t,\lambda)$ we can introduce the kernel of the resolvent of L in the corresponding Ω_p and using the contour integration method, derive the completeness relation for the FAS of L.

Third, use the Wronskian relation of L to analyze the mapping $\mathscr{F}$ from the potentials of L to the set of sewing functions $G_{sp}(x,t,\lambda)$ that determine the scattering data of L. Thus one can prove that the inverse scattering method is a generalization of the Fourier transform.

References

[1] S. Novikov, S. Manakov, L. Pitaevskii, V. Zakharov. *Theory of Solitons: The Inverse Scattering Method*, Plenum, Consultants Bureau, New York (1984).

[2] V. S. Gerdjikov. *Generalised Fourier transforms for the soliton equations. Gauge covariant formulation.* Inverse Problems **2,** n. 1, 51–74, (1986).

[3] V. S. Gerdjikov, G. Vilasi, A. B. Yanovski. *Integrable Hamiltonian Hierarchies. Spectral and Geometric Methods* Lecture Notes in Physics **748**, Springer Verlag, Berlin, Heidelberg, New York (2008). ISBN: 978-3-540-77054-1.

[4] V. S. Gerdjikov. Riemann-Hilbert Problems with canonical normalization and families of commuting operators. Pliska Stud. Math. Bulgar. **21**, 201–216 (2012); **arXiv:1204.2928v1 [nlin.SI]**.

[5] L. A. Dickey. Soliton equations and Hamiltonian systems. World scientific, (2003).

[6] A. V. Mikhailov. *The Reduction Problem and the Inverse Scattering Problem*, Physica D **3D** (1981) 73-117.

Trajectory Divergence Measures

Jordan Genoff

Let a trajectory in the real vector space $\mathbb{R}^n$ be the totally ordered subset $\mathbf{S} = \{\vec{s}\}$, which is the path of a moving point and generated by a vector function $\vec{s_c}(t) : \mathbb{R} \to \mathbb{R}^n$ of time t in the continuous case, or by a vector function $\vec{s_d}(i) : \mathbb{Z} \to \mathbb{R}^n$ of step i in the discrete case. A trajectory evolves only if the function argument changes monotonically. In most practical applications the argument takes values in a finite interval – for the continuous case $t \in \mathbb{R} : t \in [t_0, t_0 + \tau]$, where $t_0 \geq 0$ is the initial moment and $\tau > 0$ is the finite duration, or in the discrete case $i \in \mathbb{Z} : i \in [1, N]$, where $N \geq 1$ is the finite number of steps.

When applied to trajectories, the concept of divergence is about the way an evolving trajectory is getting away from something – another evolving trajectory or a fixed point in space. Motivated entirely by the requirements of a specific computer simulation results' analysis, this paper presents several divergence measures for the discrete case trajectories only. In order to simplify notation, the general discrete case vector function $\vec{s_d}(i)$ will be denoted just $\vec{s}(i)$, or if a subscript is present, it will refer to a certain trajectory, as in $\mathbf{S}_s = \{\vec{s_s}(i) \mid i \in [1, N_s]\}$.

Two things about every proposed measure should be clarified in the beginning: 1) each one is trajectory-pairwise and its result is a real scalar – $D(\mathbf{S}_u, \mathbf{S}_w) : \mathbf{S}_u \times \mathbf{S}_w \to \mathbb{R}$; 2) every one requires that $N_u = N_w$, which is extremely constraining, but fortunately can be overcome by preprocessing the original $\mathbf{S}_u$ and $\mathbf{S}_w$ with dynamic time warping (DTW) without changing their paths, and thus obtaining $\mathbf{S}'_u = \{\vec{s'_u}(i) \mid i \in [1, N'_u]\}$ and $\mathbf{S}'_w = \{\vec{s'_w}(i) \mid i \in [1, N'_w]\}$, where $N'_u = N'_w \geq max(N_u, N_w)$, and then calculating $D(\mathbf{S}'_u, \mathbf{S}'_w)$ instead of $D(\mathbf{S}_u, \mathbf{S}_w)$.

Every proposed measure is assessed towards how appropriate it is for solving each of the following problems: 1) Given two trajectory pairs $\{\mathbf{S}_u, \mathbf{S}_{w_u}\}$ and $\{\mathbf{S}_v, \mathbf{S}_{w_v}\}$ with generally $N'_u = N'_{w_u} \neq N'_v = N'_{w_v}$ after the DTW phase, it should be possible by calculating $D(\mathbf{S}'_u, \mathbf{S}'_{w_u})$ and $D(\mathbf{S}'_v, \mathbf{S}'_{w_v})$ to estimate which original pair is more divergent than the other one; 2) Based on the setting of problem 1 and assuming $\mathbf{S}_w \equiv \mathbf{S}_{w_u} \equiv \mathbf{S}_{w_v}$ with $N'_u = N'_v = N'_w \geq max(N_u, N_v, N_w)$ after the DTW phase, it should be possible by calculating $D(\mathbf{S}'_u, \mathbf{S}'_w)$ and $D(\mathbf{S}'_v, \mathbf{S}'_w)$ to estimate which one of $\mathbf{S}_u$ and $\mathbf{S}_v$ is more divergent from $\mathbf{S}_w$ than the other one; 3) Based on the setting of problem 1 and assuming $\vec{s_{w_u}}(i) = \vec{s_u}(1), \forall i \in [1, N_{w_u} = N_u]$ and $\vec{s_{w_v}}(i) = \vec{s_v}(1), \forall i \in [1, N_{w_v} = N_v]$, without DTW phase it should be possible by calculating $D(\mathbf{S}_u, \mathbf{S}_{w_u})$ and $D(\mathbf{S}_v, \mathbf{S}_{w_v})$ to estimate how much divergent is each trajectory regarding its initial point and which one is more divergent than the other.

All proposed measures are calculated by accumulating some partial divergence at each step. Depending on the partial divergence estimation technique, they can be divided in two groups: distance based (kinematics grounded) – they rely, each one in some way, on $\| \vec{s_u}(i) - \vec{s_w}(i) \|$ and $\| \vec{s_u}(i+1) - \vec{s_w}(i+1) \|$; and "stretch" based (dynamics grounded), which try to extract the "forces" that make trajectories diverge – they utilize in some way $((\vec{s_u}(i+1) - \vec{s_u}(i)) \cdot (\vec{s_u}(i) - \vec{s_w}(i))) / \| \vec{s_u}(i) - \vec{s_w}(i) \|$ and $((\vec{s_w}(i+1) - \vec{s_w}(i)) \cdot (\vec{s_u}(i) - \vec{s_w}(i))) / \| \vec{s_u}(i) - \vec{s_w}(i) \|$, and as this may not be enough, then both $((\vec{s_u}(i+1) - \vec{s_u}(i)) \cdot (\vec{s_u}(i+1) - \vec{s_w}(i+1))) / \| \vec{s_u}(i+1) - \vec{s_w}(i+1) \|$ and $((\vec{s_w}(i+1) - \vec{s_w}(i)) \cdot (\vec{s_u}(i+1) - \vec{s_w}(i+1))) / \| \vec{s_u}(i+1) - \vec{s_w}(i+1) \|$, too. Partial divergence accumulation is done in a Minkowski distance-like manner, which partitions all mea-

sures in three other groups, according to p: p is even; p is odd and partial divergence absolute value is used; p is odd and partial divergence value is used as is. Most measures produce their results in the closed interval $[0, 1]$, but some, specifically intended to solve problem 3, do not obey this. All measures are designed to be invariant to congruent and similarity transformations.

A thorough experimental investigation of all formulated measures on boundary and nominal case trajectory pairs is done, in order to rate them as most applicable to solve the above stated problems. Future developments will consider the continuous case for only those measures, which will prove most effective in practice.

2D CT Data Reconstruction from Radiographic Images, Generated by Scanners with Static 1D Detectors

Péter Balázs, Stanislav Harizanov

In industrial Computed Tomography (CT) a three-dimensional digitization of a scanned physical object is generated, using a series of two-dimensional radiographic images. The gray-scale pixel intensity for each of the planar images is proportional to the corresponding X-ray amount that penetrates through the object along a given direction and is captured by a flat panel detector. In processes, where images are obtained by counting particles, Poisson noise occurs and is typically the dominant noise component. Poisson noise is non-additive and generates a non-structured noise in the final 3D reconstruction that cannot be theoretically treated.

This paper is devoted to scanners, using one-dimensional static detectors. In this setup, the object moves with a constant speed and the two-dimensional radiographic images are generated via "gluing" row data together. Since the number of image rows n_1 is usually high and the scanned object is thinner than the detector size, we can analyze in detail the scanner noise characteristics as certain columns of the radiographic image (the ones of pure background information) correspond to n_1 different measurements of the same X-ray quantity. We perform such statistical analysis and propose an efficient numerical algorithm for 2D noise removal, adapted to the noise specifics.

The most general model for mixed Poisson-Gaussian noise in CT assumes

$$\mathbf{f} \sim \alpha P(\alpha^{-1}\mathbf{u}) + \mathcal{N}(\mu, \sigma^2),$$

where $\mathbf{f}$ is a 2D radiographic image, $\mathbf{u}$ is the true noise-free data, α is scaling parameter, μ is the mean of the Gaussian component, and σ is its standard deviation. Those three parameters should depend only on the acquisition device and should be uncorrelated to the spatial position of the detector entry. Assuming that Poisson and Gaussian noise components are realization of independent random variables, we conclude that

$$E(\mathbf{f}) = \mathbf{u} + \mu; \qquad Var(\mathbf{f}) = \alpha\mathbf{u} + \sigma^2 = \alpha E(\mathbf{f}) + \underbrace{\sigma^2 - \alpha\mu}_{\beta}$$

Thus, one can apply the Generalized Anscombe Transform

$$T_G(\mathbf{f}) = \frac{2}{\alpha}\sqrt{\alpha\mathbf{f} + \frac{3}{8}\alpha^2 + \sigma^2 - \alpha\mu} = \frac{2}{\alpha}\sqrt{\alpha\mathbf{f} + \frac{3}{8}\alpha^2 + \beta},$$

which is a Variance Stabilizing Transformation (VST) and transforms the mixed noise into a purely Gaussian one with zero mean and unit variance. The parameters α and β can be numerically estimated via Least-Squares fit of (part) of the static background information. More precisely, denote by $\mathbf{I}$ an a priori fixed set of detector entries. For each $i \in \mathbf{I}$ compute its sample mean and variance via

$$\hat{\mu}_i = \frac{1}{n_1}\sum_{j=1}^{n_1}\mathbf{f}_{ji}; \qquad \hat{v}_i = \frac{1}{n_1 - 1}\sum_{j=1}^{n_1}(\mathbf{f}_{ji} - \hat{\mu}_i)^2.$$

Then solve the overdetermined system of linear equations

$$\alpha\hat{\mu} + \beta\mathbf{1} = \hat{\mathbf{v}}$$

in the Least-Squares sense, i.e., consider the 2×2 system

$$\left(\begin{array}{cc} \langle \hat{\mu}, \mathbf{1} \rangle & \langle \mathbf{1}, \mathbf{1} \rangle \\ \langle \hat{\mu}, \hat{\mu} \rangle & \langle \mathbf{1}, \hat{\mu} \rangle \end{array} \right) \left(\begin{array}{c} \alpha \\ \beta \end{array} \right) = \left(\begin{array}{c} \langle \hat{\mathbf{v}}, \mathbf{1} \rangle \\ \langle \hat{\mathbf{v}}, \hat{\mu} \rangle \end{array} \right).$$

For noise removal, we follow the constraint Total Variation (TV) minimization model

$$\underset{u \in [0,v]^N}{\arg\min} \, \| \, |\nabla u| \, \|_1 \quad \text{subject to} \quad \|T_G(u) - T_G(\mathbf{f})\|_2^2 \le N, \tag{1}$$

where N is the image size, v – its maximal gray-scale intensity (either 255 for 8-bit bitmap images, or 65535 for 16-bit bitmap images), and ∇ – the discrete gradient operator with Dirichlet boundary conditions, based on forward finite differences. A modified version of the numerical algorithm proposed in [1] can be used for efficiently solving (1).

The proposed theoretical framework has been tested on real industrial CT data, generated by the *3D Tire Scanner* of *GriffSoft* (`https://www.griffsoft.hu/tartalom/ /222255/3d_abroncs_szkenner`). First, static images were studied for detailed analysis of the noise (each row of the image is a chronological realization of the same noise-free input, as no motion is applied during the scanning process). Once the noise parameters had been estimated, various tires were scanned and the proposed numerical algorithm was executed on the generated radiographic images. The quality of the data visually and quantitatively improved.

References

[1] S. Harizanov, J. C. Pesquet, and G. Steidl. Epigraphical Projection for Solving Least Squares Anscombe Transformed Constrained Optimization Problems. In *Scale-Space and Variational Methods in Computer Vision (SSVM 2013)*, A. Kuijper et al., (eds.), LNCS 7893, 125–136, Springer-Verlag: Berlin, 2013.

Comparison analysis on two numerical solvers for fractional Laplace problems

Stanislav Harizanov, Svetozar Margenov

The interest in fractional diffusion models is motivated by fractional calculus and its numerous applications related to anomalous diffusion, e.g., underground flow, diffusion in fractal domains, dynamics of protein molecules, and heat conduction with memory, to name just a few. Other possible applications of very active development are in the area of image processing and stochastic PDEs. For instance, problems with fractional power of graph Laplacians appear in image segmentation.

In this experimental paper we compare the performance of two numerical solvers [1] and [2] for the fractional Laplace problem

$$(-\Delta)^{\alpha}\mathbf{u} = \mathbf{f}, \qquad \Omega = [0,1]^d, \quad d = 1,2,$$

with homogeneous Dirichlet boundary conditions. On a uniform grid with mesh-size $h = 1/(N+1)$, the discrete 3-point stencil approximation of $-\Delta$ in 1D has the form $\mathbb{A} = h^{-2}tridiag(-1,2,-1)$, while in 2D we work with the discrete 5-point stencil approximation

$$\mathbb{A} = h^{-2}tridiag\left(-I_N, \mathbb{A}_{1,1}, -I_N\right), \quad \mathbb{A}_{1,1} = tridiag(-1,4,-1).$$

For $(-\Delta)^{\alpha}$ we consider the corresponding discrete approximation $\mathbb{A}^{\alpha}$.

Both numerical solvers involve a positive combination of evaluations of $(t_iI+\mathbb{A})^{-1}\mathbf{f}$, with $t_i \geq 0$ and their accuracy increases with the number of summands. The origin of t_i however differs for the two approaches. In [1] $\{t_i\}_1^k$ are related to the nodes of an exponentially convergent k-quadrature rule for evaluating

$$\frac{2\sin(\pi\alpha)}{\pi} \int_0^{\infty} t^{2\alpha-1} \left(I + t^2\mathbb{A}\right)^{-1} dt,$$

while in [2] $t_0 = 0$ and $\{t_i\}_1^k$ are the poles of the (k,k)-best uniform rational approximation (BURA) for $t^{1-\alpha}$ in $[0,1]$.
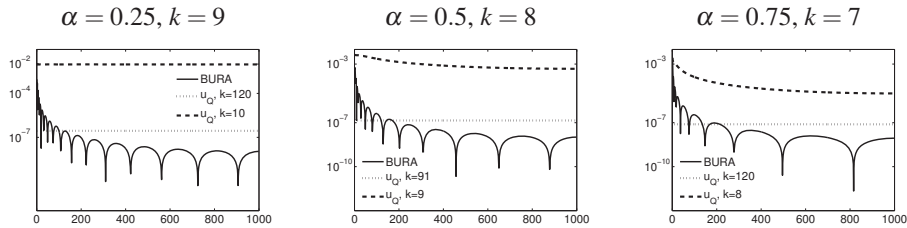
Figure 1: 1D ℓ_2-Relative error analysis over the eigenvectors of $\mathbb{A}$ ($h = 10^{-3}$)

In 1D we know explicitly the eigenvalues and the eigenvectors of $\mathbb{A}$, so we can compute the exact solution $\mathbf{u}_e$ of the problem. Thus, we can evaluate the true ℓ_2 relative error $\|\mathbf{u} -$

Solver	$\alpha = 0.25, k = 9$		$\alpha = 0.50, k = 8$		$\alpha = 0.75, k = 7$	
	ℓ_2-error	ℓ_∞-error	ℓ_2-error	ℓ_∞-error	ℓ_2-error	ℓ_∞-error
u_{BURA}	2.689e-4	5.551e-4	2.411e-4	6.322e-4	5.215e-4	1.190e-3
u_Q	9.375e-3	9.568e-3	4.008e-3	4.093e-3	1.500e-3	1.823e-3

Table 1: Comparison of 2D relative errors in ℓ_2 and ℓ_∞ norms for the checkerboard function, $h = 2^{-11}$. As a reference solution we use u_Q with $k = \{120, 91, 120\}$

$\mathbf{u}_e\|_2/\|\mathbf{f}\|_2$ for both solvers if we let $\mathbf{f}$ run over all eigenvectors. For standard discretization step $h = 10^{-3}$ the errors are illustrated on Fig. 1. We choose $\alpha = \{0.25, 0.50, 0.75\}$ and apart from k-solutions we investigate 120-quadrature solutions $\mathbf{u}_Q$ ($\alpha = \{0.25, 0.75\}$) and 91-quadrature solutions $\mathbf{u}_Q$ ($\alpha = 0.5$), which theoretically guarantee errors of order 10^{-7}. We observe that the accuracy of the BURA solver exceeds the one of the quadrature rule with the same computational complexity, and except for the low spectrum of $\mathbb{A}$ is comparable to the one of the benchmark (see Fig. 1). Only for $\alpha = 0.75$ and the first eigenvector of $\mathbb{A}$ we have similar ℓ_2 errors for $\mathbf{u}_{BURA}$ and $\mathbf{u}_Q$ of magnitude $\approx 3 \cdot 10^{-3}$.

$$\alpha = 0.25, k = 9 \qquad \alpha = 0.5, k = 8 \qquad \alpha = 0.75, k = 7$$
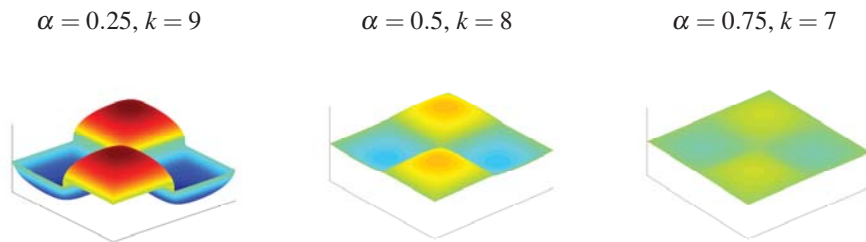
Figure 2: BURA-approximation of $\mathbb{A}^{-\alpha}\mathbf{f}$ for the checkerboard function $\mathbf{f}$ ($h = 2^{-11}$)

In 2D we compare the two solvers on the checkerboard function, that is 1 in $[0, 0.5]^2 \times [0.5, 1]^2$, and -1 elsewhere in the unit square. The higher accuracy of $\mathbf{u}_{BURA}$ with respect to $\mathbf{u}_Q$ for fixed k is again confirmed. Additionally, we observe that the ℓ_∞ relative error behaves similarly to the ℓ_2 one, although there is no theoretical estimate available for the former.

References

[1] A. Bonito, J. Pasciak. Numerical approximation of fractional powers of elliptic operators. *Mathematics of Computation* 84(295), 2083–2110, 2015.

[2] S. Harizanov, R. Lazarov, S. Margenov, P. Marinov, Y. Vutov. Optimal solvers for linear systems with fractional powers of sparse SPD matrices. submitted, posted as arXiv:1612.04846v1 (December 2016)

Improved Cranial Sutures Visualization via Digital Image Processing

Stanislav Harizanov, Silviya Nikolova, Diana Toneva, Ivan Georgiev

Reliable non-destructive evaluation of the calcified tissues in each of the three calvarial layers is an active research topic with huge practical importance. Micro-computed tomography (μCT) is a highly accurate such tool for both qualitative and quantitative analysis that generates clean, high-resolution images. However, μCT is entirely inapplicable *in vivo*. Thus, one works with Medical CT, instead. Here, resolution is quite low (typically around $0.5mm$ in x and y direction, and not less than $0.3mm$ in the z direction). As a result, the generated tomograms (a single slice from the 3D CT volume reconstruction) are not as detailed as needed. In this paper we investigate the possibility to extract meaningful information about the structure of the cranial sutures from both a single tomogram and the whole 3D reconstruction of medical CT data, generated for diagnostic purpose.

It is well-known that the dominant noise component in CT scanning is the Poisson one, which, unlike the Gaussian case, cannot be attacked with standard linear filters. The presence of noise significantly decreases the quality of the result and the reliability of its analysis. On top of that, medical data is typically not row when given for analysis but artificially blurred via convolution with a Gaussian kernel. Such a procedure reduces the noise level, but in the same time decreases the contrast along the image edges. Thus, useful information about the sutures shape and properties is lost.

We propose and study a different approach, based on penalized total variation (TV) minimization

$$\bar{\mathbf{u}} = \underset{u \in [0,v]^N}{\arg\min} \| \, |\nabla u| \, \|_1 + \lambda DF(Hu, H\mathbf{f}),$$

where $\mathbf{f} \in [0,v]^N$ is the input (gray-scale!) CT data, N is the image size, $H \in \mathbb{R}^{n \times N}$ is the degradation (blur) operator, $\nabla \in \mathbb{R}^{N \times 2N}$ is the discrete gradient operator, and DF is a convex function, measuring data fidelity. The model depends on two parameters - the standard deviation σ of the Gaussian kernel and the penalizer λ, which plays a balancing role between regularization and data fidelity. We conduct various numerical experiments on both single tomograms and the whole 3D volume reconstruction for different choices of σ and λ. For properly tuned parameters, we observe improved visual quality of the skull sutures, allowing for more accurate classification of their characteristics.

Parallelization of a finite difference algorithm for solving systems of 2D Sine-Gordon equations

Ivan Hristov, Radoslava Hristova, Stefka Dimova

We consider systems of 2D perturbed Sine-Gordon equations :

$$S(\varphi_{tt} + \alpha\varphi_t + \sin\varphi - \gamma) = \Delta\varphi, \quad (x,y) \in \Omega \subset R^2 \tag{1}$$

Here Δ is the 2D Laplace operator. Ω is a given rectangular domain in R^2. S is the $N_{eq} \times N_{eq}$ cyclic tridiagonal matrix:

$$S = \begin{pmatrix} 1 & s & 0 & . & 0 & s \\ s & 1 & s & 0 & . & 0 \\ . & . & . & . & . & . \\ . & . & . & . & . & . \\ 0 & . & 0 & s & 1 & s \\ s & . & 0 & 0 & s & 1 \end{pmatrix}$$

N_{eq} is the number of equations. The unknown is the column vector $\varphi(x,y,t) = (\varphi_1, ..., \varphi_{N_{eq}})^T$. Neumann boundary conditions are posed:

$$\frac{\partial\varphi}{\partial\overrightarrow{n}}|\partial\Omega = 0 \tag{2}$$

A finite difference algorithm for solving the above systems is proposed. Since we have a quasi 3D model in space, in some cases computational domain size may be pretty large and also a very long time integration is needed. Therefore we need serious computational resources to simulate the above system in reasonable time.

The goal of the work is to make a parallel program that use effectively as much resource from a given CPU-cluster as needed, depending on the computational domain size of the problem. We propose and realize a fully hybrid MPI+OpenMP parallelization strategy, i.e. one MPI process per cluster node and OpenMP threads inside the node. Three levels of parallelism are explored: MPI processes at the outer level, OpenMP threads at the middle level and SIMD parallelism (vectorization) at the inner level.

We test our program on the CPU-platform of the IICT-BAS cluster and on the HybriLIT cluster, JINR, Dubna, Russia. A very good performance scalability is observed.

As a simulation example we give the standing wave solutions corresponding to the so called cavity resonances in Intrinsic Josephson junctions.

Biomolecular studies in coarse-grain approaches: the good, the bad, and the beautiful

N. Ilieva, P. Petkov, E. Lilkova, R. Marinova, A.J. Niemi, J. He, and L. Litov

In biomolecular modelling, computational challenges are based on the system size on the one side and the characteristic time scales on the other. The necessity for time steps of the order of a few femtoseconds and the nature of the underlying biophysical and biochemical processes poses severe limitations on the time span of the investigated phenomena.
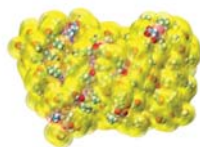
Figure 1: Interlaced all-atom and coarse-grain representations of system A.

We discuss the possibilities for efficient acceleration of biomolecular simulations by appropriate system representations. In particular, we analyze the applicability of coarse-grain (CG) approaches in the investigations of conformation-dependent processes, to put forward the advantages of synergistic protocols from complementary approaches that are able to extend the boundaries of the underlying physical modelling techniques. We exemplify our considerations by three particular cases: a study of tagging influence on human interferon gamma binding affinity within MARTINI coarse-grain approach (system A), peptide-membrane interaction of the antimicrobial peptide indolicidine with a model bacterial membrane (system B), and protein folding simulations of the villin headpiece VHP35 based on a coarsening of its generalised backbone bond angles (system C). For all three systems, CG results were controlled by a full or partial coverage with all-atom simulations.

Table 2: Performance comparison for AA and CG simulatons of systems A and B.

	simulation type	number of particles	box dimensions [Å^3]	nodes/ MPI processes/ threads per MPI	performance [ns/day]
A	AA	147557	186x89x89	12/16/2	52.7
A	CG	33812	174x174x174	16/16/2	1756.16
B	AA	170697	107x107x146	4/4/6 + 1 GPU per node	31.44
B	CG	34152	114x114x140	4/1/24 + 1 GPU per node	786.003

By reducing the level of detail in the representation of the system (Fig. 1), CG approaches do overcome the time- and length- scale restrictions in biomolecular modelling. This allows for a 25- to 35-fold increase of the computed evolution per day, both on homogeneous and hybrid architectures (see Table 1). The loss of resolution, however, has to be carefully weighted. CG-MD simulations allowed in the case of system A to reveal the blocking mechanism of the
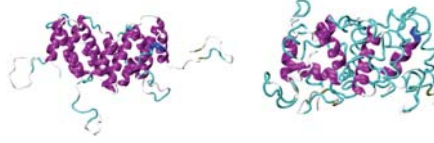
Figure 2: The final state of system A after all-atom MD simulation (left) and the corresponding CG-MD f̶ [obscured] l-at̶ [obscured]
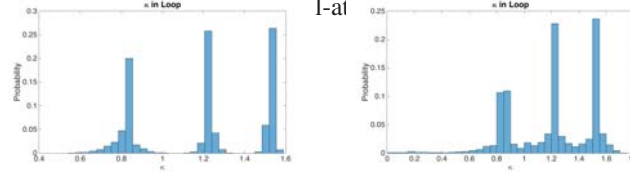
Figure 3: Distribution of generalised bond angles of the first loop in VHP35 (PDB ID 1yrf) for a backfolding (left) and a misfolding (right) MC-MD generated evolution.

tagg-peptide in the process of hIFNγ binding to its receptor, and in the case of system B, to observe impact dynamics some 50 times faster. However, as seen in Fig. 2, a conformation analysis might be misleading.

In our multistage MC-MD approach to protein folding dynamics, generalised bond angles κ_i are subjected to a coarsening procedure through the defining them tangent vectors of the Frenet frames in the positions of the α carbons of the protein backbone

$$t_i^{(p)} \rightarrow \frac{t_{2j-1}^{(p)} + t_{2j}^{(p)}}{|t_{2j-1}^{(p)} + t_{2j}^{(p)}|} = t_j^{(p+1)}$$

$$\cos \kappa_i^{(p)} = t_{i+1}^{(p)} t_i^{(p)} \rightarrow t_{j+1}^{(p+1)} t_j^{(p+1)} = \cos \kappa_j^{(p+1)}$$

In this approach, the protein structure is recovered with an accuracy of about 1 Å and fine conformation changes can be detected and analysed, as seen from the bond angle distribution of a backfolding and a misfolding conformations, obtained through it (Fig. 3). Thus, the generalised bond angle based coarsening proves itself not only a computationally efficient but also highly sensitive complementary approach in investigating protein dynamics and interactions.

Machine learning approach for classification task

Ivan Ivanov

In this article we are going to build a model, that filters as many of the inaccurate prices as possible and as little accurate prices as possible, based on the provided data for prices displayed on Skyscanner and later booked by their users. The definition of "accurate" comes form data about Skyscanner user's perception of the problem and is set to USD +4.0, meaning that if a booked price is more than $4 above the price we displayed, it is considered inaccurate.

We use the Random Forest algorithm in python with the help of python machine learning library - Scikit-Learn. Scikit-learn provides a rich environment with state of the art implementations of many well known machine learning algorithms, while maintaining an easy to use interface tightly integrated with the Python language.

Data set

The Skyscanner data is a csv file, which contains 942896 rows and 15 columns with different data types and we need of data preprocessing. As other classifiers, forest classifiers have to be fitted with two arrays: a sparse or dense array X of size [n samples, n features] holding the training samples, and an array Y of size [n samples] holding the target values (class labels) for the training samples. We set a new column with labels - 0 for difference in price under $4 and 1 for difference in price over $4.

Most implementations of random forest (and many other machine learning algorithms) that accept categorical inputs are either just automating the encoding of categorical features for us or using a method that becomes computationally intractable for large numbers of categories. For the first iteration we apply LabelEncoder() from scikit-learn on all dataset. The LabelEncoder is a way to encode class levels and also fill missing values with zeros. In the next step we apply MinMaxScaler() from scikit-learn to scale features to lie between a given minimum and maximum value, that the maximum absolute value of each feature is scaled to unit size. The motivation to use this scaling include robustness to very small standard deviations of features and preserving zero entries in sparse data.

Classification results

After preprocessing, we split the data on a train set, test set and validation set in ratio 80:20:20. Now we train the model using the training set, predict output with test set and check accuracy. We get ACC = 0.9086589705110325.

Using a pretrained model and validation set we obtain:
$Accuracy = Number\_Of\_Acurate\_Data\_Points/Total\_Data\_Points =$
$((TP + TN)/\#testset) = 0.908459890553$

Validation set : 188 584 samples.
TP – 4 667
TN – 166 654
FN – 16 604
FP – 659
Positive – price, that should be remove from Skyscanner site.
Negative – price, that remain on Skyscanner site.

Variable importance results

Variable importances from our model:

```
0 : Search_Date
1 : Search_Time
2 : Skyscanner_Price_USD
3 : Country
4 : Partner
5 : Airline
6 : Origin
7 : Destination
8 : Departure_Date
9 : Departure_Time
10 : Original_Currency
11 : Passengers_Adult
12 : Passengers_Child
13 : Passengers_Baby
```
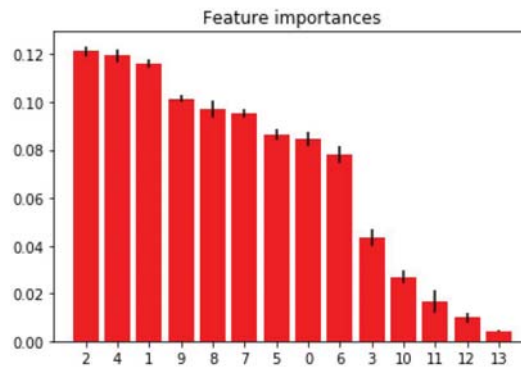

Conclusion

In this work, Random Forests were successfully applied to the feature selection to classify Skyscanner flight prices. Future work will be a feature engineering to improve the Random Forests results.

References

[1] https://en.wikipedia.org/wiki/Machine_learning#cite_note-1

[2] http://scikit-learn.org/dev/_downloads/scikit-learn-docs.pdf

[3] https://www.kdnuggets.com/2016/08/10-algorithms-machine-learning-engineers.html

[4] V. F. Rodriguez-Galiano, B. Ghimire, J. Rogan, M. Chica-Olmo, and J. P. Rigol-Sanchez, Anassessment of the effectiveness of a Random Forest classifier for land-cover classification, ISPRS J. Photogramm. vol. 67, no. 1, pp. 93-104, Jan. 2012.

[5] A. Liaw and M. Wiener. Classification and regression by randomForest. R News, 2(3), 2002.

[6] L. Breiman, Random Forests, Machine Learning, 45(1), 5-32, 2001.

Performing a moving average operation with an FPGA device

Vladimir Ivanov , Todor Stoilov

A large amount of the practical applications in information technologies dealing with the problems of development system for processing enormous data stream in real time mode. A typical representative of such a practical application is the "moving average" (MA) procedure used to "smooth out" data.

The starting point for the practical solution of this task in real-time mode is the use of Field Programmable Gate Array (FPGA) devices. The projects realized with this class of utensils can be modified, adopt different dimensions and structures. As a result of this they prove to be significantly more promising for a product, both from the positions of current and future changes in it, as well as from its rapid exit on the market. The large logic resources and built-in hardware features of FPGAs allow for the realization of the MA device in various modifications.

In the work, it is shown that the classic description of the MA procedure can be treated as a FIR filter with single weighting coefficients which. In a large number of averaged data, the realization based on the conventional FPGA structure becomes not profitable.

Taking this fact into account, in the article, the MA procedure is presented with a recursive digital filter. This approach offers a more compact solution for its implementation in an FPGA device, based on the use of a DSP48A1 block and several shift registers. The work presents a result of practical modeling, designing and simulation of the MA device. It is implemented in the Web Pack environment under the conditions closest to the real ones. In the work are presented the block diagram of the device and its location in the resources of the FPGA chip XC6SLX4 of the series Spartan6. An estimate of the dynamic range and performance of the developed device was also made and given.

In general, the article contributes to lowering the high degree of abstractness of digital signal processing by means of the modern FPGA element base, which often hinders rethinking the intuitive concepts of classical analog technology, and allows the use of the presented material for other applications.

Exact traveling wave solutions of a class of reaction-diffusion equations

Ivan P. Jordanov, Nikolay K. Vitanov

Reaction-diffusion equations have many applications for describing different kinds of processes in physics, chemistry, biology, etc. Traveling wave solutions of these equations are of special interest as they describe the motion of wave fronts or the motion of boundary between two different states existing in the studied system. In this presentation we apply the modified method of simplest equation [1-3] for obtaining exact traveling solutions of nonlinear reaction-diffusion PDEs from the following class

$$\tau \rho_{tt} + \rho_t = D\rho_{xx} + \sum_{i=1}^{n} \alpha_n \rho^n \tag{1}$$

where n is a natural number and α_n are parameters. A balance equation is obtained that regulates the kind of the used simplest equation and the length of the solution. The characteristics of the the obtained traveling wave solution are visualized and discussed. The connection of the traveling wave solutions of the model equations to processes of the modelled systems is discussed too.

References

[1] Nikolay K. Vitanov, Zlatinka I. Dimitrova, Holger Kantz. Modified method of simplest equation and its application to nonlinear PDEs. *Applied Mathematics and Computation* **216**, 2587 - 2595 (2010).

[2] Nikolay K. Vitanov. Modified method of simplest equation: Powerful tool for obtaining exact and approximate traveling-wave solutions of nonlinear PDEs. *Communications in Nonlinear Science and Numerical Simulation* **16**, 1176 - 1185 (2011).

[3] Nikolay K. Vitanov, Zlatinka I. Dimitrova, Kaloyan N. Vitanov. Modified method of simplest equation for obtaining exact analytical solutions of nonlinear partial differential equations: further development of the methodology with applications. *Applied Mathematics and Computation* **269**, 363 - 378 (2015).

The 6-th CompMath Competition

S. Bouyuklieva S. Kapralov

CompMath is a competition among university and high school students in the field of Computer Mathematics. It serves as an excellent teaching tool for using computer algebra systems for solving mathematical problems. Math education, and more generally the STEM education are of great importance to society. At the same time it is apparent that contemporary math education is in a deep crisis and that it requires a major shift from teaching manual calculation techniques towards computer-based solution techniques.

The 6-th National Student Olympiad in Computer Mathematics (CompMath-2017) was held in October 27-29, 2017 at Technical University - Varna, Bulgaria. Students from 10 universities participated in the competition. They competed in two groups - group A for students studying Mathematics, Informatics or Computer Science (52 contestants), and group B for students from Technical Universities (36 contestants).

The students had to solve 30 math problems in 4 hours using a computer algebra system like Maple, Mathematica, Maxima, MATLAB or MuPad. These problems were divided into two parts - 20 easier and 10 harder problems, and the participants had two hours to solve the problems for each of both parts. For the first time there were participants working in Python. These were three students from the American University in Blagoevgrad.

The hardest problem for the students in group A was the following:

Find the canonical form of the curve c: $2x^2 + 6xy + 5y^2 + 2x - 4y + 24 = 0$ *and plot its graph (using the obtained canonical equation). Compute the area of the figure bounded by the curve c.*

Actually, this is a standard problem from Analytic Geometry and it is not difficult to solve by hand. But the students were confused how to solve it with a mathematical software.

For the students in group B the hardest problem was:

Find the global extrema of the function $f(x,y) = x^2 + 4y^2$ *on the closed area determined by the inequalities* $x^2 + (y+1)^2 \leq 4$ *and* $-1 \leq y \leq x+1$.

This problem was given to the students in group A, too. The solution needs deeper mathematical background and therefore the students with such knowledge worked more successfully on it.

Other interesting problems that made it hard for most participants were the following:

Find the largest integer a, such that the area of the figure bounded by the curve $y = e^{x^2}$ *and the lines* $x = 0$, $x = a$, $y = 0$, *is smaller than* 2017^{2017}.

Calculate the volume of the region enclosed by the surfaces $x^2 + y^2 + z^2 = 1$, $x^2 + y^2 - z = 0$.

The function $\pi(n) : N \rightarrow N$ gives the number of primes less than or equal to n.
In 2010 Pierre Dusart proved that

$\pi(n) > \frac{n}{ln(n)-1}$ for any $x \geq N_1$ and $\pi(n) < \frac{n}{ln(n)-1,1}$ for any $x > N_2$.
Find the integers N_1 and N_2, if it is known that $4000 \leq N_1 \leq 6000$ *and* $55000 \leq N_2 \leq 65000$.

In accordance with the practice of the international high school student science olimpiads 50% of participants won medals. Five students in group A and four students in group B won gold medals.

More information about the competition could be found on the bilingual website: http://www.compmath.eu/. All problems from prior years are published there.

The next edition of CompMath will be organized in the fourth weekend of October 2018 at Pamporovo mountain resort and will be hosted by Plovdiv University.

The organizers hope to have successful cooperation with BGSIAM in promoting this unique competition on the world stage.

Generalized nets: a new approach to model a hashtag linguistic network on Twitter

K.G. Kapanova, S. Fidanova

In the last few years the micro-blogging platform Twitter has played a significant role in the communication of civil uprisings, political events or natural disasters. One of the reasons is the adoption of the hashtag, which represents a short word or phrase that follows the hash sign (#). These semantic elements captured the topics behind the tweets and allowed the information flow to bypass traditional social network structure. The hashtags provide a way for users to embed metadata in their posts achieving several important communicative functions: they can indicate the specific semantic domain of the post, link the post to an existing topic, or provide a range of complex meanings in social media texts. In this paper, Generalized nets are applied as a tool to model the structural characteristics of a hashtag linguistic network through which possible communities of interests emerge, and to investigate the information propagation patterns resulting from the uncoordinated actions of users in the underlying semantic hashtag space. Generalized nets (GN) are extensions of the Petri nets by providing functional and topological aspects unavailable in Petri nets. The study of hashtag networks from a generalized nets perspective enables us to investigate in a deeper manner each element of the GN, substituting it with another, more detailed network in order to be examined in depth. The result is an improved understanding of topological connections of the data and the ability to dynamically add new details to expand the network and as a result discover underlying structural complexities unable to be discovered through traditional network analysis tool due to the prohibitive computational cost. Analysis is performed on a collection of Tweets and results are presented.

Testing performance and scalability of the hybrid MPI-2/OpenMP model on the heterogeneous supercomputer "Avitohol"

Vyara Koleva-Efremova

Over the last years, high performance computer systems called supercomputers is used to solve complex tasks arising in different research areas of physics, medicine and meteorology. Following the Moore's law, the power of supercomputers is doubled each 18 months until now, and this tendency is expected to remain in force with the development of new GPGPU devices and co-processors. The usage of such extreme-scale parallel computer systems for scientific computations is highly relevant, due to two main reasons - the price/performance and speed of development (time to market). The high performance of supercomputers depends not only on the hardware architecture model, but also on the different open source libraries as MPI and OpenMP standards for parallel implementation.

In this paper we compare the performance and scalability of the unified MPI-2 and corresponding a hybrid model of MPI-2 with OpenMP routines for two different benchmark tests using the heterogenius HPC system - Avitohol [3]. It consists of 150 computational servers HP SL250s Gen8, equipped with two Intel Xeon E5-2650v2 CPUs and two Intel Xeon Phi 7120P co-processors, 64 GB RAM, two 500 GB hard drives, interconnected with non-blocking FDR InfiniBand running at 56 Gbp/s line speed. The total number of cores is 20700 and the total RAM is 9600 GB, respectively [1,2]. In this study we investigated the communication time of our benchmark tests when we use uniform MPI (shared and two-sided) implementation versus OpenMP and MPI-2 implementations.

The two benchmarks used communication patterns ranging from light to heavy communication traffic: point-to-point message passing and shared memory programming. The synchronization mechanisms are necessary when using one-side communication and overhead an implementation. Each implementation was run using 16 bytes, 32 Kbytes and 1Mbyte messages. Tests were run with 2, 4, 8, 16, 32, 64, 128, 256, 320 and 640 MPI processes using two MPI processes per node (one MPI process per socket). We chose 320 and 640 processes because these numbers correspond to using one and two cabinets respectively in this setup. The tests were also run on Intel Xeon Phi co-processors and the results were compared.

In summary, the benchmark applications written using MPI shared programming have an execution time that is smaller than MPI two-sided implementation. The non-blocking (asynchronous) two-sided communication has significant advantage over the blocking MPI two-sided communication. MPI shared programming has a memory consumption that is considerably less than MPI two-sided programming and comparable to the OpenMP memory consumption. Both MPI and OpenMP are easy to use. MPI-2 has limitations overcome in version 3.0. The hybrid OpenMP+MPI model provides better memory consumption compared with the uniform model. The two levels of parallelism provides better load balancing but creates conditions for many topology and threads-safety problems.

The obtained results are helpful in cases we need to run specific applications on a heterogeneous HPC system - Avitohol and to choose the best approach for parallel implementation.

References

[1] A. Radenski, T. Gurov, et al., Big Data Techniques, Systems, Applications, and Platforms: Case Studies from Academia, in: "Annals of Computer Science and Information Systems", Volume 8,"Proceedings of the 2016 Federated Conference on Computer Science and Information Systems" FedCSIS'16, pp. 883 - 888, Sep, 2016. DOI: http://dx.doi.org/10.15439/978-83-60810-90-3.

[2] E. Atanassov, T. Gurov, A. Karaivanova, S. Ivanovska, M. Durchova and D. Dimitrov, On the Parallelization Approaches for Intel MIC Architecture, Citation: AIP Conf. Proc. 1773, 070001 (2016), DOI: http://dx.doi.org/10.1063/1.4964983.

[3] ACDC at IICT-BAS, http://www.hpc.acad.bg/ .

Methods of life expectancy analysis of Bulgarian population in the period 2001 - 2015

Tsvetanka Kovacheva

Abstract. In the present paper the dynamics of the mortality and the life expectancy of the population in Bulgaria for the period 2001-2015, depending on age and gender, are analyzed. On the basis of given probabilities of dying and life expectancies , the life tables for so-called conditional generation for ages 100 years and over were constructed. Two types of life tables were calculated by using an established methodology: complete with one year age intervals and abridged with 5-year age intervals. The data were taken from the National Statistical Institute. Initially, from the complete life tables, the child mortality was examined for a 15-year period to determine its trend. The dynamics of mortality and the life expectancy for males and females in the country were presented graphically and were compared. The ratio of male and female deaths to all thirteen life tables was calculated.

The life expectation was used as convenient summary measure of the mortality of a population. The changes in life expectancies were used for summarizing mortality changes of a population. However, the connection between life expectation and mortality rate at a particular age is not a particularly simple one. Different approaches for investigation and explanation change of life expectancy in terms of mortality change have been proposed using discrete or continuous methods. In the paper were discussed the methods of Arriaga, Pollard and United Nation for decomposition of the difference between two life expectancies over time. These three methods are compared using two groups of data on abridged life tables for Bulgarian males and females for the first sub-period 2001-2003 and the last sub-period 2013-2015.

References

[1] Arriaga, E. Measuring and Explaining the Change in Life Expectancies, Demography 21: 83-96, 1984

[2] Life tables, Republic Bulgaria, National Statistical Institute, www.nsi.bg

[3] Pollard, J. H. On the Decomposition of Changes in Expectation of Life and Differentials in Life Expectancy, Demography 25 (2): 265-276, 1988

[4] United Nations. World population trends, population development interrelations and population policies, v.1, Population trends, ST/ESA/Ser.A/93, New York: United Nations, Department of International Economic and Social Affairs: 193, 1985

Adaptive Moving Mesh Central-Upwind Schemes for the Saint-Venant Systems of Shallow Water Equations

Alexander Kurganov

It is well-known that solutions of the Saint-Venant system of shallow water equations may be nonsmooth and thus they are understood in the weak sense. Therefore, finite-volume methods, which are based on integral formulation of hyperbolic system of PDEs, are appropriate numerical tool for computing this type of solutions. In the framework of finite-volume Godunov-type schemes, the solution, which is assumed to be available at a certain time level, is first reconstructed (approximated) globally in space using a piecewise polynomial function and then evolved in time to the next time level by solving the studied hyperbolic system subject to piecewise polynomial initial data. The evolution step is performed by integrating the system over a space-time control volume. Depending on the way the control volumes are selected, Godunov-type schemes can be split into two classes: upwind and central. To design upwind schemes, the numerical fluxes along the boundaries of the control volumes are to be computed by solving (generalized) Riemann problems, arising at each cell interface at the reconstruction step. Central schemes are much simpler since in the central framework, the fluxes are evaluated away from discontinuities and thus no (generalized) Riemann problems need to be solved. Therefore, central schemes can be applied as a black-box solver to a variety of hyperbolic systems. However, compared to their upwind counterparts, central schemes contain larger amount of numerical diffusion, which may oversmear nonsmooth solutions. To reduce the numerical diffusion present in central schemes, we have developed central-upwind schemes, which I will present in the first part of my talk.

Application of the central-upwind to the Saint-Venant system requires development of several techniques, which will guarantee that a delicate balance between the flux and source terms is respected and that the positivity of the computed water depth is not disrupted. To achieve these goals we have developed a well-balanced positivity preserving central-upwind schemes, which I will present in the second part of my talk. In the last part of my talk, I will show how one can achieve even higher resolution as well as to improve the efficiency of central-upwind schemes by developing new adaptive moving mesh (AMM) central-upwind schemes on both adaptive one-dimensional nonuniform grids and two-dimensional structured quadrilateral meshes. After evolving the solutions to the new time level, the grid points are redistributed according to the moving mesh PDE, and then the solution is projected onto the new mesh in a conservative manner. In order to preserve the positivity of the computed water depth, several measures are taken. First, we either make sure that the reconstructed values of the water surface stay above the corresponding values of the bottom topography or use the positivity preserving reconstructions for the water depth. Second, we use a draining time-step technique to ensure that the water depth remains positive during the evolution step. Third, we propose special corrections of the solution projection step in (almost) dry areas. I will demonstrate the ability of the proposed AMM central-upwind schemes to significantly improve quality of the computed solution in a number of numerical examples.

On the group analysis of differential equations on the group $SL(2,R)$

Georgi Kostadinov, Hristo Melemov

The aim of this paper is to analyse the existence of polynomial solutions of the initial value problem defined by the linear differential equation.

$$\dot{g}(t) = A(t)g(t), \ \ g(0) = E \tag{1}$$

where $g(t) \in G = SL(2,R)$, the special linear group and $A(t)$ is a polynomial matrix bellowing to the algebra $sl(2,R)$. Obviously we have $A(t) = dR_{g(t)}^{-1}\dot{g}(t)$, where $R_{g(t)}$ denotes the right translation in G. We choose a basis of $sl(2,R)$, [2]:

$$H = \begin{pmatrix} 1 & 0 \\ 0 & -1 \end{pmatrix}, X = \begin{pmatrix} 0 & 1 \\ 0 & 0 \end{pmatrix}, Y = \begin{pmatrix} 0 & 0 \\ 1 & 0 \end{pmatrix}$$

with commutators $[X,Y] = H$, $[H,X] = 2X$, $[H,Y] = -2Y$. To the nilpotent elements X and Y correspond 1-parameter subgroups:

$$\exp tX = \begin{pmatrix} 1 & t \\ 0 & 1 \end{pmatrix} \ and \ \exp tY = \begin{pmatrix} 1 & 0 \\ t & 1 \end{pmatrix}.$$

As well known they satisfy the equations:

$$\dot{g}(t) = \begin{pmatrix} 0 & 1 \\ 0 & 0 \end{pmatrix} g(t) \ and \ \dot{g}(t) = \begin{pmatrix} 0 & 0 \\ 1 & 0 \end{pmatrix} g(t).$$

The curve $g(t) = \exp tX \exp tY$ satisfies the equation $\dot{g}(t) = B(t)g(t)$. Here $B(t) = X + Ad(\exp tX)Y$. More generally the curve

$$g(t) = \exp tX_1 \exp tX_2 \cdots \exp tX_n \tag{2}$$

is a solution of the equation $\dot{g}(t) = A(t)g(t)$ with

$$A(t) = X_1 + Ad(\exp tX_1)X_2 + \cdots + Ad(\exp tX_1 \exp tX_2 \cdots \exp tX_{n-1})X_n. \tag{3}$$

Here X_i, $i = 1, 2 \cdots, n$ stand for the nilpotent elements X and Y of $sl(2,R)$. Let us have $A(t) = \begin{pmatrix} a(t) & b(t) \\ c(t) & -a(t) \end{pmatrix}$, where $a(t) = a_0 + a_1 t + \cdots + a_k t^k$,
$b(t) = b_0 + b_1 t + \cdots + b_l t^l$ and $c(t) = c_0 + c_1 t + \cdots + c_m t^m$. We identify this polynomial matrix with the curve in $sl(2,R)$, $\alpha(t) = a(t)H + b(t)X + c(t)Y = (a(t), b(t), c(t))$. By using the adjoint representation of the group $G = SL(2,R)$ in the algebra $sl(2,R)$ we may state the following necessary conditions for the existence of polynomial solutions of the form (2).

Theorem 0.1 *If the system (1) admits a polynomial solution (2), the following conditions are fulfilled:*

(i) *The leading terms of $A(t)$ satisfy the equality:* $\frac{a_k t^k}{c_m t^m} = \frac{b_l t^l}{-a_k t^k}$,

(ii) *The initial value of the curve $\alpha(t)$ is $\alpha(0) = b_0 X$ or $\alpha(0) = c_0 Y$,*

(iii) *The derivatives of the vector function $\alpha : R \to sl(2,R)$ satisfy at $t = 0$ $\alpha^{(j)} = (*,0,0)$ or $\alpha^{(j)} = (0,*,*)$, where $j = 1, \cdots, n$. The stars stand for real numbers.*

Thus we get a recurrent way for constructing explicitly polynomial solutions.

One may consider as well k-th order "tangent" vectors of $sl(2,R)$: $\tilde{X} = \begin{pmatrix} 0 & t^k \\ 0 & 0 \end{pmatrix}$ and $\tilde{Y} = \begin{pmatrix} 0 & 0 \\ t^k & 0 \end{pmatrix}$. In this case we get polynomial curves of the form

$\tilde{g}(t) = \exp t^{k_1} X_1 \exp t^{k_2} X_2 \cdots \exp t^{k_n} X_n$, where k_i, $i = 1,2\cdots,n$ are positive integers, but the Theorem is not true for the corresponding system. This situation requires an additional analysis.

Comment. In the theory of homogeneous spaces $M = G/H$, H is the isotropic subgroup. The vector fields on M corresponding to the action of H vanish at the initial point. Here we have $\tilde{X}(0) = \vec{0}$, $\tilde{Y}(0) = \vec{0}$ and by that there arise changes in the behaviour of the corresponding curve $\tilde{\alpha}(t)$. Many authors have been studied this problems [1], [3].

References

[1] Turbiner A., *Lie-algebraic approach to the theory of polynomial solutions*, Comm. Math. Phys., CPT-92/P.2679

[2] Vilenkin N., *Special function and representation group theory*, Moskow Nauka 1965.

[3] Blanes S., *Optimization of Lie group methods for differential equations*, Elsevier Science B.V.2002.

On Digital Watermarking for Audio Signals

Hristo Kostadinov, Nikolai Manev

We investigate the possibility of embedding robust against compression watermark in musical audio files. The method used for embedding is a combination of key-dependable dither modulation [1] and "Haar" wavelet. Examples of using this method for MP3 compression have been already proposed, see [2]. Our goal is to investigate systematically this approach to the embedding in audio files.

To specify parameters of both transformations we need a good knowledge of statistical characteristics of the process of compression. The compression itself can be considered as a communication channel whose statistical characteristics are sensitive to the compressed musical genre. We study only the most used compression methods, MP3 and Advance Audio Coding (AAC), and collect statistical data for different musical genres.

The next step is to analyze how changes are spread under inverse "Haar" wavelet transformation. This knowledge together with statistic of compression channel are important to select the right value for the step of quantizer and dither modulation.

The process of embedding and retrieving the watermark can be regarded as a binary communication channel. We investigate its statistic to give recommendation what error correcting codes to be used.

At the end we analyze the whole process for its embedding capacitate and robustness.

References

[1] B. Chen and G.W. Wornell, Quantization index modulation: A class of provably good methods for digital watermarking and information embedding, IEEE Trans. on Information Theory, vol. 47 no.4, pp. 1423–1443, 2001.

[2] R. Martinez-Noriega, M. Nakano, B. Kurkoski, and K. Yamaguchi, High Payload Audio Watermarking: toward Channel Characterization of MP3 Compression, Journal of Information Hiding and Multimedia Signal Processing, vol. 2, no. 2, 91-107, (2011).

Effcient Numerical Evaluation of Fokas' Transform Solution of the Heat Equation on the Half-Line

Mohamed Lachaab, Peter Turner, Athanassios Fokas

A new method has been recently introduced by Fokas (one of the authors) for solving a large class of partial differential equations (PDEs). The new method (Fokas, 1997 and 2002; Fokas and Sung, 2004; Fokas and Pellouni, 2005; Fokas et al., 2009), which is referred to as the uni ed transform, contains the classical methods as special cases and gives solutions to many PDEs where the classical methods cannot. The key to this method is the global relation which combines specified and unknown values of the solution or its derivatives on the boundary.

This method, however, arises a problem: the transform solution is an infinite contour integral in the complex plane that needs to be evaluated numerically. For the heat equation on the half-line, for example, this method constructs the solution $q(x;t)$ as an integral in the complex plane involving an x-transform of the initial condition and a t-transform of the boundary condition. To evaluate the integral, Flyer-Fokas (2008) and Fokas et al. (2009) deformed and parametrized the contour of integration to a path in the region where the integrand decays exponentially fast for large k, then used the simple trapezoidal rule on a truncated interval directly. However, this truncation method introduces large error when the integrand decays slowly (small x values).

In this paper, we evaluate the integral using a different accurate approach. First, we bound the tail of the integrand using the partition-extrapolation method of Lyness. Second, we estimate the integral on the remaining finite interval using the Romberg integration to an absolute accuracy. Our method improves the truncation estimates of the tail and the solution in general compared to that obtained by the direct truncation method. Also, the Romberg integration uses less function evaluations than that of MATLAB quadl.m subroutine.

A mathematical analysis concerning the effect of step-feeding on performance of constructed wetlands

Konstantinos Liolios, Krassimir Georgiev, Ivan Georgiev

Step-feeding (SF) describes the case when the wastewater is introduced to a Constructed Wetland (CW) at several points along the flow path in a gradational way [1, 2]. The purpose of this alternative feeding technique for the CW, is to increase its performance [3, 4]. In the present study this problem is analyzed mathematically. First, the P-TIS (P Tanks In Series) methodology [1], based on Finite Volume Method (FVM), is used. In this case, the operation of SF in a series of Continuous Stirred-Tank Reactors (CSTR) under steady conditions, by using the volumetric degradation coefficient λ, is analyzed. Then, the SF procedure is mathematically investigated, when the CW is operated like a Plug Flow Reactor (PFR).
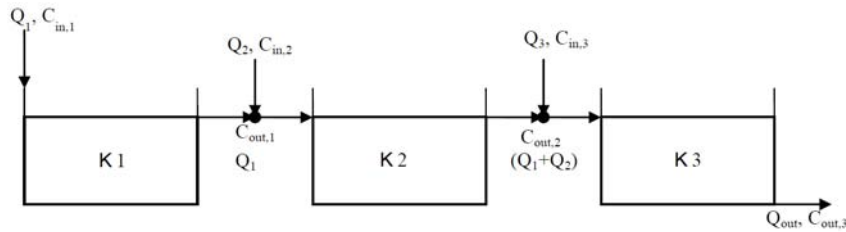
Initially, the TIS (Tanks In Series) methodology [5, 6] is used, where the tank is splitted in three (P = 3) equal cells. This system of CWs is shown in Figure 1. The volume of each cell is:

$$V_1 = V_2 = V_3 = \frac{V_p}{3} \tag{1}$$

The total inflowing wastewater flow rate $Q = Q_{in}$ was distributed in three inflowing points: $x_0 = 0$, $x_1 = 1m$ and $x_2 = 2m$. If x, y, z are the corresponding percentages of Q in each position, when it is: $Q_1 = x \cdot Q$, $Q_2 = y \cdot Q$ and $Q_3 = z \cdot Q$, where x, y, z must fulfil the condition: $x + y + z = 1$.

The concentration of the above system of CWs at the outlet, $C_{out}, 3$, is:

$$C_{out,3} = C_{out} = \frac{C_{in,3}}{1 + (HRT_3 \lambda_3)} \tag{2}$$

where $HRT_3 = V_3/Qin$ is the Hydraulic Residence Time.

For the case that CW is operated without SF, i.e., $x = 1$ and $y = z = 0$, and when λ is equal for all the cells ($\lambda_1 = \lambda_2 = \lambda_3 = \lambda$), the above equation (2) gives the well-known TIS equation [1, 5]:

$$C'_{out,3} = \frac{C}{1 + \left(\frac{\lambda \cdot HRT}{3}\right)^3} \qquad (3)$$

The CWs can be also considered that they operate as Plug Flow Reactors (PFR). For this case, and when λ is equal for all the cells, the concentration $C_{out,3}$ is:

$$C_{out,3} = C \cdot \left[z + y e^{-\lambda \frac{HRT}{x+y}} + x e^{-\lambda HRT \frac{2x+y}{x(x+y)}} \right] e^{-\lambda HRT} \qquad (4)$$

The above equation (4) is equal with the PFR equation [1, 5], when CW is operated without SF, for $HRT = V_p / Q_{in}$:

$$C'_{out,3} = C \cdot e^{-\lambda HRT} \qquad (5)$$

Thus, for both cases (when the system of CWs is operated as CSTR and as PRF), the purpose of the present study is to check mathematically if SF improves the performance of the CW. It means, by using a numerical example, to compare if the value of $C_{out,3}$ is smaller than $C'_{out,3}$.

References

[1] Kadlec, R.H., Wallace, S., Treatment Wetlands. CRC Press, Boca Raton, USA (2009)

[2] Saeed, T., Sun, G., A review on nitrogen and organics removal mechanisms in subsurface flow constructed wetlands: Dependency on environmental parameters, operating conditions and supporting media. J. Environ. Manage. 112, 429-448 (2012)

[3] Liolios, K.A., Moutsopoulos, K.N., Tsihrintzis, V.A., Modelling alternative feeding techniques in HSF constructed wetlands. Environ. Proces. 3(1), 47-63 (2016)

[4] Meng, P., Pei, H., Hu, W., Shao, Y., Li, Z., How to increase microbial degradation in constructed wetlands: Influencing factors and improvement measures. Bioresource Techn. 157, 316-326 (2014)

[5] Tchobanoglous, G., Schroeder, E., Water Quality. Addison-Wesley Pub. Comp., Amsterdam. (1987)

[6] Chen, S., Wang, G.T., Xue, S.K., Modeling BOD removal in constructed wetlands with mixing cell method. J. Environ. Eng. 125(1), 64-71 (1999)

Influence of glycosilation on human interferon gamma dynamics – setting up the stage

E. Lilkova, N. Ilieva, P. Petkov, L. Litov

Interferon-γ (IFNγ) is a pleiotropic cytokine, which plays a key role in regulating the initiation and the course of immunopathologic processes. It exerts its effects by a high affinity interaction with a species-specific receptor complex (IFNγR).

Natural human IFNγ (hIFNγ) is a glycoprotein with two N-glycosilation sites in each monomer chain – ASN^{25} and ASN^{97}, which are independently and differentially glycosilated. Two fractions are naturally isolated with molecular weights of 20 kDa and 25 kDa. The lower weighted fraction is monoglycosilated, i.e. glycan chains are attached only to one of the ASN residues, whereas the second fraction is glycosilated at both sites. The chemical composition of the predominantly occurring oligosaccharide sequences (41% of the glycans at ASN^{25} and 34% of the glycans at ASN^{97}) in the native hIFNγ are shown in Figure 1.
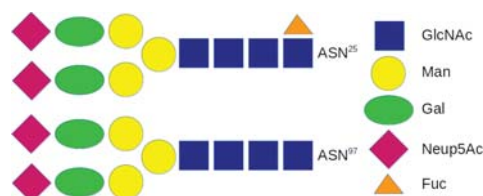
Figure 1: Chemical composition of the most often isolated oligosaccharide chains of native hIFNγ.

Although glycosilation is not crucial for hIFNγ activity, it has been shown that N-linked oligosaccharides promote the folding and dimerization of the recombinant cytokine. N-glycosilation also protects hIFNγ from proteolytic degradation, thus influencing its circulatory half-life.

Recently, for studying the properties of hIFNγ and its mutants, a technology has been developed for expressing them labeled with a specific tag peptide added to the N-terminus of the cytokine. A somewhat unexpected observation was that if the labeled hIFNγ was glycosilated, the marker could not be removed. Each of the complex glycan residues increases the molecular weight of hIFNγ by approximately 3-4 kDa, so they are relatively large. It was therefore suggested that the carbohydrates probably cover much of the surface of the cytokine and thus completely or partially protect the tag peptide from proteases. This hypothesis cannot be tested experimentally, which necessitates its *in silico* verification using molecular dynamics (MD) simulations. For this purpose, the structures of mono- and diglycosilated hIFNγ need to be modelled.

Here, we report the development of model structures of monoglycosilated at either ASN^{25} or ASN^{97} or diglycosilated full-length native and N-terminally tagged hIFNγ dimers. The glycosilation anchors were modelled using the GlyProt server (`http://www.glycosciences.de/modeling/glyprot/php/main.php`). The glycan

structures, corresponding to Figure 1, were then build using the Glycan Reader of the molecular dynamics simulation setup server CHARMM-GUI (`http://www.charmm-gui.org/?doc=input/glycan`). The structures were parameterized using the CHARMM 36 force field and then equilibrated. A sample initial structure of diglycosilated full-length hIFNγ is shown in Figure 2. The production MD simulations were performed with the package GROMACS 2016.1. We report preliminary results on the interaction of the carbohydrate chains with the receptor-binding sites in the cytokine and with its flexible highly positively charged C-termini. The obtained models will be used in studies of the influence of hIFNγ glycosilation on receptor binding.
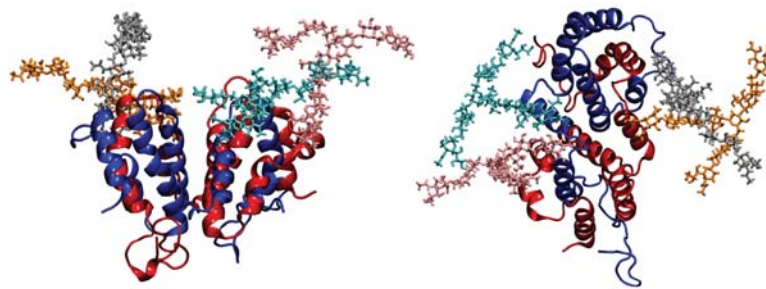
Figure 2: Front and top projections of the developed model structure of diglycosilated full-length hIFNγ. The two protein monomers are depicted in ribbons in red and blue respectively. The glycans are depicted in licorice as follows: ASN_A^{25} – silver, ASN_A^{97} – cyan, ASN_B^{25} – pink, and ASN_B^{97} – orange.

Initial calibration of MEMS accelerometers, used for measuring inclination and toolface

Galina S. Lyutskanova-Zhekova, Tihomir B. Ivanov, Spasimir I. Nonev

Microelectromechanical systems (MEMS) sensors have wide range of applications. Amongst their advantages are their miniature size and low-cost. A significant requirement for their applicability, however, is to account for different errors, deterministic as well as stochastic, that are present in the work of the device. In particular, we are interested in accounting for sensor's offset and scaling errors. There exist different approaches for correcting those errors (see, e.g., [1, 2] and the references therein). Most of them are connected with the idea of comparing the sensors' outputs, when the device is standing still, with the vector of gravitational acceleration.

One particular application of accelerometer sensors is determining orientation in space. In the present work, we propose a new objective function, whose minimization gives an estimate of the calibration coefficients. The latter takes into account the specifics of measuring toolface and inclination, in seek of better accuracy, when the device is used for this purpose. To the best of our knowledge, it has not been mentioned in the literature. We propose an algorithm for initial calibration of MEMS sensors, based on the aforementioned objective function. It is described in detail, because, even though, some of the steps are standard from the point of view of a numerical analyst, this could be helpful for an engineer or applied scientist, looking to make a concrete implementation for applied purposes.

On the basis of numerical experiments with sensor data, we compare the accuracy of the proposed algorithm with classical methods. We show that it has an advantage, when sensors are to be used for orientation purposes.

References

[1] P. Aggarwal, Z. Syed, X. Niu, N. El-Sheimy, A standard testing and calibration procedure for low cost MEMS inertial sensors and units, The Journal of Navigation 61 (2008) 323–336.

[2] G. Aydemir, A. Saranli, Characterization and calibration of MEMS inertial sensors for state and parameter estimation applications, Measurement 45 (2012) 1210–1225.

Cluster formation from disordered peptides in water solution: a coarse-grain molecular dynamics approach

R. Marinova, P. Petkov, N. Ilieva, E. Lilkova, L. Litov

The increased resistance of bacteria towards conventional antibiotics imposes a pressing need for the development of alternative therapies. Antimicrobial peptides (AMPs) are an important part of the innate immune defense system of many organisms. Their broad-spectrum antimicrobial activity against bacteria, viruses and fungi bears a high potential to combat microbial infections.

The objective of this study is to scrutinize the very initial – or even preparatory – stages of the antimicrobial mode of action of one particular class of AMPs — the disordered antimicrobial peptides. More specifically, we want to find out if these peptides attack their target, the bacterial membrane, individually or after having formed certain larger-scale structures. To this end, we employ a coarse-grain molecular dynamics approach. The sample peptide itself — the indolicidin (IL) — is a promising candidate for future clinical applications because of its activity against Gram-negative and Gram-positive bacteria.
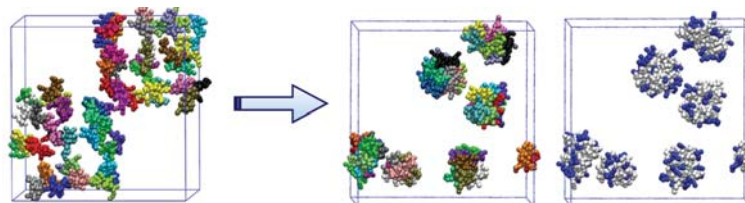
Figure 1: Initial configuration of the system II at concentration of 21.9mM (left) and the configuration of the system at the end of simulation (right). The different IL monomers are presented in different. Clusters are formed with a central hydrophobic core (white) and charged amino acids at the edges (blue).

We performed coarse-grain molecular dynamics (CG-MD) simulations of IL solutions with different concentrations (10.9 mM, 21.9 mM, 26.6 mM, and 99.4 mM, referred to systems I to IV, respectively) at T=310K. For studying the temperature dependence of the observed processes, system III was also simulated at a higher temperature, T=330 K. The influence of the finite simulation box and of the periodic boundary conditions was investigated through a series of simulations at a constant concentration (26.6mM) and variable simulation box volumes.

The results show saturation of the solution at concentration of at 99.4mM. Under a certain threshold value (between 99.4mM and 26.6mM) IL aggregates in globular amphipathic structures with a central hydrophobic core and positively charged regions near to the peptide's termini (Figure 1). A summary of the results of the different simulations is given in Table 1. In system III, ten clusters were formed at T=310K, whereas at T=330K their number increased to 13 (Figure 2). At both temperatures, however, the largest cluster contained 23

Initial Box size [nm × nm × nm]	Number of peptides	$V^{-1/3}$ [nm^{-3}]	Average cluster size [#peptides]	Maximal cluster size [#peptides]
$15 \times 15 \times 7.5$	27	0.084	9	13
$15 \times 15 \times 15$	54	0.067	9	11
$15 \times 15 \times 30$	108	0.053	11	23

Table 3: Aggregation parameters in different simulation box volume.

peptide units. In both cases the topology of the self-assembled structures remains unchanged, with a similar cluster-formation pattern.
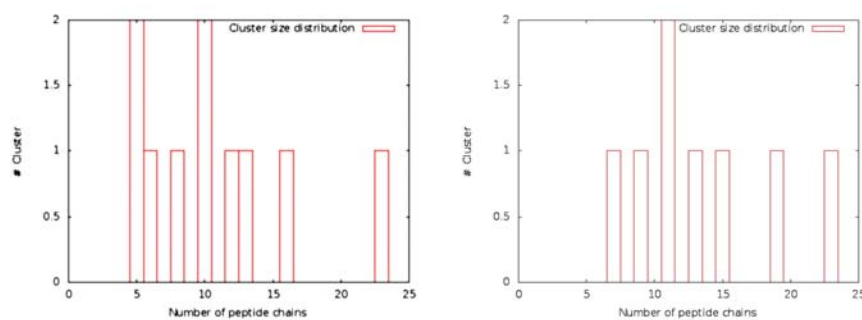
Figure 2: Cluster size distribution for system III at T=310K (left panel) and T=330K (right panel).

Our results reveal the proper understanding of the AMPs dynamics prior to the impact with the bacterial membrane as an indispensable element in the analysis of their antimicrobial action. The knowledge on the aggregation process, the structure and size of the clusters so-formed may pave the way for designing of peptides with predefined properties and thus, novel antibacterials to overcome the threatening bacterial multi-drug resistance.

A functional expansion and a new set of rapidly convergent series involving zeta values

Lubomir Markov

The origin of the interesting subject of series involving values of the Riemann zeta function may be traced back to a classical paper by Euler [5], where he establishes, in equivalent form, the following representation for $\zeta(3)$:

$$\zeta(3) = \frac{\pi^2}{7} - \frac{4\pi^2}{7} \sum_{k=1}^{\infty} \frac{\zeta(2k)}{(2k+1)(2k+2)2^{2k}}.$$

This series has since been rediscovered several times, most recently by Ewell [6], who derives it following a method of Choe [3], which method is itself a modified Euler argument (see [1]). It is clear that the above sum converges much more rapidly than the defining series of $\zeta(3) = \sum_{n=1}^{\infty} \frac{1}{n^3}$. In recent years there has been a substantial amount of research regarding such rapidly convergent representations, and a large number of series have been evaluated in closed form, in terms of virtually all important constants of mathematics. (See primarily Srivastava's expository article [8] and the book by Srivastava and Choi [9], but also the papers [2], [4], [11].) As a rather suggestive example of the progress achieved, one may note the formula

$$\zeta(3) = -\frac{120\pi^2}{1573} \sum_{k=0}^{\infty} \frac{8576k^2 + 24286k + 17283}{(2k+1)(2k+2)(2k+3)(2k+4)(2k+5)(2k+6)(2k+7)} \frac{\zeta(2k)}{2^{2k}},$$

discovered recently by Srivastava and Tsumura [10, equation (4.6)]. The purpose of the present work is to investigate series representations (believed to be new) of certain special functions related to polylogarithms (see [7]). These representations are then used to obtain new rapidly convergent series involving zeta values. We also indicate in passing another proof of Euler's famous result:

$$\zeta(2) = \sum_{n=1}^{\infty} \frac{1}{n^2} = \frac{\pi^2}{6}.$$

References

[1] R. Ayoub, Euler and the Zeta function, *Amer. Math. Monthly* **81** (1974), 1067-1086

[2] M.-P. Chen and H.M. Srivastava, Some families of series representations for the Riemann $\zeta(3)$, *Result. Math.* **33** (1998), 179-197

[3] R. Choe, An elementary proof of $\sum_{n=1}^{\infty} \frac{1}{n^2} = \frac{\pi^2}{6}$, *Amer. Math. Monthly* **94** (1987), 662-663

[4] A. Dąbrowski, A note on the values of the Riemann Zeta Function at positive odd integers, *Nieuw Arch. Wisk.* **14** (1996), 199-207

[5] L. Euler, Exercitationes analyticae, *Novi Comment. Acad. Sci. Imp. Petropol.* **17** (1772), 173-204

[6] J. Ewell, A new series representation for $\zeta(3)$, *Amer. Math. Monthly* **97** (1990), 219-220

[7] L. Lewin, *Polylogarithms and Associated Functions*, Elsevier (North-Holland), New York/London/Amsterdam, 1981

[8] H.M. Srivastava, Some properties and results involving the zeta and associated functions, *Funct. Anal. Approx. Comput.* **7** (2015), 89-133

[9] H.M. Srivastava and J. Choi, *Series Associated with the Zeta and Related Functions*, Kluwer Academic Publishers, Dordrecht/Boston/London, 2001

[10] H.M. Srivastava and H. Tsumura, Inductive construction of rapidly convergent series representations for $\zeta(2n+1)$, *Internat. J. Comput. Math.* **80** (2003), 1161-1173

[11] N.-Y. Zhang and K.S. Williams, Some series representations of $\zeta(2n+1)$, *Rocky Mountain J. Math.* **23** (1993), 1581-1591

High-order Artificial Compressibility for the Navier-Stokes Equations

J.L. Guermond and P.D. Minev

We introduce a generalization of the artificial compressibility method for approximation of the incompressible Navier-Stokes equations. It allows for the construction of schemes of any order in time that require the solution of a fixed number of vectorial parabolic problems, depending only on the desired order of the scheme. These problems have a condition number that scales like $O(\delta t h^2)$, with δt being the time step and h being the spatial grid size. This approach has several advantages in comparison to the traditional pro- jection schemes widely used for the unsteady Navier-Stokes equations. First, it allows for the construction of schemes of any order for both, the veloc- ity and pressure, while the best proven accuracy achievable by a projection scheme is second order on the velocity and 3/2 order on the pressure. Second, the projection schemes require the solution of an elliptic scalar problem for the pressure that has a condition number $O(h^2)$, in addition to a vectorial parabolic problem for the velocity. This makes them slower if iterative meth- ods are used to solve the linear systems, and less efficient if implemented on a parallel cluster. Further, we will discuss the approach for solving the linear system resulting from the momentum equation and more particularly, we will present an unconditionally stable split version of the scheme that treats the mixed derivatives in the grad div operator fully explicitly. Finally, we will present a one step version of the high order scheme that opens the door to time step control algorithms. The accuracy and stability of the resulting schemes will be demonstrated on examples with manufactured solutions.

Digital Security Future Objectives Foresight Modelling and Analytical Assessment

Zlatogor Minchev

Understanding the digital future security challenges, risks, gaps and divides is a comprehensive task that requires combination of both expert knowledge with suitable modelling and assessment techniques implementation [1]. The current study gives an exploration approach, using a hypergraph modelling that is further used for risks [2] and extended to utilities problem space assessment and representation. This provides a working context for understanding the problem from both static and dynamic perspective, resulting a final system effectiveness assessment. Risk and utility are represented as multiparameter probabilistic functions, similar to [2] and their practical results implementation is illustrated via an experimental software environment - I-SCIP - EA. The results provide a system of systems interpretation that gives a hypergraph arcs dynamics model coping, that could be implemented into the transition cycles discretisation, assuming a multitrajectory stochastic problem meeting [3]. Finally, some foresight digital security modelling examples, concerning future web technologies development security foresight expectations are presented, producing digital transformation [1], [3] supportive interpretation with the outlined ideas.

References

[1] Minchev, Z. Analytical Challenges to Modern Digital Transformation. In Proceedings of Education and Research in the Information Society, 10th Edition, pp. 38-47, 2017, ISSN:1314-0752, DOI:10.13140/RG.2.2.31856.05125

[2] Minchev, Z., Dukov, G., Boyadzhiev, D., Mateev, P. In Future Cyber Attacks Modelling and Forecasting. ESGI 120 Problems and Final Reports Book, pp. 77-86, 2016, DOI:10.13140/RG.2.2.10132.30088

[3] Minchev, Z. Security Challenges to Digital Ecosystems Dynamic Transformation. In Proceedings of BISEC 2017, October 18, Belgrade Metropolitan University, pp. 6-10, 2017, ISBN:978-86-89755-14-5, DOI:10.13140/RG.2.2.32354.84160

Simulated Annealing Method for Metal Nanoparticle Structures Optimization

Vladimir Myasnichenko, Nikolay Sdobnyakov, Leoneed Kirilov, Rossen Mikhov, Stefka Fidanova

The goal of this work is to develop an efficient method for search a metal and bimetal nanoparticle structures with the lowest possible potential energy. In the search for the most effective particle structures, the problem of global optimization arises. In computational complexity theory, global optimization problems are NP-hard, meaning that they cannot be solved in polynomial time. The randomly searching through all possible minima on a potential energy surface is impractical. Instead, computer algorithms were written to search for minima that are believed to be close to the global minimum (GM). In other words, the GM was approximated using time-efficient optimization strategies. The difficulty of global optimization of atomic clusters is even greater for nano-alloys, where permutation of unlike atoms likewise leads to many more isomers [1,2]. A comparison between the two search techniques, molecular dynamics and the basin-hopping [3,4] Monte Carlo, has been performed in [5]. It was found that the basin-hopping algorithm is more efficient than a molecular dynamics minimization approach in the investigation of the most stable conformations for metal clusters. Given severe difficulty of finding the GM, the simulated annealing (SA) algorithm was selected as main strategy. At the first step we use the lattice Monte-Carlo method with different lattices. And then we relax the resulting nanoparticle structures at low temperature within molecular dynamics, choosing the one of them as approximation of global minimum. The convergence of a class of Metropolis-type Markov-chain annealing algorithms for global optimization of a smooth function was established in [6]. Metropolis Monte Carlo with SA procedure was used to search for GM configurations (up to 3000 atoms) of transition metal's nanoparticles in [7].

References

[1] Jellinek J., Krissinel E.B. NinAlm alloy clusters: analysis of structural forms and their energy ordering, Chem. Phys. Lett. 1996. Vol. 258, 1-2. P. 283-292.

[2] Lloyd L.D., Johnston R.L., Salhi S., Wilson N.T. Theoretical investigation of isomer stability in platinum-palladium nanoalloy clusters, J. Mater. Chem. 2004. Vol. 14, 11. P. 1691-1704.

[3] Wales D.J., Doye J.P. Global Optimization by Basin-Hopping and the Lowest Energy Structures of Lennard-Jones Clusters Containing up to 110 Atoms: Condensed Matter; Atomic and Molecular Clusters, J. Phys. Chem. A. 1997. Vol. 101, 28. P. 5111-5116.

[4] Wales D.J. Global Optimization of Clusters, Crystals, and Biomolecules, Science. 1999. Vol. 285, 5432. P. 1368-1372.

[5] Sebetci a., Guvenc Z.B. Global minima for free Pt_N clusters (N = 22-56): a comparison between the searches with a molecular dynamics approach and a basin-hopping algorithm, Eur. Phys. J. D. 2004. Vol. 30, 1. P. 71-79.

[6] Gelfand S.B., Mitter S.K. Metropolis-Type Annealing Algorithms for Global Optimization in Rᵈ, SIAM J. Control Optim. 1993. Vol. 31, 1. P. 111-131.

[7] Myshlyavtsev A. V., Stishenko P. V., Svalova A.I. A systematic computational study of the structure crossover and coordination number distribution of metallic nanoparticles, Phys. Chem. Chem. Phys. 2017. Vol. 19, 27. P. 17895-17903.

Gaussian Model Deformation of an Abdominal Aortic Aneurysm Caused by the Interaction between the Wall Elasticity and the Average Blood Pressure

Nikola Nikolov, Sonia Tabakova, Stefan Radev

The initiation and growth of malformations in the abdominal part of the aorta (AA) are some of the reasons for human mortality. This important human organ possesses such mechanical characteristics, which are difficult for in vivo measurements. The work and the state of all other organs and systems keeping the metabolism depend on the optimal function of the aorta. Therefore the in silico (numerical simulations) study of the aortic mechanical behaviour depending on its elastic properties and the blood flow parameters becomes a powerful tool to predict the deviations on its optimal functioning. Such optimal functions are generally expressed by the aortic work in compliance with the heart pulses. That is closely related to the elasticity and geometrical form of the aorta as well as the blood flow parameters, and definitely to the interaction between the two continuous media: fluid and structure. The proper combinations of aortic elasticity and blood flow pressure play an important part in the compliance/stiffness of the cardiovascular system, and the undesirable declinations could even lead to dissections or ruptures.

In the present work, the Fluid Structure Interaction method (FSI of ANSYS software) is applied to model a pulsatile blood flow in a cylindrical elastic tube with a damaged part described by a Gaussian profile. The numerical experiment is performed at Young modulus of 500, 1000 and 1500kPa and average blood pressure in the range of 0 to 20kPa.

Depending on the pulsatile fluid flow (Fig.1), different pulsatile stress strain states are established along the tube length and tube thickness, Fig. 2 and 3. At the combination of the different aortic wall elasticity with different average blood pressure, three basic regimes of the deformation of the Gaussian AAA profile are observed: stably-pulsating deforming regime, Fig. 2 and 3, with constantly pulsating stress and strain in the damaged part of the tube leading to stably pulsating AAA volume around a constant profile in dependence on the initial one; unstably-pulsating reversible deforming regime with increasing pulsating reversible stress and strain in the damaged part leading to pulsating growth of the AAA volume, where it is possible not to reach a rupture of the AAA at a smooth decrease of the average constant blood pressure; unstably-nonpulsating nonreversible deforming regime with non reversible linearly increasing stress and strain in the damaged part leading to a sharp increase of the AAA volume and rupture, where it is not possible to reverse the system in a smooth stable pulsatile regime.

The reported three regimes are observed at Young modulus of 500kPa. Stable deforming regimes are observed with average pressure upto 13.5kPa, while sharp increasing AAA volume and rupture are observed with average pressure of 20kPa. Stable deforming regimes with different profiles of pulsating AAA volumes, Fig. 2, are observed with Young modu-
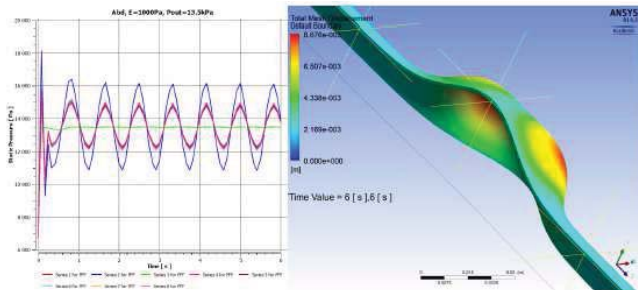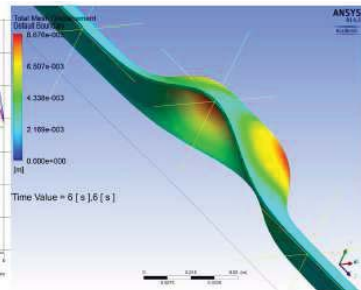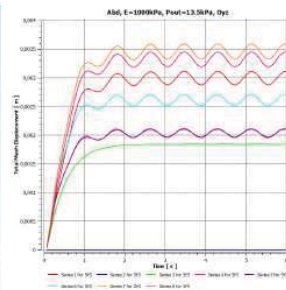
Fig.1   Fig. 2   Fig.3

lus of 1000 and 1500kPa under average blood pressure values in the whole discussed interval.

In the real case, the real forms of the AAA volumes deviate from the observed model forms here, Fig. 2, at least because of the material anisotropy and non-homogeneity in the boundary conditions. The model forms, established here, together with the corresponding stress strain states, boundary conditions and the mechanical characteristics of the tube wall and fluid flow, define a parametrical space in which the clinically measured data determine a subspace optimal to keep the living functions. Correspondent interpretations of the obtained numerical data are available from this point of view.

EM Estimation of the Parameters in Latent Mallows' Models

Nikolay I. Nikolov, Eugenia Stoimenova

A full ranking of N items simply assigns a complete ordering to the items. Any such ranking vector can be viewed as an element π of the permutation group $\mathscr{S}_N$ generated by the first N positive integers. There are various probability methods for modelling rank data. Some models have larger probabilities for rankings that are "close" to a "modal" ranking π_0. One such example is the Mallows' model, given by

$$P_{\theta,\pi_0}(\pi) = e^{\theta d(\pi,\pi_0) - \psi(\theta)} \quad \text{for } \pi \in \mathscr{S}_N, \tag{1}$$

where θ is a real parameter ($\theta \in \mathbb{R}$), $d(\cdot,\cdot)$ is a metric on $\mathscr{S}_N$, π_0 is a fixed ranking and $\psi(\theta)$ is a normalizing constant. When $\theta > 0$, π_0 is a *modal* ranking, for $\theta < 0$, π_0 is an *antimode*, and for $\theta = 0$, P_{θ,π_0} is the uniform distribution. If $d(\cdot,\cdot)$ is right-invariant, then the distribution of $d(\pi,\pi_0)$ for uniformly chosen permutation $\pi \sim Uniform(\mathscr{S}_N)$ does not depend on π_0 and the Mallows' model could be significantly simplified. In this situation, it is easy to show that $\psi(\theta) = \log(N!m(\theta))$, where $m(t)$ is the moment generating function of $d(\pi,\pi_0)$. The special cases, when $d(\cdot,\cdot)$ is Kendall's tau and Spearman's rho, are first investigated by Mallows. Later on, models based on Cayley's distance and Hamming distance are considered by Fligner and Verducci. For all these examples of simple Mallows' model (1), there are explicit maximum likelihood estimates of the unknown parameters θ and π_0.

One effective approach to extend model (1) is to assume that there are K latent groups, $G_1, G_2, \ldots, G_K$ in the population and that the distributions of the rankings within each group can be described by model (1), i.e.

$$P_{\theta_j,\pi_{0,j}}(\pi) = e^{\theta_j d(\pi,\pi_{0,j}) - \psi(\theta_j)}, \quad \pi \in \mathscr{S}_N,$$

where θ_j is a real parameter and $\pi_{0,j}$ is the "modal" ranking in group G_j, for $j = 1, 2, \ldots, K$. Then the overall density for this latent Mallows' model is

$$P_{\vec{\theta},\vec{p},\vec{\pi}_0}(\pi) = \sum_{j=1}^{K} p_j e^{\theta_j d(\pi,\pi_{0,j}) - \psi(\theta_j)}, \quad \pi \in \mathscr{S}_N, \tag{2}$$

for $\vec{\theta} = (\theta_1, \theta_2, \ldots, \theta_K)$, $\vec{\pi}_0 = (\pi_{0,1}, \pi_{0,2}, \ldots, \pi_{0,K})$ and $\vec{p} = (p_1, p_2, \ldots, p_K)$. Since the probability p_j represents the proportion of the population in group G_j, for $j = 1, 2, \ldots, K$, the elements of $\vec{p}$ have to sum up to 1, i.e. $\sum_{j=1}^{K} p_j = 1$.

In this talk we propose an algorithm to find maximum likelihood estimates of the unknown parameters $\vec{\theta}$, $\vec{p}$ and $\vec{\pi}_0$ of model (2) by making use of the EM algorithm. The aim of the algorithm is to find the expected value of the loglikelihood function $\ell(\vec{\theta}, \vec{p}, \vec{\pi}_0, \vec{\pi}, G)$ for given initial approximations of $\vec{\theta}$, $\vec{p}$ and $\vec{\pi}_0$ (*E-step*). This expectation is usually denoted by

$$Q^{(t)}\left(\vec{\theta}, \vec{p}, \vec{\pi}_0, \vec{\pi}\right) = \mathbf{E}_{G|\vec{\theta}^{(t)}, \vec{p}^{(t)}, \vec{\pi}_0^{(t)}, \vec{\pi}}\left[\ell(\vec{\theta}, \vec{p}, \vec{\pi}_0, \vec{\pi}, G)\right]$$

for initial values $\vec{\theta}^{(t)}, \vec{p}^{(t)}$ and $\vec{\pi}_0^{(t)}$. The next step is to maximize $Q^{(t)}\left(\vec{\theta}, \vec{p}, \vec{\pi}_0, \vec{\pi}\right)$ with respect to $\vec{\theta}, \vec{p}$ and $\vec{\pi}_0$ (*M-step*), i.e.

$$\left(\vec{\theta}^{(t+1)}, \vec{p}^{(t+1)}, \vec{\pi}_0^{(t+1)}\right) = \underset{\left(\vec{\theta}, \vec{p}, \vec{\pi}_0\right)}{\operatorname{argmax}} \left\{Q^{(t)}\left(\vec{\theta}, \vec{p}, \vec{\pi}_0, \vec{\pi}\right)\right\}.$$

The obtained maximum likelihood estimators $\vec{\theta}^{(t+1)}, \vec{p}^{(t+1)}$ and $\vec{\pi}_0^{(t+1)}$ are then substituted in the *E-step* for calculating new values of $Q^{(t+1)}\left(\vec{\theta}, \vec{p}, \vec{\pi}_0, \vec{\pi}\right)$ and so on. This procedure continues until some optimal criteria is reached, for example if the change of the likelihood function is relatively small. We illustrate the accuracy of the proposed estimation algorithm with a simulation study.

The derivaties of any polynomial as a linear combination of finite differences with step one

Inna Nikolova

In this paper we represent the derivative of any polynomial as a linear combination of finite differences with step one. The problem appeared in a special representation of orthogonal polynomials. As a corollary we obtain the solution of the following problem: Given a polynomial in the basis $(-x)_k$ represent its derivatives again in the basis $(-x)_k$. There is nothing easier than finding derivatives of a polynomial when it is represented in the basis x^k but when it is represented in the basis $(-x)_k = (-x)(-x+1)(-x+2)\dots(-x+k-1)$ the situation is different. To find some derivative of higher order using the usual approach one needs first to change the basis, moreover the result is again in the basis x^k and one needs to change the basis again. More over there is no closed expression for the derivatives since usually we change the basis step by step. The considered representation allows sticking to the basis $(-x)_k$. We use the following approach. Represent the values of the polynomial in the points $x+k, k=1\dots n$ in terms of the forward finite differences. Then represent the same values in terms of the exact Teylor expansion of the polynomial and thus form a linear system in which the derivatives are considered as unknowns and the finite differences forwards are given. The finite differences from their side are represented in the basis $(-x)_k$. The solution of the linear system is not easy. We find it in terms of the elementary symmetric functions of the first n integers, which are sometimes called Stirling numbers of first kind. However we prefer the notation for the elementary symmetric functions, since during the solution we use elementary functions of several numbers which are not necessarily consecutive integers. The result is

$$p_n(x)^{(j)} = \sum_{l=j}^{n} (-1)^{l-j} \frac{j!}{l!} \sigma_{l-j}(1,2,\dots,l-1)\Delta^l p_n(x)$$

Or

$$p_n(x)^{(j)} = \sum_{l=j}^{n} (-1)^{l-j} \frac{j!}{l!} \begin{bmatrix} l \\ j \end{bmatrix} \Delta^l p_n(x),$$

where by

$$\begin{bmatrix} l \\ j \end{bmatrix}$$

we denote the unsigned Stirling number of first kind.

Exact traveling wave solutions of a generalized Kawahara equation

Elena Nikolova, Zlatinka Dimitrova

We apply the modified method of simplest equation [1-3] for obtaining exact traveling solutions of nonlinear PDEs to a generalized Kawahara equation

$$\mu u^r u_t + \alpha u^n u_x + \beta u^p u_{xxx} - \delta u_{xxxxx} = 0 \tag{1}$$

where r, n, and p are natural numbers and α, β, δ and μ are parameters. Several kinds of ordinary differential equations are used as simplest equations. The obtained kinds of waves are visualized and their properties are studied. We discuss the application of some of the solution for description of nonlinear capillary gravity waves.

References

[1] Nikolay K. Vitanov. Modified method of simplest equation: Powerful tool for obtaining exact and approximate traveling-wave solutions of nonlinear PDEs. *Communications in Nonlinear Science and Numerical Simulation* **16**, 1176 - 1185 (2011).

[2] Nkolay K. Vitanov, Zlatinka I. Dimitrova, Kaloyan N. Vitanov. Modified method of simplest equation for obtaining exact analytical solutions of nonlinear partial differential equations: further development of the methodology with applications. *Applied Mathematics and Computation* **269**, 363 - 378 (2015).

[3] Nikolay K. Vitanov. Application of simplest equations of Bernoulli and Riccati kind for obtaining exact traveling-wave solutions for a class of PDEs with polynomial nonlinearity *Communication in Nonlinear Science and Numerical Simulation* **15**, 2050 - 2060 (2010).

Evolution equation for propagation of blood pressure waves in an artery with an aneurysm: exact solution obtained by the modified method of simplest equation

Elena Nikolova

The theoretical investigation of pulse wave propagation in human arteries has a long history starting from ancient times until today. Over the past decade, however, the scientific eforts have been concentrated on theoretical investigations of nonlinear wave propagation in injured arteries. Evolution equations for propagation of pressure waves in a normal artery and in a tapered aorta have been presented in [1, 2]. In all these studies, the artery is treated as a straight circularly cylindrical elastic tube without or with a geometrical imperfection. The blood is modeled as an incompressible inviscid fluid.

In the present work we shall focus on consideration of the blood flow through an artery with a local dilatation (an aneurysm). Motivated by investigations in [1,2], we shall derive an evolution equation for propagation of nonlinear waves of the blood pressure perturbation through an injured artery. For the purpose we use two types equations to model the motion the arterial wall with a local dilatation (an aneurysm) and the motion of the fluid (the blood). The aneurismal artery is considered as a thin-walled straight hyper-elastic tube with a dilatation, as the longitudinal motion of arterial wall is assumed to be negligible. Unlike [1,2] the blood is modeled as an incompressible Newtonian fluid, as the viscous effects are presented in an appropriate manner. By applying a reductive perturbation method to the basic equations they are reduced to a version of the perturbed Korteweg-deVries (KdV) equation with variable coefficients. Exact traveling-wave solution of the evolulution equation is derived by applying the modified metod of simplest equation [3-5]. The ordinary differential equation of Bernulli is used as simplest equation. The obtained traveling-wave solution is numerically simulated. It is established that in absence of a local arterial dilatation thre are not waves. Bur, solitary waves appear in presence of a local dilatation. In addition, the amplitude and the wavelength of these waves are depended on basic geometric characteristics of the aneurysm, such as the maximal aneurysm diameter and the aneurysm length.

References

[1] Elgarayhi, A., E. K.El-Shewy, A. A. Mahmoud, A. Elhakem. Propagation of Nonlinear Pressure Waves in Blood. Hindawi Publishing Corporation, *ISRN Computational Biology*, Article ID 436267, 5 pages,(2013).

[2] J.C. Misra, M.K. Patra. A study of solitary waves in a tapered aorta by using the theory of solitons. *CAMWA* **54**, 242–254 (2007).

[3] Nikolay K. Vitanov. Application of simplest equations of Bernoulli and Riccati kind for obtaining exact traveling-wave solutions for a class of PDEs with polynomial nonlinearity *Communication in Nonlinear Science and Numerical Simulation* **15**, 2050 - 2060 (2010).

[4] Nikolay K. Vitanov. Modified method of simplest equation: Powerful tool for obtaining exact and approximate traveling-wave solutions of nonlinear PDEs. *Communications in Nonlinear Science and Numerical Simulation* **16**, 1176 - 1185 (2011).

[5] Nkolay K. Vitanov, Zlatinka I. Dimitrova, Kaloyan N. Vitanov. Modified method of simplest equation for obtaining exact analytical solutions of nonlinear partial differential equations: further development of the methodology with applications. *Applied Mathematics and Computation* **269**, 363 - 378 (2015).

Orientation selectivity tuning of a spike timing neural network model of the first layer of the human visual cortex

Simona Nedelcheva, Petia Koprinkova-Hristova

A spike timing neural network model of the first layer of the human visual cortex was implemented using NEST simulator. It consists of a receptive layer, a layer of lateral geniculate nucleus (LGN) neurons and a recurrent layer of cortex neurons. The receptive layer consists of ON/OFF filters mimicking the photoreceptor cells in the retina, composed by difference between two dimensional Gaussian functions. The parameters influencing the filters reaction to changes in light intensity at their spacial position are variances of the center and surround Gaussian functions respectively. The second (LGN) layer consists of integrate and fire neurons, one per each photoreceptor, having experimentally determined parameters taken from literature. These neurons transform the continuous generating current coming from the photoreceptor into discrete signal called spike train with corresponding frequency. The third layer of the model consist of integrate and fire neurons, each one with Gabor function receptive filed that determines its connectivity with neighboring neurons in dependence on their space positions and orientation selectivity. The main parameters influencing the orientation selectivity of each neuron depend on the corresponding Gabor function parameters. Recent investigations of the human brain showed that spatial organization of the visual cortex has orientation columns, each one having different orientation selectivity. The present paper investigates an approach to design of spacial organization into orientation columns of the third layer of the presented model. The influence of the parameter values determining the photoreceptor's size as well as the spacial structure of the orientation columns and the overall model orientation selectivity were investigated. The aim was to tune our model to recognize spacial orientation of the visual stimuli having different shape and orientation. The simulation investigations were carried out with stimuli representing rectangular shapes with different size and orientation moving through the visual field with different speed and having different starting positions.

Investigation of as-cast light alloys by selected homogenization techniques with microstructure effects

Ludmila Parashkevova, Pedro Egizabal

Objectives:

In the present contribution, upgrading the findings of previous works, new models are proposed for evaluation of effective mechanical properties of light alloys regarded as multiphase composites. These models are aimed to improve the mechanical properties predictions of two groups light alloys: die cast Mg alloys AZ and metal foams with closed cells. The presented models are variants of mean field homogenization approach and Differential Homogenization Method, (DHM), both accounting for microstructure size effects. The microstructure - properties relationships for AZ Mg alloy with Continuous (C) and Discontinuous (D) intermetallic phase precipitations are investigated applying two different approaches. The basic differences between cases (C) and (D) consist of arrangement and volume fraction of harder phase Mg17Al12. The microstructure of the alloy type (C) is characterizing by 10-20 volume % hard particles embedded into the softer matrix. The second microstructure type (D) corresponds to a composite with low volume fraction (10-20 %) of harder matrix phase, which contains (80-90 %) inclusions of softer material – alpha Mg. The type of microstructure depends mainly on the applied cooling regime and chemical composition of the alloy. As far as in the most AZ alloys Al is supersaturated in the melt, the precipitation type, rate and the amount of intermetallic phase are controlled by the thermal manufacturing conditions.

The elastic behavior of metal foams with closed pores is simulated applying DHM, where the size sensitive variant of Mori-Tanaka scheme is used as a basic "dilute case" procedure. The method is developed to closed form solutions of corresponding system of differential equations.

Results:

In case of continuous distribution of Mg17Al12 into alpha Mg matrix the variant of Mori-Tanaka homogenization method, described in [1] was used. For the case (D) of discontinuous distribution of the gamma phase Mg17Al12 around the grains, formed by alpha Mg, a new variant of DHM is suggested accounting for size effects. The elastic moduli of the composite with low matrix volume fraction are solutions of the differential system. In that system a special term reprezents the size sensitivity of the model through the average diameter of alpha phase and a length parameter of gamma phase. The elastic-plastic behavior of different AZ alloys is compared applying appropriate models. According to our theory, the alloy with continuously precipitated gamma phase demonstrates better ductility and higher maximal elongation at tension than the alloy with the same chemical composition but with discontinuously distributed phase, (Fig.1). Such behavior is experimentally proven.

For the case of metal foams the model, presented in differential form, is modified for a composite of high porosity, where the closed pores play the role of second phase,[2]. Here the analytical predictions for the elastic constants of metal foam are calculated at different size effects and Young's modulus at arbitrary porosity is compared to experimental data for Al based foams available in the literature,[3], see Fig.2.
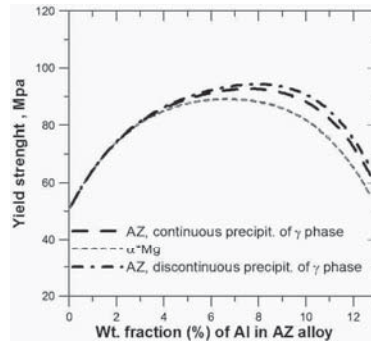
Figure 1: Comparison of initial yield stress of AZ alloy for microstructures with different type of Mg17Al12
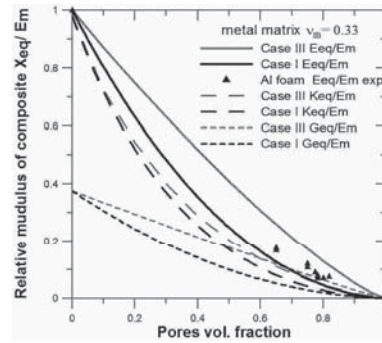
Figure 2: Relative elastic Young's, bulk and shear moduli for Al foam depending on porosity.

References

[1] Parashkevova, L., Egizabal, P., In: Adv. Computing in Industrial Mathematics: 11th Ann. Meet. of the Bulg. Sect. of SIAM, Dec. 20-22, 2016, Sofia, Bulgaria, editors: K. Georgiev, M. Todorov, I. Georgiev, pp.145-157, Springer (2018)

[2] Parashkevova, L.: Some considerations on modelling and homogenization of multi-phase light alloys,13th CTAM, 6-10 Sept. 2017, Sofia, MATEC,(in print)

[3] Kovacik, J., Simancik, F., Scripta Materialia, **39**, 239–246 (1998)

Experimental investigation of the influence of the non-condensable gas on the heat transfer during the condensation of different tubular structures

P. Petrova, B. Petrova, S. Chaoushev

Over the last decades, overall energy consumption has risen dramatically. Economic growth, as well as the growing world population and increased consumption, led to increased energy consumption in industrial processes and this requires the use of renewable energy sources. Realizing a more efficient use of energy is of great importance in almost all areas of our society, also in heat exchange processes. These processes are responsible for a significant part of the world's energy needs. For example, in the chemical industry, different heat exchangers find wide application in evaporation and condensation processes. The main purpose of these processes is to improve heat exchange so as to obtain the highest possible heat transfer coefficients. Negative effects on heat exchange and heat transfer coefficients, where the efficiency of the plant used is reduced, include inert gases such as air, nitrogen, etc. In this case, diffusion is of great importance. The temperature difference decreases and heat exchange is reduced. The presence of an inert gas has a different effect on pipes of different structures. A wide range of technical applications includes not only smooth pipes, but also tubes which, by increasing their contact surface, improve heat exchange. This development of their geometry is accomplished by the presence of various structures such as grooving or ribbing on their tubular surface. This research represents an overview of the influence of the non-condensable gas on the heat transfer during the condensation of different tubular structures. For this aim, four different copper tubes were examined in terms of their external heat transfer coefficients. The measurements were carried out using an evaporator/condenser test rig at one saturation temperature and with different volume fractions of the non-condensable gas. The evaluation was done utilizing the modified Wilson Plot Method. The measurement data was optimized with the Matlab program. The program uses various known models for describing the internal and external heat exchange and determines for each combination of models (internal / external) correlation coefficients so that, on the principle of the smallest square deviation, the calculated values for the heat transfer coefficients can maximally approximate to the experimental ones. Four correlation models for internal heat exchange and two models for external heat exchange were used. The results in the presence of non-condensable gases and without non-condensable gases were compared with each other. A decrease in the heat transfer during the condensation was observed with the increase of the volume fraction of the non-condensable gas.

Pohodhaev identities as conservation laws for semi-linear elliptic-hyperbolic equations

Nedyu Popivanov

It is well known result of Pohozhaev (1965), that the homogeneous Dirichlet problem for semilinear elliptic equations $\Delta u + u|u|^{p-2}$, in a bounded subset Ω of R^n , with $n > 2$, permits only the trivial solution if the domain is star-shaped, the solution is sufficiently regular, and the power of nonlinearity $p > 2^*(n) := 2n/(n-2)$, where the latter quantity is the critical exponent in the Sobolev embedding of $H_0^1(\Omega)$ into $L^p(\Omega)$ for $p < 2^*(n)$. To the opposite of this fact, in the case $2 < p < 2^*(n)$ there exist nontrivial solutions. In the last 50 years the Pohozhaev identities and results have been used and extended for a large class of elliptic problems. Let us mention now that in [1], [2] it has been shown that the nonexistence principle in supercritical case also holds for certain two dimensional problems for the mixed elliptic-hyperbolic Gellersted operator L (instead of Δ), with some appropriate boundary conditions. It is also valid for a large class of such problems even in higher dimensions [3]. In dimension 2, such operators have a long-standing connection with transonic fluid flow. Of course, the critical Sobolev embedding in this case is for a suitable weighted version of $H_0^1(\Omega)$ into $L^p(\Omega)$. As usual, in the BVP for such mixed elliptic-hyperbolic Gellersted operator L, the boundary data are given only on the proper subset of the boundary of Ω. To compensate the lack of a boundary condition on a part of boundary, a sharp Hardy-Sobolev inequality is used, as was first done in [1], [2] and later in [3], [4], [5]. Some further results, already published or in progress, prepared jointly with colleagues from Italy and Norway will be also discussed.

References

[1] Lupo D., Payne K., Critical exponents for semi-linear equations of mixed elliptic-hyperbolic types, Comm. Pure Appl. Math. (2003), V.56, P. 403-424.

[2] Lupo D., Payne K., Conservation laws for equations of mixed elliptic-hyperbolic type, Duke Math. J., 2005, V. 127, P. 251-290.

[3] Lupo D., Payne K., Popivanov N., Nonexistence of nontrivial solutions for supercritical equations of mixed elliptic-hyperbolic type, Progress in Non-Linear Differential Equations and Their Applications, Birkhäuser Verlag Basel, V. 66 (2005), P. 371-390.

[4] Lupo D., Payne K., Popivanov N., On the degenerate hyperbolic Goursat problem for linear and nonlinear equations of Tricomi type, Nonlinear Analysis, Series A: Theory, Methods and Appl. (2014), V. 108, P. 29-56.

[5] Dechevsky L., Payne K.R., Popivanov N., Nonexistence of Nontrivial Generalized Solution for 2-D and 3-D Quasilinear Mixed Type Equation Problems, AIP Conference Proceedings (in print).

Sparse time-frequency representations and uncertainty on finite Abelian groups

Peter Rashkov

Uncertainty principles establish restrictions on how well localized the Fourier transform of a well localized function can be and vice versa [1]. In the case of a function f defined on a finite Abelian group $\mathfrak{G}$, localization is generally expressed through the cardinality of the support of the function, $\|f\|_0$. Due to its relevance for compressed sensing and, in particular, for the recovery of lossy signals under the assumption of restricted spectral content [2], the uncertainty principle for functions on finite Abelian groups has drawn renewed interest. In this realm, a classical result on uncertainty states that the product of the number of nonzero entries in a vector representing a nontrivial function $\|f\|_0$ on an Abelian group and the number of nonzero entries in its Fourier transform $\|\hat{f}\|_0$ is not smaller than the order of the group $|\mathfrak{G}|$ [1]. Furthermore, the quantity $\theta(\mathfrak{G},k) = \min\{\|\hat{f}\|_0 : 0 < \|f\|_0 \le k\}$, can be explicitly computed for $\mathfrak{G} = \mathbb{Z}_p$ (p prime)[3], and estimated from below for nontrivial finite Abelian groups of nonprime order [4].

In particular, we consider dictionaries $\mathscr{D} = \{g_0, g_1, \ldots, g_{N-1}\}$ of N vectors in $\mathbb{C}^{\mathfrak{G}}$. For $k \le n = |\mathfrak{G}|$ we examine the set of vectors having a sparse representation in $\mathscr{D}$,

$$\mathfrak{s}_k^{\mathscr{D}} = \{f \in \mathbb{C}^{\mathfrak{G}} : f = \sum_r c_r g_r, \text{ with } \|c\|_0 \le k\}.$$

A fundamental question is how many entries of $f \in \mathfrak{s}_k^{\mathscr{D}}$ need to be known (or stored), in order that $c \in \mathbb{C}^n$ with $f = \sum_r c_r g_r$ and $\|c\|_0 \le k$, and therefore f, be uniquely determined by the known data?

To this end, we define $\psi(\mathscr{D},k) := \min\{\|f\|_0 : f \in \mathfrak{s}_k^{\mathscr{D}}\}$. It is well known that any $f \in \mathfrak{S}_k^{\mathscr{D}}$ is fully determined by any choice of $n - \psi(\mathscr{D},2k) + 1$ entries of f[2, 5]. Consider $\mathscr{D}$ to be the Fourier dictionary, that is, set of characters ξ on $\mathfrak{G}$ (continuous homomorphisms $\xi : \mathfrak{G} \to S^1$). $\mathscr{D}$ can be identified with the dual group $\mathfrak{G}'$, and the uncertainty principle implies

$$\psi(\mathscr{D},k) = \min\{\|f\|_0 : f \in \mathfrak{s}_k^{\mathscr{D}}\} = \min\{\|\hat{f}\|_0 : \|f\|_0 \le k\} = \theta(\mathfrak{G},k),$$

yielding an explicit lower bound for the number of known data which are sufficient to recover a sparse vector f in this dictionary.

In [6, 7] the focus is on extending these results to *sparse time-frequency representations* in the Gabor dictionary $\mathscr{G}$, consisting of the time-frequency shifts of a prototype *window function* $g \in \mathbb{C}^{\mathfrak{G}}$, $\pi(x,\xi)g(t) = g(t-x)\xi(t)$ with $x \in \mathfrak{G}, \xi \in \mathfrak{G}'$. Our interest is in similar results relating the support sizes of functions and their *short-time Fourier transforms* $V_g f : \mathfrak{G} \times \mathfrak{G}' \to \mathbb{C}$, defined by $V_g f(x,\xi) = f \cdot \pi(x,\xi)g$. The short-time Fourier transform measures the local frequency content of a function with respect to a given window. Due to this dependence, only weak bounds can be expected to hold for all windows. In [6] we have established stronger results by instead restricting our attention to bounds that hold for almost every window function, that is, we allow an exceptional set of measure zero.

We search for a relation between the representations using a Gabor dictionary and a Fourier dictionary. In [6] we demonstrated that for cyclic groups $\mathbb{Z}_n$ of *prime order* and almost every

$g \in \mathbb{C}^n$, it holds that for $k \leq n$, $\psi(\mathscr{G}, k) = \theta(\mathbb{Z}_n, k)$. Rudimentary numerical experiments gave some indication that equality holds also for *cyclic groups* $\mathbb{Z}_n$ with $n \leq 6$ [7]. This does not hold for all Abelian groups of finite order, per following counterexample: for any $g \in \mathbb{Z}_2 \times \mathbb{Z}_2$, we have $\psi(\mathscr{G}, 4) = 0$ while $\theta(\mathbb{Z}_2 \times \mathbb{Z}_2, 4) = 1$. Therefore, a question was posed whether for any cyclic group $\mathbb{Z}_n$, for almost every $g \in \mathbb{C}^n$ does it hold that for $k \leq n$, $\psi(\mathscr{G}, k) = \theta(\mathbb{Z}_n, k)$. An affirmative answer was given recently in [8].

References

[1] D. Donoho, P. Stark. Uncertainty principles and signal recovery. *SIAM J. Appl. Math.* **49** 906-931, 1989.

[2] E. Candes, J. Romberg, T. Tao. Robust uncertainty principles: Exact signal reconstruction from highly incomplete frequency information. *IEEE Trans. Inform. Th.* **56** 489-509, 2006.

[3] T. Tao. An uncertainty principle for cyclic groups of prime order. *Math. Res. Lett.* **12** 121-127, 2005.

[4] R. Meshulam. An uncertainty inequality for finite abelian groups. *Eur. J. Combin.* **27** 227-254, 2006.

[5] D. Donoho. Compressed sensing. *IEEE Trans. Inform. Th.* **52** 1289-1306, 2006.

[6] F. Krahmer, G.E. Pfander, P. Rashkov. Uncertainty in time-frequency represen-tations on finite abelian groups and applications, *Appl. Comput. Harmon. Analysis* **25** 209-225, 2008.

[7] F. Krahmer, G.E. Pfander, P. Rashkov. An open question on the existence of Gabor frames in general linear position. In: S. Dahlke, et al. (Eds.) *Structured Decompositions and Efficient Algorithms*, Schloss Dagstuhl - Leibniz-Zentrum für Informatik, Germany, 2009.

[8] R.D. Malikiosis. A note on Gabor frames in finite dimensions. *Appl. Comput. Harmon. Analysis* **38** 318-330, 2015.

A European Technology Platform for MSO

Wil Schilders

The current and future technological and economic development of the industrial Europe is characterized by a steadily growing complexity of modern products and processes, as well as ever shorter innovation cycles. Principal issues which must be addressed are the scarcity of resources, recycling, climate change, assessment of the risks to the environment and society, as well as increased automation and a holistic view of the life cycle of a product. The long-term and sustainable solution to these problems is only possible through an intensive support of the development procedures of new products and production processes via a holistic mathematical Modeling, Simulation and Optimization (MSO) approach, where in each case parallel to each product or process a virtual product or process (the digital twin) is generated. On this basis a simulation of functionality and design, as well as of long-term effects and risks, one is able to design optimized products and sustainable process controls. In addition to the classic areas of mechanical and vehicle engineering in which a modularized and component- based development on the basis of mathematical models is already established, this approach is also essential in the development of Industry 4.0 as a key technology and a decisive competitive advantage. This procedure also plays a central role in all other fields of science, economy and society and the aim must be to strengthen the leading position of Europe in this system- oriented approach. Success of the above mentioned approach relies heavily on the further advancement of Mathematical Technologies. Mathematical Technologies play already an essential role in almost all areas of industrial and societal relevance. As numerous success stories show, Mathematical Technologies, in particular Modelling, Simulation and Optimization tools, provide real and production processes, analysing data, enabling virtual prototyping of new products and reducing costs. Mathematical Technologies find application in a wide range of scientific and technological fields, and it is expected that in the coming years, with the increased use of technology and availability of ever more power-ful high performance computers, the impact of MSO tools will become even more significant.

There is a clear need to bring together the existing European National Networks of Research Centres for Industrial and Applied Mathematical Technologies, to ensure a common effort towards one main and shared objective: providing the industrial and scientific communities with a single coordinated and comprehensive infrastructure for Mathematical Modelling, Simulation and Optimization, and resulting research programs. This is organized on a European scale by EU-MATHS-IN – a European Network of Mathematics for Industry and Innovation. This network is a collaboration of national organizations from currently 17 European countries. The promoting partners of EU-MATHS-IN are the European Mathematical Society and the European Consortium for Mathematics in Industry. The primary objective of this network is to discuss success stories and share experiences and best practices of organizing collaborative research projects with industry, as well as to discuss and brainstorm about joint future activities.

One of the major obstacles to be addressed is the low visibility of mathematical technologies in European programs. We will also discuss measures facilitating awareness about existing expertise in Europe and knowledge transfer. Currently, together with renowned industry partners, EU-MATHS-IN is discussing the set-up of a so-called European Technology Platform for Mathematical Modeling, Simulation and Optimization. In the talk, the preparations for this will be discussed: there have been several workshops in Amsterdam to discuss in-depth with industry, and recently a larger research workshop was organized in Leiden at the Lorentz Center (see poster below).

Comparative study of Hierarchical and Traditional Solvers for Dense Systems of Linear Equations on Xeon Phi Processors

D. Slavchev, S. Margenov

This study is motivated by HPC simulation of laminar flow around airfoils. The Boundary Element Method (BEM) is applied for numerical solution of the related integral equation, taking into account the advantages of BEM in the case of exterior domain. The most computationally expensive part of the algorithm is solving a dense system of linear algebraic equations (SLAE). We examine several libraries that solve it using traditional methods (PLASMA and MKL only) and one (STRUMPACK) using decomposition of the coefficient matrix into a hierarchical matrix thus changing the problem into solving a sparse system.

The scalability analysis is focused on strong parallel speed-up and parallel efficiency. The BEM matrix is fully populated, and the algorithmic complexity is dominated by the solution of BEM linear algebraic system. However, the computation of BEM matrix also takes substantial part of the total time.

Traditional methods for solving a system of Linear algebraic equations use some variant of Gausian Elimination. This process is $O(N^3)$ complexity problem, where N is the number of unknowns (elements used in the BEM). We solve the SLAE using MKL and PLASMA parallel solvers on Intel Xeon Phi processors and compare the results. Another method for solving SLAE is based on the theory of hierarchical matrices (H- matrices) to transform the dense matrix of coefficients into a sparse matrix thus allowing the use of methods tailored for sparse matrices. The H-matrices methods are initially developed for matrices produce by the BEM therefore they are applicable to our case. H-matrices methods use the structure of the matrix to produce a sparse matrix approximation of the original matrix.

This promises a lower time needed for the solution of the resulting SLAE (petentially down to $O(NlogN)$) but adds an additional step - the approximation of the original dense matrix with a sparse one. In order to measure the parallel speed up of this method and to compare it with the traditional ones we use the STRUctured Matrices PACKage (STRUMPACK) library. It uses Hierarchically Semi-Separable (HSS) representation for the sparse matrix.

The numerical tests are ran on a single node on the Avitohol Cluster at the Institute of Communication and Information Technologies. More information about it could be found at http://www.iict.bas.bg/avitohol/index.html.

Memristor Computing

Angela Slavova, Ronald Tetzlaff

Neuromorphic circuits can be considered for energy efficient computing based on biological principles in future electronic systems. Thereby, memristors are assumed in neuron models and for synapses in several recent investigations in order to overcome the limits of conventional von Neumann architectures by taking these devices as memory elements and as well as devices for computation also in bio-inspired artificial neural networks.

Cellular Neural Networks (CNN) are universal high-speed computing systems with stored programmability and are already based on the principle of distributed computing with memory. The dynamical behavior of these spatiotemporal systems will be exploited to solve multidimensional signal processing and classification problems. For example, reaction-diffusion systems can be represented by state equations of so called reaction-diffusion CNN showing the emergence of complex behavior (e.g. pattern formation) based on local activity and especially on a parameter subset called the "edge of chaos".

We shall present the dynamics of hysteresis CNN model with memristor synapses (M-HCNN). In order to study the dynamics of the obtained M-HCNN model we shall apply theory of local activity. In this way we shall determine the edge of chaos domain in the parameters' set for the model under consideration. We shall provide two examples of the application in image processing. The processing results do not change under the variations of the memristor weights. This is due to the influence of the binary quantization of the output signals. However, in order to obtain stable solution we need more iterations when some variations arise in the templates. This can reflect in the speed of the M-HCNN performance without change of the quality of the final results.

Multisoliton Interactions in Schrödinger and Manakov Dynamical Systems with Nonlinear Gain/Loss and External Potentials

Michail Todorov, Vladimir Gerdjikov

We analyze the N-soliton interactions in adiabatic approximations for the nonlinear Schrödinger equation:

$$i\frac{\partial u}{\partial t} + \frac{1}{2}\frac{\partial^2 u}{\partial x^2} + |u|u = i(\gamma u + \beta|u|^2 u + \eta|u|^4 u) + V(x)u, \quad u = u(x,t) \tag{1}$$

in the presence of three types of perturbation terms: a) periodic external potential $V(x) = A\cos(\Omega x + \Omega_0)$ and b) non-conservative gain/loss terms the form. Similar analysis is performed also for the perturbed Manakov system:

$$i\frac{\partial \mathbf{u}}{\partial t} + \frac{1}{2}\frac{\partial^2 \mathbf{u}}{\partial x^2} + (\mathbf{u}^\dagger,\mathbf{u})\mathbf{u} = i[\gamma\mathbf{u} + \beta(\mathbf{u}^\dagger,\mathbf{u})\mathbf{u} + \eta(\mathbf{u}^\dagger,\mathbf{u})^2\mathbf{u}] + V(x)\mathbf{u}, \quad \mathbf{u} = \mathbf{u}(x,t). \tag{2}$$

Both equations (1) and (2) find a wide range of applications including optics, Bose-Einstein condensation, fluid dynamics and plasma physics, and many more, see [1, 2].

The adiabatic method first specifies the initial condition which is an N-soliton train whose parameters satisfy the adiabaticity condition. Then we derive a dynamical system for the soliton parameters, known as the perturbed complex Toda chain (PCTC), see [3, 4, 5] and the references therein.

Then we compare the numerical solutions of (1) and (2) with the numerical solutions of PCTC. Our conclusion is that the above perturbations are compatible with the adiabatic approximation if the equation

$$\frac{\partial v_k}{\partial t} = \gamma + \frac{8}{3}\beta v_k^2 + \frac{128}{15}\eta v_k^4$$

allows bounded solutions. This is possible if $\beta \simeq -1.5\gamma$ and $\eta \ll \beta$. We have found very good agreement between the PCTC and the nonlinear Schrödinger and Manakov 5-soliton trains.

References

[1] P. G. Kevrekidis, D. J. Frantzeskakis, and R. Carretero-González (Eds.), *Emergent Nonlinear Phenomena in Bose-Einstein Condensates. Theory and Experiment* (Springer-Verlag, Berlin, 2008); R. Carretero-González, D. J. Frantzeskakis, and P. G. Kevrekidis, *Nonlinearity* **21**, R139 (2008).

[2] P. G. Kevrekidis, D. J. Frantzeskakis, and R. Carretero-González, *The Defocusing Nonlinear Schrödinger Equation* (SIAM, Philadelphia, 2015).

[3] M. D. Todorov, V. S. Gerdjikov, and A. V. Kyuldjiev. Multi-soliton interactions for the Manakov system under composite external potentials, *Proceedings of the Estonian Academy of Sciences, Phys.-Math. Series* **64**(3), 368–378 (2015), doi: 10.3176/proc.2015.3S.07.

[4] V. S. Gerdjikov, A. V. Kyuldjiev, and M. D. Todorov, Manakov Solitons and Effects of External Potential Wells, *Discrete and Continuous Dynamical Systems*, Supplement **2015**, pp. 505–514 (2015), doi:10.3934/proc.2015.0505.

[5] R. Carretero-González, V. S. Gerdjikov, and M. D. Todorov, *N*-soliton Interactions: Effects of Linear and Nonlinear Gain/loss, in *AMiTaNS'17*, AIP CP, vol. 1895, American Institute of Physics, Melville, NY, paper 040001, 10p., 2017, doi: http://doi.org/10.1063/1.5007368.

Sound Vectorization with Genetic Algorithms

Petar Tomov, Iliyan Zankinski, Todor Balabanov

Introduction In the audio based multimedia there are two common directions - WAVE audio and MIDI audio. The WAVE audio represents direct air vibrations assembled into a complex sound. On the other side MIDI audio is a sequence of musical events stating the order in which different musical notes should be played by different musical instruments. WAVE is a raw sound format and MIDI is a form of vector sound format. MIDI audio was developed with the progress of electronic musical instruments. It is an information representation standard which is very useful for real time audio information exchange and efficient file storage. To transform MIDI to WAVE is an easy task for the modern computers. It is done even inside the hardware sound cards by the module called MIDI synthesizer. The opposite transformation from WAVE to MIDI is relatively complex problem even for the modern computers. It is like a human that listens to the music and writing the notes corresponding to it. Some audio information is not needed in WAVE or MP3 form but in MIDI (such as games background music). In these situations the WAVE information should be transformed in a group of simple MIDI events. This process of sound data transformation is related to information reduction. The process is transformation of true sounds into a set of simple musical events. The problem of vectorization is very well known in literature and one of the most impressive implementations has been done with the image of Mona Lisa. The goal of this project was to approximate the picture of Mona Lisa by no more than 50 polygons. The colors and the points of the polygons were optimized with GAs. The same principles can be applied in sounds vectorization where WAVE information is transformed into a MIDI sequence.

Proposed Solution The model proposed is based on Genetic Algorithms (GA). GA is applied over a set of MIDI events. It is an unsupervised system which takes digital WAVE sounds as input and generates simplified, stylized vector data as output. A WAVE sound usually contains details that are not relevant for the audio quality and increase the cost of computations. Simplification of WAVE sounds is a process to eliminate the most useless elements, while retaining the perceptually dominant elements. Simplification of WAVE sound is used in the area of music composition and game development. In sounds simplification and vectorization digital WAVE samples are the input and generated simplified, stylized vector data are the output. The objective of sounds simplification by vectorization is to split the original sound into simple MIDI events. In this study MIDI events were chosen as approximation primitives to be used for sound reconstruction. Each MIDI event is described by its type, status and time. Each individual in the GA's population consists of an ordered set of events and a fitness value. The fitness value is calculated as Euclidean distance between the approximate sound and the original sound. The approximated sound is assembled by MIDI events. As an initial step GA population is initialized with randomly generated sets of events. Type, status and time are taken randomly for each event . During GA's evolutionary process individuals are selected from the population, crossover, mutation, evaluation and survival are applied so that the sound approximation is approved. In this study a binary crossover is chosen. Mutation is applied as time shifting and status change of one event in the individual. During evaluation phase the approximated sound is compared with the original sound. The result of the com-

parison is used as a fitness value of the individual. During the survival process it is decided which individual to be kept, the newly created or the already existing. The only stopping criteria used is the total number of sound evaluations.

Conclusions Experiments show that using GA may be very efficient and sound approximation is relatively accurate in the limits of the sound simplification. Optimization convergence is related to the probabilistic nature of GA. Sound comparison is time consuming and slows down the optimization process. As further research, it could be suitable for GA to be implemented as distributed computing algorithm. Such a distributed implementation is efficiently applicable for the class of evolutionary algorithms GA is a part of. The set of events can be treated as a multidimensional space and optimization can provide much better results.

Slot Machine Reels Reconstruction with Genetic Algorithms

Petar Tomov, Iliyan Zankinski, Todor Balabanov

Introduction This paper focuses on a very well know problem in the slot machine gambling games development - reverse engineering of the virtual reels. Virtual reels are trade secretes of the manufacturer usually. They are a discrete random distribution of the game symbols. The value for return to player (RTP) is adjusted by the placement of the symbols. If the RTP needs to be checked (without access to the game source code) a reconstruction of the virtual reels is necessary. Such check starts with visual observation of the game screens or by image processing of game screen-shots. This research proposes Genetic Algorithm (GA) as search technique for slot machines virtual reels reconstruction.

Slot Machine Reels For better understanding of the problem a brief description of the slot machine reels will be given. One of the basic concepts of the slots are the spinning reels. In the beginning slots were mechanical. Reels were driven to spin by manual handle. Nowadays slots are generally computerized. It means that mechanical reels are replaced with virtual reels. There is no handle anymore, but a button and a pseudo-random number generator (PRNG) are used for the outcome. Win is calculated according to symbols patterns that appear on the screen after the reels have stopped spinning. A known pay table defines how valuable each symbol on the screen is. More frequent symbols are less profitable and less frequent symbols are much more profitable and informative for reels reconstruction process. The accuracy of game RTP is used to measure reels reconstruction quality. If the reconstruction is good enough the RTP will be close to the RTP published by the manufacturer. When the game is produced the desired RTP is adjusted by mathematicians and game designers. Their job is to populate game reels with proper symbols in proper discrete distribution. The process of reels reconstruction is pretty similar to the process of the new reels construction. The only difference is about symbols classification patterns and the requirement this patterns to be presented in the reconstructed reels.

Proposed Solution Virtual reels analysis starts with screen pattern classification as image processing (http://github.com/ TodorBalabanov/Slot-Machine-Symbols-Capture). Classified patterns are used as pieces in the reconstructed sequence of the reels. A list of the classified patterns is the input for the algorithm (http://github.com/ TodorBalabanov/Slot-Machine-Reel-Mosaicing). The software implementation uses Apache Commons Genetic Algorithms Framework. Chromosomes are characters sequences of the symbols available in the slot game. The crossover operator is chosen to be a single cut point. It is the preferred way because strips of the symbols should be kept as much in order as possible. Crossover rate is experimentally chosen to be 90%. Mutation operator is done in the simplest possible way by swapping two symbols in a single reel. Mutation rate is experimentally chosen to be 10%. Tournament selection with arity value of 2 is used for reproducing parents choosing. Population of 23 individuals is selected experimentally. Reels reconstruction problem is highly combinatorial and because of this maximum running time is chosen as optimization stopping criteria. When the problem is highly combinatorial it is useful to apply elitism rule as it is applied in this research with rate of 10%. The most complex part in the solution proposed is

the fitness function organization. Five different components were involved in fitness function composition: 1) Number of wrong patterns found in the reconstructed reel, but not presented in classified patterns; 2) Number of missing patterns which should be presented in the reconstructed reel, because they are presented in the classified patterns; 3) Number of patterns which repeats more than once in the reconstructed reel; 4) Length of the reconstructed reel; 5) Euclidean distance of symbols frequencies between reconstructed reel and classified patterns. These five components can be separated in two groups of constraints - first and second are hard constraints (should not be violated) and the other three are soft constraints (can be violated). The most important criteria is related to wrong patterns. If in the reconstructed reel there are unobserved patterns it means that the reconstructed reel is generally wrong and the desired RTP will not be achieved. Secondly most important criteria is related to the missing patterns. If the patterns were observed, but they are missing in the reconstructed reel it means that the reel is not close enough to the original reel. Repeating patterns (third constraint) are not desirable, because they extend the length of the reconstructed reel, but can be accepted. Reconstructed reels are better accepted when they are as short as possible (fourth constraint), but length can vary. The final constraint is about the Euclidean closeness between the reconstructed reel and the classified patterns. Symbols frequencies are calculated for the classified patterns in the beginning of the algorithm. At each fitness function calculation symbols frequencies are calculated for each reconstructed reel. The reconstructed reel gets closer to the real reel when symbol frequencies are close.

Conclustions Experiments show that absolutely automatic reconstruction is not possible with GA technique, but with some manual adjustments reconstructed reels are close to originals at least as RTP achieved. As further research it will be interesting reconstruction approach to be extended to optimization with Context-Sensitive Grammars (CSG).

Change-point analysis as a tool to detect abrupt Cosmic ray muons variations

Assen Tchorbadjieff, Ivo Angelov

Recently, there have been an increasing number of studies using Big Data. They rely on large datasets of time series to detect artificial or natural patterns in processes of sciences or economy. However, many of them suffer for insufficient data quality processing for estimation of used data consistency. The most possible outcome due to lack of rigid data quality process is data contamination with abrupt drifts and regime shifts. The impossibility for their detection causes production of wrong statistical estimates and leads to wrong conclusions and decisions.

Possible software tools for detection of regime shifts are delivered from change-point methods [1]. Such kind of statistical data proceeding is applied to experimentally acquired time series from cosmic ray measurements at peak Moussala (2925 masl). The observed parameters are muons produced in cosmic ray cascades in atmosphere and parallelly acquired atmosphere and meta- data [2].

However, a major drawback with the most of the currently available change-point methods is the challenge of complex temporal variations due to compound processes similar to cosmic rays cascades and also possible detectors drifts. In this study, we examine different approaches for change-point detection in compound particle counting process. They are implemented for R statistical environment and tested for different statistical distributions as Normal, Gamma or Poisson.

References

[1] Chen, J., A. K. Gupta, A. K.: On Change Point Detection and Estimation. Communications in Statistics - Simulation and Computation, 30(3), 665–697 (2001)

[2] Angelov, I.I., Malamova, E.S., Stamenov, J. N.: Muon Telescopes at Basic Environmental Observatory Moussala and South-West University–Blagoevgrad. Sun Geosphere, 3(1), 20–25 (2008)

Performance Analysis of Effective Methods for Solving Band Matrix SLEs after Parabolic Nonlinear PDEs

Milena Veneva, Alexander Ayriyan

Systems of linear algebraic equations (SLEs) with pentadiagonal (PD) and tridiagonal (TD) coefficient matrices arise after discretization of partial differential equations (PDEs), using finite difference methods (FDM) or finite element methods (FEM). Methods for numerical solving of SLEs with such matrices which take into account the band structure of the matrices are needed. The methods known in the literature usually require the matrix to possess special characteristics so as the method to be stable, e.g. diagonally dominance, positive definiteness, etc. which are not always feasible.

In [1], a finite difference scheme with first-order approximation of a parabolic PDE was built that leads to a TD SLE with a diagonally dominant coefficient matrix. The system was solved using the Thomas method. However, a difference scheme with second-order approximation ([2]) leads to a matrix which does not have any of the above-mentioned special characteristics. The numerical algorithms for solving multidimensional governing equation, using FDM (e.g. alternating direction implicit (ADI) algorithms), ask for a repeated SLE solution. This explains the importance of the existence of effective methods for the SLE solution stage.

Two different approaches for solving SLEs with pentadiagonal and tridiagonal coefficient matrices were explored by us in [2] – diagonal dominantization and symbolic algorithms. These approaches led to five algorithms – numerical algorithms based on LU decomposition (for PD ([3]) and TD matrices), modified numerical algorithm for solving SLEs with a PD matrix, and symbolic algorithms (for PD ([3]) and TD ([4]) matrices). The numerical experiments with the five methods in our previous paper were conducted on a PC. Here, we are going to suggest an iterative method which is also not restrictive on the coefficient matrix, namely the strongly implicit procedure (SIP), also known as the Stone method. This method uses the incomplete LU (ILU(0)) decomposition. An application of the Hotelling-Bodewig iterative algorithm is suggested as a replacement of the standard forward-backward substitutions. The upsides and the downsides of the SIP method are discussed. The complexity of all the investigated methods is presented.

It is a well-known fact that solving problems of the computational linear algebra with sparse matrices is crucial for the effectiveness of most of the programs for computer modelling of processes which are described with the help of differential equations, especially when solving complex problems with big dimension. However, this is exactly how most of the computational science problems look like and hence usually they cannot be model on ordinary PCs for a reasonable amount of time. This enforces the usage of supercomputers and clusters for solving such big problems. Therefore, the aim and the main contribution of this paper is to investigate the performance characteristics of the considered methods being executed on modern (as of 2017) computer clusters. To that purpose, the experimental setup and the results from the conducted computations on the individual computer systems are presented and discussed.

References

[1] Ayriyan, A., Buša Jr., J., Donets, E. E., Grigorian, H., Pribiš, J.: Algorithm and simulation of heat conduction process for design of a thin multilayer technical device. Applied Thermal Engineering. Elsevier. **94**, 151–158 (2016) doi: 10.1016/j.applthermaleng.2015.10.095

[2] Veneva, M., Ayriyan, A.: Effective Methods for Solving Band SLEs after Parabolic Nonlinear PDEs. Submitted to European Physics Journal – Web of Conferences (EPJ-WoC), arXiv: 1710.00428 [math.NA]

[3] Askar, S. S., Karawia, A. A.: On Solving Pentadiagonal Linear Systems via Transformations. Mathematical Problems in Engineering. Hindawi Publishing Corporation. **2015**, 9 (2015) doi: 10.1155/2015/232456

[4] El-Mikkawy, M.: A Generalized Symbolic Thomas Algorithm. Applied Mathematics **3**, 4, 342–345 (2012) doi: 10.4236/am.2012.34052

Hermitian and Pseudo-Hermitian Reduction of the GMV Auxilliary System. Spectral Properties of the Recursion Operators

Alexandar Yanovski and Tihomir Valchev

We consider the auxiliary linear problem

$$\tilde{L}^0 \psi = (\mathrm{i}\partial_x - \lambda S)\psi = 0, \quad S = \begin{pmatrix} 0 & u & v \\ \varepsilon u^* & 0 & 0 \\ v^* & 0 & 0 \end{pmatrix}, \quad \varepsilon = \pm 1 \qquad (1)$$

and the theory of the expansions over the adjoint solutions related to it.

In the above u, v (the potentials) are smooth complex valued functions on x belonging to the real line and $*$ stands for the complex conjugation. In addition, the functions u and v satisfy the relation:

$$\varepsilon |u|^2 + |v|^2 = 1 \qquad (2)$$

The functions u, v must satisfy also some asymptotic conditions when $x \to \pm\infty$, for the systems of nonlinear evolution equations associated to $\tilde{L}^0$ the most reasonable are constant asymptoitics. We adopt the following convention. When ε is in some formulas and it is a number, then it will be $+1$ or -1. When it is used as index or label it will be either $+$ or $-$. For example, we call the above system GMV$_\varepsilon$ system. Thus GMV$_+$ is the usual GMV system (obtained for the first time by Gerdjikov-Mikhailov and Vachev).

The GMV$_+$ system arises naturally when one looks for integrable system having a Lax representation $[L, A] = 0$ with L and A subject to Mikhailov-type reduction requirements. This is also true for both GMV$_\pm$ systems. Indeed, the Mikhailov reduction group G_0 acting on the fundamental solutions of the system (1) could be defined as generated by the two elements g_1 and g_2 acting in the following way:

$$g_1(\psi)(x, \lambda) = \left[Q_\varepsilon \psi(x, \lambda^*)^\dagger Q_\varepsilon \right]^{-1}, \quad Q_\varepsilon = \mathrm{diag}(1, \varepsilon, 1), \ \varepsilon = \pm 1$$
$$g_2(\psi)(x, \lambda) = H\psi(x, -\lambda)H, \quad H = \mathrm{diag}(-1, 1, 1) \qquad (3)$$

where $\dagger$ denotes Hermitian conjugation. Since $g_1 g_2 = g_2 g_1$ and $g_1^2 = g_2^2 = \mathrm{id}$, $G_0 = \mathbb{Z}_2 \times \mathbb{Z}_2$. We shall call the reduction defined by g_1, g_2 for $\varepsilon = 1$ Hermitian reduction and the reduction defined by g_1, g_2 for $\varepsilon = -1$ pseudo-Hermitian reduction. The requirement that G_0 is a reduction group immediately gives that the coefficients of the pencil of L-A pairs

$$\tilde{L}^0, \quad \tilde{A} = \mathrm{i}\partial_t \psi + \left(\sum_{k=0}^{n} \lambda^k \tilde{A}_k \right), \quad \tilde{A}_k \in \mathrm{sl}(3, \mathbb{C}) \qquad (4)$$

must satisfy:

$$HSH = -S, \quad H\tilde{A}_k H = (-1)^k \tilde{A}_k$$
$$Q_\varepsilon S^\dagger Q_\varepsilon = S, \quad Q_\varepsilon \tilde{A}_k^\dagger Q_\varepsilon = \tilde{A}_k \qquad (5)$$

which gives a hierarchy of nonlinear evolution equations (NLEEs) (or soliton equations) solvable via $\tilde{L}^0$.

As it can be checked the matrix S has constant eigenvalues and as a result $S(x)$ takes values in the orbit $\mathcal{O}_{J_0}(\mathrm{SU}(\varepsilon))$ of the element $J_0 = \mathrm{diag}(1, 0 - 1)$ with respect to the adjoint representation of the group $SU(\varepsilon)$ where the notation $\mathrm{SU}(\varepsilon)$ stands for $\mathrm{SU}(3)$ for $\varepsilon = +$ and for $\mathrm{SU}(2,1)$ for $\varepsilon = -$ (it is a submanifold of $\mathfrak{isu}(\varepsilon)$ of course, where $\mathfrak{su}(\varepsilon)$ are the corresponding Lie algebras).

Our approach to the $\mathrm{GMV}_\pm$ system is based on the fact that it is gauge equivalent to a Generalized Zakharov-Shabat auxiliary systems (GZS systems) on the algebra $\mathrm{sl}(3, \mathbb{C})$ which in our case takes the form:

$$L^0 \psi = (\mathrm{i}\partial_x + q(x) - \lambda J_0)\,\psi = 0 \tag{6}$$

If we denote the space of diagonal matrices in $\mathrm{sl}(3, \mathbb{C})$ by $\mathfrak{h}$ (it is the Cartan subalgebra of $\mathrm{sl}(3, \mathbb{C})$ the potential $q(x)$ belongs to the orthogonal complement $\mathfrak{h}_{J_0}^\perp$ of $\mathfrak{h}$ with respect to the Killing form. When u, v are smooth and tend to their constant asymptotic values sufficiently fast, then $q(x)$ converges sufficiently fast to 0 when $x \to \pm\infty$ and is smooth. The concept of gauge transformation, gauge equivalent auxiliary problems and gauge equivalent soliton equations, originates from the famous work of Zakharov and Takhtajan [4] where it has been used to solve an equation that is a classical analogue of equations describing waves in magnetic chains (spin $1/2$) - the so called Heisenberg Ferromagnet equation. It has been shown that it is gauge equivalent to the famous nonlinear Schrödinger equation. Later the result has been generalized to the soliton equations hierarchies associated with the corresponding gauge-equivalent auxiliary problems, to the conservation laws of these NLEEs, the hierarchies of their Hamiltonian structures etc. This has been achieved by generalizing the so-called AKNS approach [1] (Generating Operators or Recursion Operators) approach. Initially this has been done in the $\mathrm{sl}(2, \mathbb{C})$ case, next in the case of GZS system on arbitrary semisimple Lie algebra and this theory is referred as the gauge-covariant theory of the Recursion Operators related to the GZS systems in canonical and pole gauge, see the monograph book [3].

Until recently the GMV system was considered only in the Hermitian case, that is GMV_+ was considered. The first paper in which GMV_+ was studied in detail was a paper by Gerdjikov-Mikhailov and Valchev [2] and in it under the asymptotic conditions ($\lim_{x\to\pm\infty} u = 0$, $\lim_{x\to\pm\infty} v = \exp \mathrm{i}\Phi_\pm$ were discussed the spectral properties of (1), were presented two operators whose product play the role of a Recursion Operator, and were given expansions over the so-called adjoint solutions.

As mentioned, the approach we use is based on gauge equivalence, using the developed theory for the GZS systems in order to study $\mathrm{GMV}_\pm$. This requires some slight modifications to the theory which was developed for different asymptotic conditions, but this difficulty is easily overcame. As a consequence, we are able to treat both $\mathrm{GMV}_\pm$ systems simultaneously and we are able to consider general asymptotic conditions $\lim_{x\to\pm\infty} u = u_0$ and $\lim_{x\to\pm\infty} v = v_0$. In a paper we submitted to publication we considered the case when there is only continuous spectrum, in the present article we shall consider also the discrete spectrum.

References

[1] Ablowitz MJ, Kaup DJ, Newell AC and Segur H, Stud. Appl. Math. **53** (1974) 249-315

[2] Gerdjikov VS, Grahovski GG, Mikhailov AV, Valchev TI, Symmetry, Integrability and Geometry: Methods and Applications SIGMA **7** (2011) 096

[3] Gerdjikov VS, Vilasi G and Yanovski AB, Integrable Hamiltonian Hierarchies - Spectral and Geometric Methods, Springer (Heidelberg) 2008

[4] Zakharov VE, Takhtajan LA , TMF **38** (1979) 26-35

Stability properties of the Repeated Richardson Extrapolation combined with some explicit Runge-Kutta methods

Z. Zlatev, I. Dimov, I. Farago, K. Georgiev, A. Havasi

The implementation and the stability properties of the Repeated Richardson Extrapolation when it is applied together with Explicit Runge–Kutta Methods is studied in this paper.

The initial–value problem for first–order non–linear systems of ordinary differential equations (ODEs) in the time interval $[a,b]$ is considered. Let us assume that it is solved approximately by some one–step numerical method of order **p** on the equidistant grid–points. Assuming furthermore that the calculations at the points $t_1, t_2, \ldots, t(n-1); t_k = t_{k-1} + h; h = \frac{b-a}{n}$ has been completed and that the calculations at point t_n have to be carried out. This means that the approximation $y(n-1)$ is available and must be used to calculate the next approximation y_n. When the Repeated Richardson Extrapolation is to be used, this can be done by performing successively in four steps:

- *Step 1*: Compute an approximation $z_n^{[1]}$ of the solution of at the point $t = t_n$ by using the selected numerical method with a large stepsize h (i.e. one step is to be performed during this process).

- *Step 2*: Compute an approximation $z_n^{[2]}$ of the solution at the point $t = t_n$ by using the selected numerical method with a medium stepsize $h/2$ (i.e. two steps are to be performed during this process).

- *Step 3*: Compute an approximation $z_n^{[3]}$ of the solution at the point $t = t_n$ by using the selected numerical method with a small stepsize $h/4$. (i.e. four steps are to be performed during this process).

- *Step 4*: Compute an approximation y_n of the solution at the point $t = t_n$ by using the approximations $z_n^{[1]}$, $z_n^{[2]}$ and $z_n^{[3]}$.

The following theorem related to the accuracy of the Repeated Richardson Extrapolation holds and it is proven:

Theorem: *Consider the solution of the system of ODEs and assume that the underlying one-step numerical method is of order of accuracy **p**. Then the order of accuracy of the Repeated Richardson Extrapolation is at least **p+2** when the right-hand-side $f(t,y)$ is **p+2** times continuously differentiable.*

This theorem shows that the order of accuracy can be increased significantly when the Repeated Richardson Extrapolation is used, but it is necessary to pay some price (to carry out seven steps instead of only one) for achieving high accuracy. It is demonstrated that the high accuracy of the Repeated Richardson Extrapolation is sometimes allowing us to increase the stepsize and, solving the problem with a sufficiently large stepsize.

Two more theorems were proven. The first of them shows that the stability function of the Repeated Richardson Extrapolation is expressed by the stability function of the underlined

one-step method, but it is different. This means that the two numerical methods, the underlying one-step method and the Repeated Richardson Extrapolation, will in general have different stability properties. This result is a motivation for studying the stability properties of the Repeated Richardson Extrapolation. The second one was proved graphically and concerns the absolute stability regions of numerical methods that are combinations of explicit Runge-Kutta methods and the Repeated Richardson Extrapolation. It wsa proved that these stability regions are always larger than the absolute stability regions of the underlying explicit Runge-Kutta methods when the conditions **p = m** and **m**=1, 2, 3, 4 are satisfied.

The following book and papers were used as a base for the reported research:

1. G. Dahlquist: *A special stability problem for linear multistep methods*, BIT, **Vol. 3** (1963), pp. 27–43.

2. J. D. Lambert: *Numerical Methods for Ordinary Differential Equations: The Initial Values Problem*, Wiley, New York, 1991.

3. L. F. Richardson: *The Deferred Approach to the Limit, I—Single Lattice*, Philosophical Transactions of the Royal Society of London, Series A, **Vol. 226** (1927), pp. 299–349.

4. Z. Zlatev, K. Georgiev and I. Dimov: *Studying absolute stability properties of the Richardson Extrapolation combined with explicit Runge-Kutta methods*, Computers and Mathematics with Applications, **Vol 67, No. 12** (2014), pp.2294–2307.

Part B

List of participants

A.Alexandrov
Institute of Information and
Communication Technologies
Bulgarian Academy of Sciences
Akad. G. Bonchev, Str., Bl. 2
Sofia, Bulgaria
e-mail: akalexandrov@iit.bas.bg

Artan Alidema
Faculty of Mathematical and Natural Science
University of Pristina, 1000 Pristina, Kosovo
E-mail: artan.alidema@uni-pr.edu

Slav Angelov
Department of Informatics
New Bulgarian University
Montevideo str., 21
1618 Sofia, Bulgaria
sangelov@nbu.bg

Maria Angelova
Institute of Biophysics and
Biomedical Engineering
Bulgarian Academy of Sciences
105 Acad G. Bonchev Str.
1113 Sofia, Bulgaria
maria.angelova@biomed.bas.bg

Vera Angelova
Institute of Information and
Communication Technologies
Bulgarian Academy of Sciences
Akad. G. Bonchev, Str., Bl. 2
Sofia, Bulgaria
vangelova@iit.bas.bg

Atanas Angov
Institute of Information and
Communication Technologies
Bulgarian Academy of Sciences
Acad. G. Bontchev str., bl. 2
1113 Sofia, Bulgaria

Owe Axelsson
Institute of Geonics
Czech Academy of Sciences
Ostrava, Czech Republic
owe.axelsson@it.uu.se

Krassimir Atanassov
Department of Bioinformatics and
Mathematical Modelling
Institute of Biophysics and
Biomedical Engineering
Bulgarian Academy of Sciences,
Sofia, Acad. G. Bonchev Str., Bl. 105
and
Intelligent Systems Laboratory
Prof. Asen Zlatarov University
8000 Bourgas, Bulgaria
krat@bas.bg

Ana Avdzhieva
Faculty of Mathematics and Informatics,
Sofia University
5 James Bourchier Blvd.
1164 Sofia, Bulgaria
aavdzhieva@fmi.uni-sofia.bg

Alexander Ayriyan
Joint Institute for Nuclear Research
Laboratory of Information Technologies
Joliot-Curie 6
141980 Dubna, Moscow region, Russia
ayriyan@jinr.ru

Todor Balabanov
Institute of Information and
Communication Technologies
Bulgarian Academy of Sciences
acad. G. Bontchev Str., block 2
1113 Sofia, Bulgaria
todorb@iinf.bas.bg

Simon Becher
Dresden University of Technology

Roumen Borisov
Institute of Mechanics
Bulgarian Academy of Sciences
Acad. G. Bonchev Str., Bl. 4
1113 Sofia, Bulgaria

S. Bouyuklieva
Dept. of Algebra and Geometry
Veliko Tarnovo University

Stefan Bushev
Institute of Metal Science
Equipment and Technologies
with Center for Hydro and Aerodynamics
Bulgarian Academy of Sciences
Shipchenski prohod Str., 67
1574 Sofia, Bulgaria
stbushev@abv.bg

S. Cherneva
Institute of mechanics
Bulgarian Academy of Sciences
Acad. G. Bonchev Str., bl. 4
1113 Sofia, Bulgaria

M. Datcheva
Institute of mechanics
Bulgarian Academy of Sciences
Acad. G. Bonchev Str., bl. 4
1113 Sofia, Bulgaria

Yuri Dimitrov
University of Forestry
Department of Mathematics and Physics
10 Kliment Ohridski Blvd., Sofia, Bulgaria

Zlatinka I. Dimitrova
"G. Nadjakov" Institute of Solid State
Physics, Bulgarian Academy of Sciences,
Blvd. Tzarigradsko Chaussee 72,
1782 Sofia, Bulgaria

Ivan Dimov
Institute of Information and
Communication Technologies
Bulgarian Academy of Sciences
Acad. G. Bonchev Str., bl. 25A
1113 Sofia, Bulgaria

Stefka Dimova
Faculty of Mathematics and Informatics,
St. Kliment Ohridski University of Sofia
5 James Bourchier Blvd
1164 Sofia, Bulgaria
dimova@fmi.uni-sofia.bg

Nina Dobrinkova
Institute of Information and
Communication Technologies
Bulgarian Academy of Sciences
Acad. G. Bontchev str., bl. 2
1113 Sofia, Bulgaria
ninabox2002@gmail.com

Peter Dojnow
Institute of Information and
Communication Technologies
Bulgarian Academy of Sciences
Acad. G. Bontchev str., bl. 25A
1113 Sofia, Bulgaria
Dojnow@svr.igic.bas.bg

Velika Dragieva
University of Forestry
10 Kliment Ohridski Blvd., Sofia, Bulgaria
dragievav@yahoo.com

Svetoslav Enkov
Faculty of Mathematics and Informatics
University of Plovdiv Paisii Hilendarski
24 Tzar Asen
4000 Plovdiv, Bulgaria
svetoslav.enkov@gmail.com

Georgi Evtimov
Institute of Information and
Communication Technologies
Bulgarian Academy of Sciences
Acad. G. Bontchev str., bl. 25A
1113 Sofia, Bulgaria
gevtimov@abv.bg

Stefka Fidanova
Institute of Information and
Communication Technologies
Bulgarian Academy of Sciences
Acad. G. Bontchev str., bl. 25A
1113 Sofia, Bulgaria
stefka@parallel.bas.bg

Athanassios S. Fokas
Department of Applied Mathematics
and Theoretical Physics,
Cambridge University, UK
T.Fokas@damtp.cam.ac.uk

Jordan Genoff
Technical University of Sofia
branch Plovdiv
63 Sankt Petersburg Blvd
4000 Plovdiv, Bulgaria
jgenoff@tu-plovdiv.bg

Ivan Georgiev
Institute of Information and
Communication Technologies
Bulgarian Academy of Sciences
Acad. G. Bonchev Str., bl. 2
and
Institute of Mathematics and Informatics
Bulgarian Academy of Sciences
Acad. G. Bonchev str., bl. 8
1113 Sofia, Bulgaria

Krassimir Georgiev
Institute of Information and
Communication Technologies
Bulgarian Academy of Sciences
Acad. G. Bontchev str., bl. 25A
1113 Sofia, Bulgaria
georgiev@parallel.bas.bg

Atanaska Georgieva
Faculty of Mathematics and Informatics
University of Plovdiv Paisii Hilendarski
24 Tzar Asen Str.
4000 Plovdiv, Bulgaria
E-mail: afi2000@abv.bg

Irina Georgieva
Institute of Mathematics and Informatics
Bulgarian Academy of Sciences
Acad. G. Bonchev Str., Block 8
1113 Sofia, Bulgaria
irina@math.bas.bg

Vladimir Gerdjikov
Institute for Nuclear Research
and Nuclear Energy
Bulgarian Academy of Sciences
72 Tsarigradsko Chaussee Blvd.
1784 Sofia, Bulgaria
and

Institute of Mathematics and Informatics
Bulgarian Academy of Sciences
Acad. G. Bonchev str., bl. 8
1113 Sofia, Bulgaria
vgerdjikov@math.bas.bg

Jean-Luc Guermond
Department of Mathematics
Texas A&M University
College Station, TX 77843
guermond@math.tamu.edu

Todor Gurov
Institute of Information and
Communication Technologies
Bulgarian Academy of Sciences
Acad. G. Bontchev str., bl. 25A
1113 Sofia, Bulgaria
gurov@parallel.bas.bg

Sylvi-Maria Gurova
Institute of Information and
Communication Technologies
Bulgarian Academy of Sciences
Acad. G. Bontchev str., bl. 25A,
1113 Sofia, Bulgaria
sm_tvg@rocketmail.com

Stanislav Harizanov
Institute of Information and
Communication Technologies
Bulgarian Academy of Sciences
Acad. G. Bonchev Str., bl. 25A
1113 Sofia, Bulgaria
sharizanov@parallel.bas.bg
and
Institute of Mathematics and Informatics
Bulgarian Academy of Sciences
Acad. G. Bonchev str., bl. 8
1113 Sofia, Bulgaria

Jianfeng He
School of Physics
Beijing Institute of Technology
5 South Zhong Guan Cun Str.
Haidian Beijing 100081, PR China
hjf@bit.edu.cn

Clemens Hofreither
Institute of Computational Mathematics
Johannes Kepler University Linz
Altenberger Str. 69
4040 Linz, Austria
chofreither@numa.uni-linz.ac.at

Ivan Hristov
Faculty of Mathematics and Informatics
St. Kliment Ohridski University of Sofia
5 James Bourchier Blvd
1164 Sofia, Bulgaria
christov_ivan@abv.bg

Radoslava Hristova
Faculty of Mathematics and Informatics
St. Kliment Ohridski University of Sofia
5 James Bourchier Blvd
1164 Sofia, Bulgaria
radoslava@fmi.uni-sofia.bg

D. Iankov
University of Freiburg
Laboratory for Compound
Semiconductor Microsystems
Freiburg, Germany

Nevena Ilieva
Institute of Information and
Communication Technologies
Bulgarian Academy of Sciences
25A, Acad. G. Bonchev Str, Block 25A
1113 Sofia, Bulgaria
nevena.ilieva@parallel.bas.bg

Vladimir Ivanov
Institute of Information and
Communication Technologies
Bulgarian Academy of Sciences
Acad. G. Bontchev str., bl. 2
1113 Sofia, Bulgaria

Ivan Ivanov
University of National and World Economy
Department of Mathematics, Sofia, Bulgaria

Tihomir B. Ivanov
Faculty of Mathematics and Informatics

Sofia University
5 James Bourchier Blvd.
1164 Sofia, Bulgaria
Institute of Mathematics and Informatics
Bulgarian Academy of Sciences
Acad. G. Bontchev str., bl. 8,
1113 Sofia, Bulgaria
tbivanov@fmi.uni-sofia.bg

Ivan P. Jordanov
University of National and World Economy
Department of Mathematics, Sofia, Bulgaria

K.G. Kapanova
Institute of Information and
Communication Technologies
Bulgarian Academy of Sciences
Acad. G. Bonchev Str., bl. 25A
1113 Sofia, Bulgaria

S. Kapralov
Dept. of Mathematics and Informatics
Technical University of Gabrovo

Leoneed Kirilov
Institute of Information and
Communication Technologies
Bulgarian Academy of Sciences
Acad. G. Bontchev str., bl. 2
1113 Sofia, Bulgaria
l_kirilov_8@abv.bg

Vyara Koleva-Efremova
Institute of Information and
Communication Technologies
Bulgarian Academy of Sciences
Acad. G. Bontchev str., bl. 25A
1113 Sofia, Bulgaria
viarakoleva@yahoo.com

Petia Koprinkova-Hristova
Institute of Information and
Communication Technologies
Bulgarian Academy of Sciences
Acad. G. Bontchev str., bl. 25-A
1113 Sofia, Bulgaria
pkoprinkova@bas.bg

118

Georgi Kostadinov
Faculty of Mathematics and Informatics
University of Plovdiv Paisii Hilendarski
24 Tzar Asen
4000 Plovdiv, Bulgaria
geokostbg@yahoo.com

Hristo Kostadinov
Institute of Mathematics and Informatics
Bulgarian Academy of Sciences
Acad. G. Bonchev str., bl. 8
1113 Sofia, Bulgaria

Tsvetanka Kovacheva
Department of Mathematics
Technical University of Varna
tsveta_kovacheva@tu-varna.bg

Alexander Kurganov
Southern University of Science and
Technology Department of Mathematics
Shenzhen, 518055, China
and
Tulane University
Mathematics Department
New Orleans, LA 70118, USA
kurganov@math.tulane.edu

V. Kyrychok
Paton Welding Institute, Kiev

Mohamed Lachaab
Institut Superieur de Gestion de Tunis
Rue de la liberte, Bardo 2000, Tunisia
mlachaab@albany.edu

Zhao-Zheng Liang School of Mathematics
and Statistics, Lanzhou University, Lanzhou,
P.R. China,
liangzz11@lzu.edu.cn

Elena Lilkova
Institute of Information and
Communication Technologies
Bulgarian Academy of Sciences
25A, Acad. G. Bonchev Str. , Block 25A
1113 Sofia, Bulgaria
elilkova@parallel.bas.bg

Konstantinos Liolios
Institute of Information and
Communication Technologies,
Bulgarian Academy of Sciences
Sofia, Bulgaria
kostisliolios@gmail.com

Leandar Litov
Sofia University "St. Kliment Ohridski"
Faculty of Physics
5 James Bourchier Blvd. 1164
Sofia, Bulgaria
leandar.litov@cern.ch

Galina S. Lyutskanova-Zhekova
Faculty of Mathematics and Informatics
Sofia University
5 James Bourchier Blvd.
1164 Sofia, Bulgaria
g.zhekova@fmi.uni-sofia.bg

Nikolai Manev
Institute of Mathematics and Informatics
Bulgarian Academy of Sciences
Acad. G. Bonchev str., bl. 8
1113 Sofia, Bulgaria

Svetozar Margenov
Institute of Information and
Communication Technologies
Bulgarian Academy of Sciences
Acad. G. Bonchev Str., bl. 25A
1113 Sofia, Bulgaria

Rositsa Marinova
Sofia University "St. Kliment Ohridski"
Faculty of Physics
Atomic Physics Department
5 James Bourchier Blvd.
1164 Sofia, Bulgaria
rosie.marinova@gmail.com

Lubomir Markov
Department of Mathematics and CS
Barry University
11300 N.E. Second Avenue
Miami Shores, FL 33161, USA
lmarkov@barry.edu

119

Gunar Matthies
Dresden University of Technology

Hristo Melemov
Faculty of Mathematics and Informatics
University of Plovdiv Paisii Hilendarski
24 Tzar Asen Str.
4000 Plovdiv, Bulgaria
hristomelemov@yahoo.com

Rossen Mikhov
Institute of Information and
Communication Technologies
Bulgarian Academy of Sciences
Acad. G. Bontchev Str., Bl. 2
1113 Sofia, Bulgaria,

Zlatogor Minchev
Institute of Information and
Communication Technologies
Bulgarian Academy of Sciences
Acad. G. Bontchev Str., Bl. 25A
zlatogor@bas.bg
and
Institute of Mathematics and Informatics
Bulgarian Academy of Sciences
Acad. G. Bonchev Str., Bl. 8
1113 Sofia, Bulgaria

Peter D. Minev
Department of Mathematical and
Statistical Sciences
677 Central Academic Building
University of Alberta, Edmonton
Canada

V. Monov
Institute of Information and
Communication Technologies
Bulgarian Academy of Sciences
Acad. G. Bontchev Str., Bl. 2
1113 Sofia, Bulgaria
vmonov@iit.bas.bg

Vladimir Myasnichenko
Tver State University
Tver, Russia
viplabs@yandex.ru

Maya Neytcheva
Department of Information Technology
Uppsala University, Sweden,
maya.neytcheva@it.uu.se

Antti Niemi
Department of Physics and Astronomy
Uppsala University
Box 256, 75105 Uppsala, Sweden
School of Physics
Beijing Institute of Technology
5 South Zhong Guan Cun Str.
Haidian Beijing 100081, PR China
Antti.Niemi@uu.edu.se

Nikolay I. Nikolov
Institute of Mathematics and Informatics
Bulgarian Academy of Sciences
Acad. G.Bontchev str., block 8
1113 Sofia, Bulgaria
n.nikolov@math.bas.bg

Elena V. Nikolova
Institute of Mechanics
Bulgarian Academy of Sciences
Acad. G. Bonchev Str., Bl. 4
1113 Sofia, Bulgaria
elena@imbm.bas.bg

Inna Nikolova
Institute of Information and
Communication Technologies
Bulgarian Academy of Sciences
125 Tsarigradsko shose, blvd, Block 2
1113 Sofia, Bulgaria
inna.petrova.nikolova@gmail.com

Silviya Nikolova
Department of Anthropology
and Anatomy
Institute of Experimental Morphology,
Pathology and Anthropology
with Museum
Bulgarian Academy of Sciences
Acad. G. Bonchev Str., bl. 25
1113 Sofia, Bulgaria
sil_nikolova@abv.bg

Spasimir I. Nonev
Faculty of Mathematics and Informatics
Sofia University
5 James Bourchier Blvd.
1164 Sofia, Bulgaria
spasimir.nonev@gmail.com

Ludmila Parashkevova
Institute of Mechanics
Bulgarian Academy of Sciences
Acad. G. Bontchev str., bl. 4
1113 Sofia, Bulgaria
lusy@imbm.bas.bg

Albena Pavlova
Department of MPC
Technical University-Sofia, Plovdiv Branch
4000 Plovdiv, Bulgaria
akosseva@gmail.com

Tania Pencheva
Institute of Biophysics and
Biomedical Engineering
Bulgarian Academy of Sciences
105 Acad G. Bonchev Str., 1113
Sofia, Bulgaria
tania.pencheva@biomed.bas.bg

Peicho Petkov
Sofia University "St. Kliment Ohridski"
Faculty of Physics
5 James Bourchier Blvd.
1164 Sofia, Bulgaria
peicho@phys.uni-sofia.bg

P. Petrova
UCTM
8 Kl. Ohridski Blvd.
1756 Sofia, Bulgaria
polina.petrova1994@gmail.com

Nedyu Popivanov
Institute of Information and
Communication Technologies
Bulgarian Academy of Sciences and
Sofia University "St. Kliment Ohridski"
nedyu@parallel.bas.bg

Stefan Radev
Institute of Mechanics
Bulgarian Academy of Sciences
Acad. G. Bontchev str., bl. 4
1113 Sofia, Bulgaria
stradev@imbm.bas.bg

Peter Rashkov
Institute of Mathematics and Informatics
Bulgarian Academy of Sciences
Akad. G. Bonchev str., bl. 8
1113 Sofia, Bulgaria
p.rashkov@math.bas.bg

Olympia Roeva
Institute of Biophysics and
Biomedical Engineering
Bulgarian Academy of Sciences
Acad. G. Bonchev str., bl.105
1113 Sofia, Bulgaria
olympia@biomed.bas.bg

Wil Schilders
Centre for Analysis, Scientific
Computing and Applications
TU Eindhoven
The Netherlands

Nikolay Sdobnyakov
Tver State University
Tver, Russia

Angela Slavova
Institute of Mathematics and Informatics
Bulgarian Academy of Sciences
Acad. G. Bontchev str., bl. 8
1113 Sofia, Bulgaria
slavova@math.bas.bg

Slavcho Slavchev
Institute of Mechanics
Bulgarian Academy of Sciences
Acad. G. Bontchev str., bl. 4,
1113 Sofia, Bulgaria
slavchogs@yahoo.com

Vladimira Souvandjieva
Faculty of Mathematics and Informatics
Sofia University "St. Kliment Ohridski"
5 James Bourchier Blvd.,
1164 Sofia, Bulgaria
vladi_96@abv.bg

Stefan Stefanov
Institute of Information and
Communication Technologies
Bulgarian Academy of Sciences
Acad. G. Bontchev str., bl. 2
1113 Sofia, Bulgaria

Todor Stoilov
Institute of Information and
Communication Technologies
Bulgarian Academy of Sciences
Acad. G. Bontchev str., bl. 2
1113 Sofia, Bulgaria

Eugenia Stoimenova
Institute of Information and
Communication Technologies
and
Institute of Mathematics and Informatics,
Bulgarian Academy of Sciences,
Acad. G.Bontchev str., block 25A,
1113 Sofia, Bulgaria
jeni@parallel.bas.bg

Dimiter Stoychev
Institute of Physical Chemistry
Bulgarian Academy of Sciences
Acad. G. Bontchev St., bl. 11
1113 Sofia, Bulgaria
stoychev@ipc.bas.bg

Sonia Tabakova
Institute of Mechanics
Bulgarian Academy of Sciences
Acad. G. Bontchev str., bl. 4
1113 Sofia, Bulgaria
stabakova@gmail.com

Assen Tchorbadjieff
Institute of Mathematics and Informatics
Bulgarian Academy of Sciences

Acad. G. Bonchev str., bl. 8
1113 Sofia, Bulgaria

Ronald Tetzlaff
Technical University of Dresden
Germany
Ronald.Tetzlaff@tu-dresden.de

Michail Todorov
Department of Applied Mathematics
and Computer Science
Technical University of Sofia
8 Kliment Ohridski, Blvd.
1000 Sofia, Bulgaria
mtod@tu-sofia.bg

Venelin Todorov
Institute of Information and
Communication Technologies
Bulgarian Academy of Sciences
Acad. G. Bonchev Str., bl. 25A
1113 Sofia, Bulgaria

Petar Tomov
Institute of Information and
Communication Technologies
Bulgarian Academy of Sciences
acad. G. Bontchev Str., block 2
1113 Sofia, Bulgaria
p.tomov@iit.bas.bg

Diana Toneva
Department of Anthropology
and Anatomy
Institute of Experimental Morphology,
Pathology and Anthropology
with Museum
Bulgarian Academy of Sciences
Acad. G. Bonchev Str., bl. 25
1113 Sofia, Bulgaria

Peter R. Turner
Clarkson University
Institute for STEM Education
305B Bertrand, H. Snell Hall
Clarkson University
Potsdam New York, 13669
pturner@clarkson.edu

T. Valchev
Institute of Mathematics and Informatics
Bulgarian Academy of Sciences
1113 Sofia, Bulgaria
tiv@math.bas.bg

Milena Veneva
Joint Institute for Nuclear Research
Laboratory of Information Technologies
Joliot-Curie 6
141980 Dubna, Moscow region, Russia
milena.p.veneva@gmail.com

Kaloyan N. Vitanov
Institute of Mechanics
Bulgarian Academy of Sciences
Acad. G. Bonchev Str., Bl. 4
1113 Sofia, Bulgaria

Nikolay K. Vitanov
Institute of Mechanics
Bulgarian Academy of Sciences,
Acad. G. Bonchev Str.,Bl. 4
1113 Sofia, Bulgaria
vitanov@imbm.bas.bg

Dennis Wenzel
Dresden University of Technology
Germany
denniswenzel2012@gmail.com

A. Yanovski
Department of Mathematics
and Applied mathematics
University of Cape Town
Rondebosch 7700
Cape Town, South Africa
Alexandar.Ianovsky@uct.ac.za

Iliyan Zankinski
Institute of Information and
Communication Technologies
Bulgarian Academy of Sciences
acad. G. Bontchev Str., block 2
1113 Sofia, Bulgaria
iliyan@hsi.iccs.bas.bg

Z. Zlatev
National Environmental Research Institute
Aarhus University
Frederiksborgvej 399, P. O. Box 358
DK-4000 Roskilde, Denmark